

https://dspace.org/

Lung mechanics: a systematic review of mechanical elasticity in lung parenchyma

Bhana, Rohail Hershil

2022

https://hdl.handle.net/10539/33871

Downloaded from a DSpace repository. https://dspace.org/

An investigation into the process mineralogy and supply of cobalt with special emphasis on the Democratic Republic of Congo

Ntebatše Rachidi 1356224

MSc Economic Geology



WITS
UNIVERSITY

A research report submitted to the Faculty of Science, University of the Witwatersrand, Johannesburg, in partial fulfilment of the requirements for the degree of Master of Science

27 January 2022, Johannesburg

Declaration

I declare that this research report is my own, unaided work. It is being submitted for the Master of Science at the University of the Witwatersrand, Johannesburg. It has not been submitted before for any degree or examination at any other University. Parts of this research report have been submitted to the Resource Policy Journal.



_____

(Signature of candidate)

27th **day of** January 2022 **at** Johannesburg

Abstract

Transitioning to a decarbonised and circular economy is paramount for climate change mitigation and sustainable development. In this research report I assess the global production trends of cobalt, an energy-transition metal (ETM), and its supply sustainability. Accurate production forecasting of ETMs is essential to understand the dynamics of energy supply security and adequately plan for a change from fossil fuel energy to renewable energy production. Evaluations of market concentrations point out that cobalt is a high-risk market characterised by production fluctuations and supply-chain complexities. Using an Auto Regressive Integrated Moving Average (ARIMA) model to forecast production, a linear increase in world production is predicted for the short term, while a Hubbert model predicts a world production decline beginning in the late 2010s. These predictions, coupled with geopolitical, socio-environmental, economic, and technological influences on the market reinforce the concern around cobalt supply sustainability. The relationship between geology and metallurgy must be reinforced as one of the most important criterion in ensuring cobalt supply sustainability. High-tech extractive metallurgy and mineral processing are essential for supplying critical raw materials (CRMs) for our modern society. The ability to effectively extract, process and beneficiate CRMs is dependent on understanding the mineralogical characteristics of ore deposits. Although alternative avenues for sourcing cobalt such as secondary urban mining and stockpiling exist, they are unlikely to become major suppliers in the short term and therefore, accurate primary production forecasting is important for ensuring energy supply security and policymaking. Increasing international interest on critical raw materials in policy spheres also heighten the necessity to anticipate the future of cobalt supply as governmental entities acknowledge the imbalance of CRMs in international trade. Well-researched and well-designed policies that incorporate environmental sustainability and non-discriminatory economic growth can facilitate an equitable shift to a greener and more circular economy. At the forefront of this shift should be ethical environmental and resource governance that recognises the inequalities in socio-economic development and energy-transition, and mandates for a just transition towards a low carbon future.

Dedication

I dedicate this research report to my grandparents, Noko and Kwenadi, for their love and encouragement that has been my anchor throughout my education.

Acknowledgements

I extend my heartfelt gratitude to my supervisors Adj. Prof Glen T. Nwaila and Dr Steven E. Zhang for their scholarly advice, guidance, and openness to listening to my ideas and developing them. Your support and keen interest in this research have been a source of motivation and have led to the successful completion of this research report.

Special thanks to Prof. Yousef Ghorbani and Dr Julie E.Bourdeau for their insightful feedback and assistance with the technicalities of writing a research report. Their insights pushed me one step further to improve the quality of my work.

I would also like to thank Claire Ceruti for her contribution to the social aspect of this report. Her insights were a reminder that science should not exist outside of society.

Thank you to Nonkuselo Madlakana for her assitance with the TIMA analysis and compilation of the results.

My sincere thanks are also extended to my friends, across different spheres of life, for their continued support and motivation.

The financial assistance of the National Research Foundation (NRF) towards this research is hereby acknowledged. Opinions expressed and conclusions arrived at, are those of the author and are not necessarily to be attributed to the NRF.

Contents

Declaration i
Abstract ii
Acknowledgements iv
List of Figures vii
List of Tables ix
Chapter 1 1
1. Introduction 1
1.1 Purpose of research 5
1.3 Aim of this research 5
1.4 Objectives 6
1.5 Key Questions 6
Chapter 2 7
2. Literature Review 7
2.1 The role of mineralogy in Cu-Co ores 7
2.2 Definition and significance of critical raw materials 7
2.3 Theoretical background of world cobalt resources and reserves 9
2.4 World cobalt demand and supply 10
2.5 Cobalt production in the Democratic Republic of Congo 12
2.6 Constraints in global transition to renewable resources 12
2.7 Sustainable extraction of mineral resources and recyclability 14
2.8 Environmental, social and governance (ESG) risks in mineral extraction industries 15
Chapter 3 18
3. Methods and Results 18
3.1 Tescan Integrated Mineral Analyser 18
3.2 Mineral resource production forecast 18
3.2.1 Autoregressive Integrated Moving Average model 19
3.2.2 Hubbert model 21
Chapter 4 23
4. Results 23
4.1 Qualitative mineralogy 23

4.2 Process Mineralogy 25
4.2.2 Elemental composition 27
4.3 World cobalt production trends 30
4.4 Forecasting cobalt production 32
4.4.1 ARIMA model forecasting results 32
4.4.2. Hubbert model forecasting results 35
Chapter 5 38
5. Discussions 38
5.1 Mineralogical effects on recovery of cobalt 38
5.1.1 Mineralogical limitations on separation 38
5.1.2 Size and liberation optimisation 39
5.1.3 Deleterious minerals and elements 40
5.2 Validity of ARIMA forecasts 41
5.3 Importance of production forecasting on cobalt supply 42
5.4 Uncertainties for cobalt market future 43
Conclusion 45
6. Concluding Remarks 45
References 46
Appendices 58

List of Figures

Figure 2.1 Critical versus non-critical classification of mineral resources based on supply risk-economic importance relationship (data from European Commission, 2020).

Figure 1.2 Risk profiles and demand projections for nine ETMs. A: Environmental, social and governance indicators ranked from very low to very high. B: Total risk scores based on resource tonnage. C: Prediced peak demand expected from low-carbon technologies as a part of current global production (dashed line). D: Estimated annual mined ore from predicted demand (modified from Lèbre et al., 2020).

Figure 4.1 Photomicrographs of samples showing mineralisation features of the samples. A: pyrite rims around chalcopyrite and quartz. B: chalcopyrite-carrollite disseminated texture. C: chalcopyrite alteration. D: chalcopyrite replacement texture. E: intensely fractured carrollite. F: bornite with basket-weave texture. G: covellite and bornite concentric banding. H: covellite inclusion in quartz matrix. Scale represents 100 µm.

Figure 4.2 Primary phase maps showing the common minerals and disseminated sample texture as detected by the TIMA. Descriptions for each sample is provided in Appendix A1 of the research report.

Figure 4.3 Elemental maps showing the distribution of the four most enriched elements (cobalt, sulphr, copper, and iron) in the samples. Full set of elemental maps and element distribution descriptions provided in Appendix B1 of this research report.

Figure 4.4 World cobalt production from 1970 to 2020. A full dataset for world production by country is provided in Appendix C1 to this research report (Brown et al., 2020)

Figure. 4.5 ARIMA forecasts for Global South countries. Green lines represent production data. Pink lines correspond to the forecasted values and their respective 95 % confidence interval (pale pink).

Figure. 4.6 ARIMA forecasts for Global North countries and the world. Green lines represent production data. Pink lines correspond to the forecasted values and their respective 95 % confidence interval (pale pink).

Figure. 4.7 Hubbert model fits for the DRC (blue line) and the world (red line). Blue and red shaded areas correspond to the 95 % confidence band for the DRC and the world, respectively. .

Figure 5.1 ARIMA cross validation forecasts of selected countries showing objective accuracy (A and C) and inaccuracy (B and D). A complete set of graphs is given in the Appendix D1 of this research report.

List of Tables

Table 4.1. Enrichment of elements in specific minerals.

Table 4.2
Production data for the DRC and world based on Hubbert model.

Chapter 1

1. Introduction

The overall trend in the supply of raw materials has been a societal cultural shift towards supply-chain robustness, localized sufficiency, reducing geopolitical tension and increasing supply sustainability (Overland, 2019). The sustainability of raw materials has been under consideration since its modern definition that was created in 1987 (World Commission on Environment and Development, 1987). The long-term supply of raw materials has never been certain and periodically, supply issues rekindle, especially as the problem of raw material sustainability is exacerbated by the increasing human population and development demands (Calvo et al., 2017). The COVID-19 pandemic has highlighted the vulnerability of a global supply and demand system that is highly optimised for supply-chain efficiency instead of resiliency and redundancy. This pandemic is the latest signal in a decade-long trend that has led policy makers and academics to examine the supply of raw materials.

Strategic or critical raw materials (CRMs) are gaining popularity in the policy sphere as various governmental entities realise that the international trade is becoming increasingly unbalanced, fragile and important for geopolitics, and correspondingly have taken steps to define assessment frameworks and produce periodically updated lists (e.g., European Commission, 2011, 2014, 2017 and 2020; Overland, 2019; Humphries, 2019). CRMs are non-substitutable raw materials in the present context, in which most consumer countries are dependent on imports, and whose supply is dominated by one or a few producers (National Research Council, 2008; Overland, 2019). Aside from their usage in many sectors, CRMs are a pivotal contribution to socio-economic development within the contemporary transition to a circular green economy (Mathieux et al., 2017) and the need to enhance the circularity of materials in response to climate change and finite resource depletion (Elshkaki et al., 2016, Ali et al., 2017; Hofmann et al., 2018). All energy-transition metals (ETMs), many of which are already CRMs, are

anticipated to face market pressures due to the intensification of the production of low-carbon technologies (Church and Crawford, 2018; Lèbre et al., 2020).

Although potential pre- and post-consumer recycling is increasing in efficiency (United Nations Environment Programme et al., 2009), the latency of supply-chain responses to the looming and unpredictable supply risk may create undesirable dynamics in the complex supply and demand system. For instance, mitigations such as new resources through urban mining, research and development of substitutes in various applications, or stockpiling during overproduction periods (Campbell, 2020) may occur asynchronously with market demand. Availability of ETMs will require forecasting of ETM production to understand and adequately plan for energy supply security and sourcing from alternative avenues. Developing and implementing green energy policies for economic growth and sustainable development is reliant on recognizing the importance of, and acting on environmental, social and governance (ESG) factors within the mineral industry, adopting rigorous environmental governance to align with climate change action (Lèbre et al, 2019) and complying to Sustainable Development Goals (SDGs) obligations.

Mineral extraction, processing, and beneficiation of Cu-Co ores in the DRC is driven by the pressure to satisfy the exponential demand of Cu and Co metals as this is key to increasing government revenues accruing from mining royalties (Shengo et al., 2019). This exponential demand necessitates continuous adaption of mining constraints, increasing low-grade ores, and environmental restraints (Shengo et al., 2019). The commercial processing industry of Katanga (DRC) is faced with the challenge of increasing mineralogical complexities of Cu-Co ores towards mixed ores as mining depths continue to increase due to the depletion of higher-grade ores near surface. This implies that suitable physical separation and flotation methods are required to meet market demand (Shengo et al., 2019; Crundwell, 2020).

Conventional beneficiation of Cu-Co ores in the DRC is conducted through gravity separation and/or froth flotation (Shengo et al., 2019). Gravity separation uses the effects of mass, volume, and shape of a particle to separate mineral constituents in

either a static or dynamic liquid medium (Shengo et al., 2019). This recovery method is constrained to pre-concentration stages in which its objective is to remove waste streams from the circuit upon adequate depletion or to extract the rich concentrate and subsequent treatment of discharge. More specifically, gravity separation techniques deployed to beneficiate Cu-Co ores in Katanga include spiral and shaking table concentration, and heavy/dense media separation (HMS) (Shengo et al., 2019). The purpose of the former technique is to attain the maximum grade of metallic ore with minimal mass recovery. Spiral and shaking table concentration is generally accepted to be better suited for coarser particles as the force of gravity is more effective on coarser particles than finer particles. Heavy media separation is a technique involving the treatment of crushed and screened ore that is then fed as a pulp into a pseudo-liquid medium of a specified density (Woollacott and Eric, 1994; Shengo et al., 2019). This allows for high-density, valuable minerals to sink while low-density, gangue materials float. The extraction technique is usually applied to particles with a diameter size differential of 0.5 to 40 mm (coarse particle size) as the efficiency of separation decreases with size due to nonlinear decreases in the settling rate of particles in suspension (Wills and Napier-Munn, 2006; Shengo et al., 2019)

Co is an ETM and is an element in the cathode within rechargeable batteries, especially Co-bearing lithium batteries (DeCarlo and Matthews, 2019), which are used in energy storage units, power tools, hybrid and electric vehicles – functions that promote the implementation of sustainable energy applications and the advancement of information and technology (ICT) (Hofmann et al., 2018). Recent evaluations of market concentrations of critical metals suggest that Co is a high-risk market that is prone to supply shortages in the international mineral market (Shedd et al., 2017; European Commission, 2020). Factors such as a low recycling rate and overall low availability of minerals to recycle (Ali et al., 2017) over the next two to three decades may cause supply challenges with critical metals, especially by-product metals such as Co. Despite this, the use of Co is sharply rising, as for example, Co in transportation alone increased 89 % from the first half of 2018 (~3800 metric tonnes) to the same period in 2019 (7200 metric tonnes) (Adamas Intelligence, 2019). It is unclear if the supply of Co can sustain such

demands in the future and what mitigations are appropriate, as the Co supply is affected by a range of economic, geopolitical, environmental sustainability and technological factors (Wilburn, 2012; Sykes et al., 2016).

Consistent with other ETMs, Co supply vulnerability can be reduced through secondary urban mining and substitution (Sykes et al., 2016; Ghorbani et al., 2021). Whether or not these approaches would address potential Co supply gaps depend on the exact market and political conditions, and hence forecasting the supply of Co is key to understanding the practicality of any secondary sources to augment the primary Co supply. In general, mitigating potential supply-chain disruptions to ensure Co supply sustainability for viable development requires both resource and environmental governance, which relies on accurate forecasts (Ali et al., 2017). In particular, accurate forecasting enables informed investment planning decisions and green energy policies for a low-carbon future and climate change mitigation strategies (Berk and Ediger, 2016).

In this study, I examine the supply of Co by means of short- and long-term forecasts for the world using production data from the British Geological Survey (BGS) of 14 countries[1] (i.e., Australia, Botswana, Brazil, Canada, China, Cuba, DRC, Finland, Morocco, New Caledonia, Russia, South Africa, Zambia, and Zimbabwe) for the period 1998-2020.

I employed two approaches that use the Auto Regressive Integrated Moving Average (ARIMA) method for short-term forecasts and a Hubbert-type single-peak parametric model for long-term forecasts. In addition to forecasting, I also explore the underlying ESG factors that underpin challenges of production. The world ARIMA-based forecast suggests a linear increase in production while the Hubbert-based forecast, more unreliably, assumes a production peak in 2015. Despite the varying objective accuracy of two types of forecasts, the general trends reflected by the forecasts are useful for scenario planning and policymaking as decadal behaviour is more relevant than monthly or yearly variability.

[1] Cobalt producing countries exceed 14, however, the selected countries provided the most consistent and reliable data throughout the analysis period. Years before the 1998-2020 analysis period contain data discrepancies.

1.1 Purpose of research

This study is a multidimensional examination of Co deportment and optimisation of recovery that extends beyond extraction and recovery to include issues surrounding foreign investment policy, economic analyses, and sustainable and ethical supply chains. As of 2015, and the foreseeable future, the DRC Co market is classified as high-risk, which is susceptible to supply chain disruptions as based on the Herfindahl-Hirschman Index. Given this projection, it is vital that examination of the socio-economic and environmental policy framework related to Co-production and beneficiation is conducted over-and-above questioning Co's global supply security. Results of this study are expected to provide crucial insights through rigorous data analyses on the adaptive potential of the DRC's and the world's Co supply and acts as a foundational resource for safeguarding energy supply security and informing policymaking.

1.2 Problem Statement

The confinement and increase of Co-production in the DRC due to a technological revolution, transition to environmentally friendly energy production, and the inherent fragility in the current global supply chain that is configured for high efficiency, highlights concerns for global Co supply security. An observed compound annual growth rate increase of 12 % from 2000 to 2015 necessitates an investigation of Co-production processes in conjunction with an examination of its supply sustainability (Shedd et al., 2017). A detailed Co deportment study, therefore, assesses the physiochemical and mineralogical characteristics to allow for effective and cost-efficient extraction and processing (Coetzee et al., 2011).

1.3 Aim of this research

The aim of this research is to conduct a Co deportment study on Cu-Co ores from the DRC which focuses on predictive mineralogy to aid optimisation of Co metallurgical recovery. A concurrent and equally important aim is to assess Co's supply sustainability and its implications for green energy policies.

1.4 Objectives

- To investigate the liberation and composition of Co bearing minerals and their potential impact on subsequent mineral processing.
- To analyse potential demand and supply based on mineral resource data.
- To examine the supply chain in accordance with UN Guiding Principles on Business and Human Rights

1.5 Key Questions

- Can this mineralogical information be used to predict the processing behaviour of Co?
- What are the socio-economic and environmental impacts associated with optimised Co recovery, production, and beneficiation? Are there potential alternatives?

Chapter 2

2. Literature Review

2.1 The role of mineralogy in Cu-Co ores

Primary copper-cobalt (Cu-Co) mineral associations occur homogenously in mineralised zones and variations are a resultant of the effect of oxidation and supergene enrichment (GRD Minproc, Technical Report, 2007). Mineral assemblages are, therefore, categorised based on the degree of alteration into oxide, mixed, and sulphide ore zones (Kalenga, 2014; Shengo et al., 2019) which influences the amount of available Co for extraction. The mineralogy of Co as influenced by its host deposits (oxidised versus mixed versus sulphide ores) has implications for the mineral processing procedures (Kalenga, 2014). The principal sulphide ore minerals mainly found in dolomites of the DRC are ore minerals chalcopyrite ($CuFeS_2$), bornite (Cu_5FeS_4) and carrollite ($CuCo_2S_4$) (Johnson, 2014). Cobalt can also occur in the form of linnaeite (Co_3S_4) or as cobaltiferous pyrite (CoS2), if it occurs in solid solution with pyrite (Crundwell et al., 2020). The main oxide[2] minerals are malachite, $Cu(OH)_2.CuCO_3$, and (true) heterogenite, CoOOH (Vanbrabant et al., 2013; Crundwell et al., 2020). This mineralogical association, in turn, affects the recovery efficiency as this is determined by the mineralogical complexity of the ores (Santoro et al., 2019). Based on Santoro et al.'s study (2019), there are two key factors that explain an incomplete recovery which include mineral liberation issues and the presence of un-recoverable elemental Co within the structure of the refractory phases.

2.2 Definition and significance of critical raw materials

The definition of CRMs has been refined over time since its introduction in literature in the 2000s. The European Commision (2010) defined CRMs as a raw material in which its supply-shortage risk (based on the level of concentration of production, and political-economic stability) and impact on its economy are considerably higher than that of other raw materials. Pommeret et al.'s (2022) highlight that CRMs are of high economical and technical importance and that

[2] Crundwell et al. (2020) highlighted that 'oxide' must be interpreted as non-sulphide considering that on the Central African Copperbelt, the minerals are mostly carbonates and hydroxides and not true oxides.

avalablity concenrs are influenced by geological and geopolitical factors. A commonality to CRM definitions is that deposits hosting these materials are quantitatively limited with an uneven geographical distribution (Hofmann et al., 2018) and unlike fossil fuel materials, they can be recycled. In the EU definition, criticality is dependent on supply risk and economic importance (Fig. 1) (Lusty and Gunn, 2015; European Commission, 2020; Blengini et al., 2017). As of 2018, upon recognizing the risk of potential supply of metals vital for economic and social security, the United States released a list of 35 critical raw materials[3], which include Co and lithium (Humphries, 2019). The 'Lithium Triangle', a cluster of lithium reserves located between Chile, Argentina and Bolivia, is an example of geopolitical competition caused by the criticality of metals. Known as the 'Triangle States', these three countries account for at least 60 % of global lithium brine reserves.Criticality for this metal is also excacerbated by China's potential monopoly given its growing interest in lithium projects with the Triangle (Heredia et al., 2020).

The supply of CRMs can also be curtailed due to political instability, which discourages mining policies, restricts trade, deters foreign investment, and reduces governance capacity. (UNEP, 2007; Tisserant and Pauliuk, 2016). Specifically, the relevance in research, science, and engineering (Graedel and Beck, 2016) especially with the increased action towards implementing greener and cleaner technologies contributes to the designation of criticality for raw materials (Hofmann et al., 2018). Graedel and Beck (2016) explained that the criticality approach[4] extends further from mineral resource availability into the resource supply chain. This approach incorporates macro-scale supply and demand dynamics.

[3] Aluminium, antimony, arsenic, barite, beryllium, bismuth, caesium, chromium, cobalt, fluorspar, gallium, germanium, graphite, hafnium, helium, indium, lithium, magnesium (composite), niobium, PGMs, potash, rubidium, scandium, tantalum, tellurium, tin, titanium (concentrate), tungsten, uranium, vanadium, and zirconium.

[4] Refers to approaches to deal with declining ore grades and subsequent technological challenges faced when extracting minerals in extreme environments.

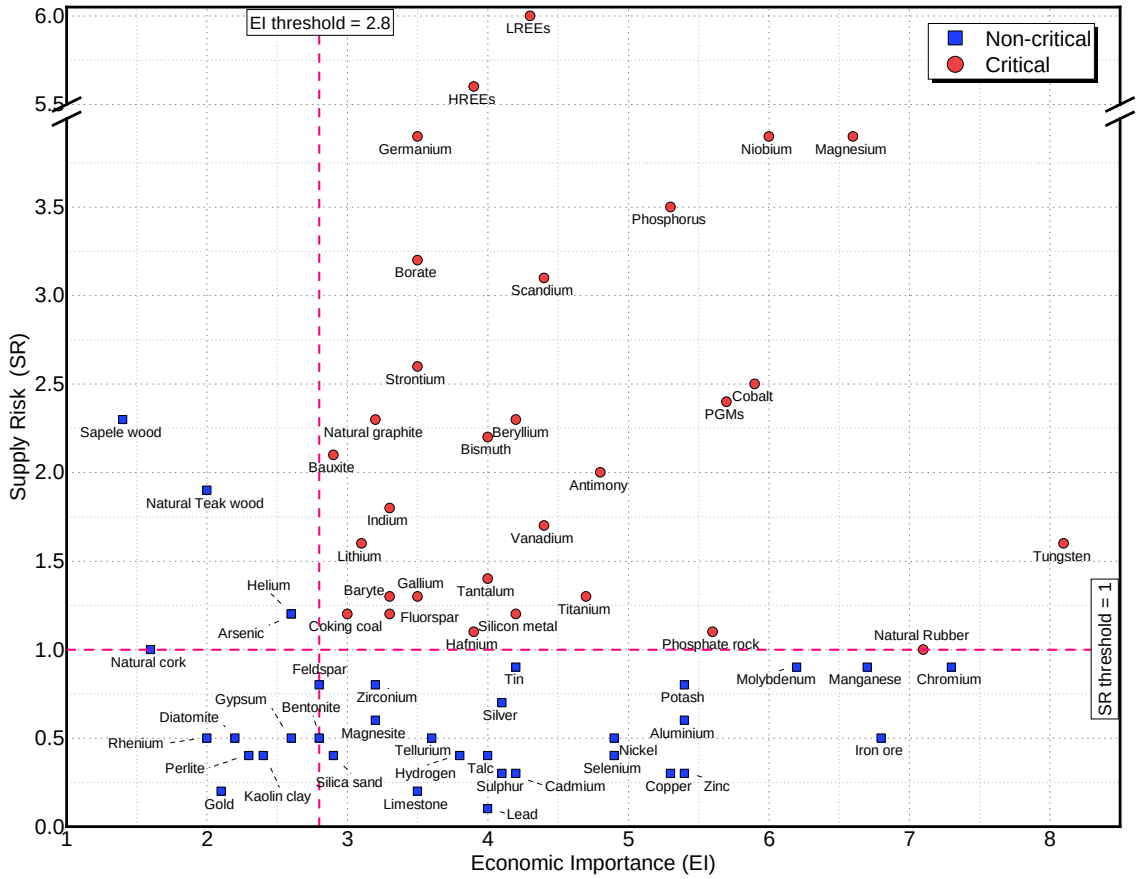


Figure 2.1 Critical versus non-critical classification of mineral resources based on supply risk-economic importance relationship (data from European Commission, 2020).

2.3 Theoretical background of world cobalt resources and reserves

Supply shortages and crises are characteristic of the Co market (Campbell, 2020). When assessing possible supply potential, a geopotential can be ascertained through geophysical and geological interpretation with the aid of modern exploration methods. From this, reserves – the percentage of total resources that are economic to extract given the available technology and energy, as well as environmentally and socially acceptable conditions (Scholz and Wellmer, 2013) – can be estimated. These estimations are either probable or proven with increasing geoscientific knowledge and confidence, as well as the application of modifying factors from the initial resource determination (SAMREC, 2016). Resources exhibit economic uncertainty but have prospects for economic extraction (SAMREC, 2016; Ali et al., 2017).

The world's terrestrial reserves of Co are estimated at approximately 25 million metric tonnes with a considerable majority of these resources located in sediment-hosted stratiform copper deposits in the Democratic Republic of Congo (DRC) and Zambia; magmatic nickel-copper sulphide deposits hosted in mafic and ultramafic rocks in Australia, Canada, Russia, and the United States; and nickel-bearing laterite deposits in Australia (Selley et al., 2018; Twite et al., 2019; United States Geological Survey, 2020; Horn et al., 2021). The inferred amount of Co within each deposit type is 60 %, 23 % and 15 %, respectively. The respective average grade of the deposit types is 0.1 – 0.4 %, 0.1 %, and 0.05 – 0.15 % (Hitzman et al., 2017; Slack et al., 2017, Cobalt Institute, 2021). Oceanic Co resources hold the potential to supplement depleting terrestrial reserves as resources in manganese nodules and oceanic crust of the Atlantic, Indian, and Pacific Oceans amount to 120 million metric tonnes (United States Geological Survey, 2020).

2.4 World cobalt demand and supply

The importance of a mineral's supply is determined by its economic importance to a geographical location and its supply potential based on metallurgical, environmental, geopolitical, and social factors (Rosyid and Adachi, 2016; Sykes et al., 2016; Hofmann et al. 2018). Krishnamurthy and Gupta (2015) constrained the geological influences of supply potential into 'discovery' and 'supply'. Discovery accounts for the relative crustal abundance and chance for a mineral of interest to concentrate into a distinct deposit. However, 'supply' refers to the ease of extraction of the ore from the ground (mine), and the ease of extraction of the mineral from the ore (process) – factors that control the potential of supplying the mineral to the market (Krishnamurthy and Gupta, 2015; Sykes et al., 2016). In the chain model of the supply-side of resources, the slowest step is the rate-limiting factor, or a bottleneck in the supply chain. Although resource availability is affected by numerous considerations (Lusty and Gunn, 2015; Sykes et al., 2016), the supply of CRMs is largely driven by geographical concentration of production (Lusty and Gunn, 2015) at both country and company scales (Shedd et al., 2017). The geographic concentration of production affects criticality in the form of: trade barriers and agreements; ease to systematic supply chain approach; import

dependency and raw materials supply; and raw material recycling and efficiency (Blengini et al., 2017). Any of these factors can potentially become a rate-limiting factor.

Increasing global demand for minerals is perpetuated by resource consumption associated with population growth, together with a progressively diverse range of applications for new technologies (Lusty and Gunn, 2015; Nurmi, 2017) and climate change mitigation through decarbonisation of economies (Lèbre et al., 2019). World demand and supply patterns will likely change globally as the Global South countries undergo intensive industrialization (UNEP, 2013; Haraguchi et al., 2017), while Global North countries incorporate more modern, metal-intensive technologies that are key for a transition to green technologies (UNEP, 2013; Rissman et al., 2020). As the consumption of resources increases in alignment to changes in the global economic and the political landscape, the supply-demand imbalances of raw materials could worsen, which may lead to price volatilities and create precarious market strategies for the technological industry (Hofmann et al., 2018). The domino effect of this could eventually pose uncertainties for the transition to a low-carbon future through clean technologies that are heavily reliant on CRMs.

In the case of Co, the supply-demand balance is strongly influenced by world production (United States Geological Survey, 2020) from 14 countries. Since 1970s, the Co market has been riddled with supply shortages relative to demand (Campbell, 2020). Growing concern has arisen because of the increasing demand for Co in rechargeable lithium-ion batteries, which are ubiquitous in modern consumer products (DeCarlo and Matthews, 2019). A forecast by Statista (2021) predicts that the global demand for Co for use in batteries will amount to 117,000 metric tonnes in 2025. The way Co market adjustments play out in response to increased demand will determine whether production, and subsequently, supply, is able to fulfill demand and address supply risk challenges. Supply risk challenges for Co are a legitimate concern, especially with the previous occurrence of the ‘cobalt crisis’. In 1978, the Co crisis exhibited a similar production situation as the 2000s with the DRC dominating production (Alonso et al., 2007). This supply risk of 1978 occurred with an even distribution of Co consumption for end uses

(Campbell, 2020). A significant risk for supply sustainability exists given the implications of the by-product nature of Co's primary production being dependent on that of copper and nickel (Shedd et al., 2017; Campbell, 2020). In the instance that Co's consumption rate is higher than copper and nickel, supply risk could be a concern (Shedd et al., 2017).

2.5 Cobalt production in the Democratic Republic of Congo

The world's Co mine production has been focused in the DRC since the 1960s (Garside, 2021). The peak production was recorded in 2018 (109,402 metric tonnes) (Brown, 2020). Throughout these 50 years, Co production in the DRC has grown by a compound annual growth rate (CAGR) of 3.9 %. The lowest production was recorded in 1993 at 2 092 metric tonnes.

The total Co production from 1970 to 2020 was recorded to be 1 565 541 metric tonnes (Brown, 2020). This production concentration in the DRC is provided through artisanal and small-scale mining (ASM) and large-scale mining (LSM). Between the two mining types, LSM in the DRC is responsible for majority of Co production in the Central African Copperbelt (CACB) (Crundwell et al.., 2020). As of 2020, Chinese ownership of Co mines is widespread in the country, with the ten top producers outside of Glencore, including companies that are owned by China Molybdenum, Zheijiang Huayou Cobalt, China Nonferrous Mining Group, Jinchuan Group, and Wanbao Mining. Under this ownership, 68 500 metric tonnes of Co were produced as hydroxide being the main product (Crundwell et al., 2020). The Roan Tailings mine owned by Eurasia Resources Group is listed as the top producer of cobalt in the CACB, producing 77 000 metric tonnes of Co, while Glencore-owned Mutanda and Kamoto mines are second and third, respectively (Crundwell et al., 2020). Artisanal and small-scale mining ongoing in the DRC are listed as the 17th top producer in the CACB as of 2020 (Crundwell et al., 2020) contributing 6 500 metric tonnes of Co.

2.6 Constraints in global transition to renewable resources

I have highlighted the importance of climate change mitigation through decarbonised economies; however, I cannot be naïve to the potential constraints in the global transition to renewable resources. Graedel and Beck's (2016)

methodology encompasses geological availability, accessibility and criticality. Criticality becomes relevant in the discourse around climate change, which leads to the restructuring of the mineral resource landscape. The three-dimensional methodology defines metal criticality on the basis of: 1) supply risk (likelihood to supply chain disruption), 2) vulnerability to supply restrictions (severity of consequences on societal needs due to disruption), and 3) environmental impacts (environmental impacts in metal supply chains). Similar methodologies are used throughout the world, for example, in the European Union's (EU) assessment methodology, supply risk and economic importance are used and there is no explicit environmental impact dimension (European Commission, 2020). Therefore, any transition to renewable resources necessitates active planning from the international community considering the dependence on CRMs (Ali et al., 2017) and ETMs.

Outside of the physical factors that present constraints in the global transition to renewable resources, from an economic perspective, the political will to fully and equitably participate in climate change mitigation is not always demonstrated. As renewable energy sources receive six times less in subsidies than fossil fuel on a global scale (Hostettler, 2015), the commercialization of renewable energy production, especially in countries heavily dependent on fossil fuel energy production, remains a challenge. The impediments to commercialization of renewable energy are often technical, financial, and market related (Kochtcheeva, 2016; Kariuki, 2018). Successful deployment of renewable technologies is dependent on the capacity to construct, maintain and monitor energy infrastructure, which requires skilled technical professionals, manufacturing capacity, and policy support at national and global levels (MacLeod and Rosei, 2015; Kochtcheeva, 2016). Deploying renewable energy also faces socio-cultural, ecological and policy barriers (Kochtcheeva, 2016). Renewable energy policy implementation is the underpinning driver for a greener and circular economy and the relationships between economic development, socio-economic structure, and environmental protection of national development plans will determine the choice in policy implementation (Thiam, 2011; Berg, 2013; Kochtcheeva, 2016). The extent to which renewable energy is incorporated into a country's developmental strategy will influence its contribution to the global responsibility of climate change

mitigation. Managing socio-environmental risks that accompany extraction should also be a priority in addressing climate change (Lèbre et al., 2020). A just transition towards a low-carbon future must be cognizant of, and plan for the increased vulnerability of developing countries to environmental consequences of ETM extractions.

2.7 Sustainable extraction of mineral resources and recyclability

High-tech extractive metallurgy and mineral processing are essential for supplying CRMs for our modern society (Ghorbani, 2018; Ghorbani et al., 2021). Given that most high-tech metals and CRMs are extracted as by-products, extraction from secondary sources is essential (Ali et al., 2017; Ghorbani, 2018; Ghorbani et al., 2021). Hence, technological advancements could facilitate improved extraction and processing efficiency. These actions align with a sustainable supply of raw materials for a greener economy. Enhanced circularity of CRMs and precise extraction and processing are approaches towards sustainability (Overland et al., 2019). In the context of Co, enhancing not only extraction/processing efficiency, but promoting increased recyclability follows the United Nations (UN) Sustainable Development Goals (UN, 2020) that are applicable to CRMs. Affordable and clean energy, decent work and economic growth, innovation and infrastructure, sustainable cities and communities, responsible consumption and production, climate action, are all Sustainable Development Goals (SDG: 7, 8, 9, 11, 12, and 13) that are dependent on the sustainable extraction and subsequent implementation of renewable energies through CRMs (Ghorbani, 2018; Ghorbani et al., 2021). As high-tech minerals are indispensable for incorporating clean technologies while promoting a circular economy, urban mines have turned into potential reservoirs for secondary high-tech metal recovery and an avenue for developing pioneering technologies with optimised extraction (Zuo et al., 2019). The development of renewable energy sources using CRMs and high-tech requires a sufficient supply of materials of interest, as this secondary production method will enable recycling to aid in supply sustainability (Ali et al., 2017). Creating maps and mineral inventories that use the recycling potential of metals can enhance production and increase the recyclability of metals (Ali et al., 2017). Such a product-focus approach

requires international standards for recyclability to ensure that recycling efficiency is enhanced as well as a strengthened relationship between public and private sectors in order to maximize on the recycling potential and create credible maps and inventories (Ali et al., 2017).

2.8 Environmental, social and governance (ESG) risks in mineral extraction industries

As consumer demand continues to rise amidst population growth, with increasing levels of human development, and decarbonization, the ESG risks are also increasingly becoming a concern in mineral extractive industries that take a progressive stance on developmental changes in society (Lèbre et al., 2019). ESG indicators are a combination of Graedel and Beck's (2016) methodology on criticality that overlaps waste, water, biodiversity (environment); land use, indigenous peoples and social vulnerability (social) with political fragility and approval and permitting (governance) indicators. Since the generation of renewable energy technologies and the creation of energy storage systems require higher metal content than its fossil fuel counterparts (UNEP, 2013; Lèbre et al., 2019), ESG indicators are crucial for safeguarding against mining-related socio-environmental risks. ESG factors are becoming more acknowledged in investor communities following the financial consequences related to ESG failures (Lèbre et al., 2019). However, it is important to reiterate that financial motives should not be the only motivating principle in changing the dynamics within the mineral extractives industry. Managing the drawbacks that coincide with ETM socio-environmental risks sit at the core of a transition to a low-carbon society that respects human rights and safeguards the environment (Lèbre et al., 2019, 2020). Findings by Lèbre et al. (2020) show that Co is an energy transition metal, in which 70 % of its resources are in high-risk contexts thus reflecting six or more ESG risks (Fig. 2.2). Furthermore, 90 % of Co resources are within high social and governance risks (Lèbre et al., 2020). ESG indicators are critical to mine projects and the production of commodities. These indicators should be included in future scenario planning in the move towards a low carbon future (Lèbre et al., 2020).

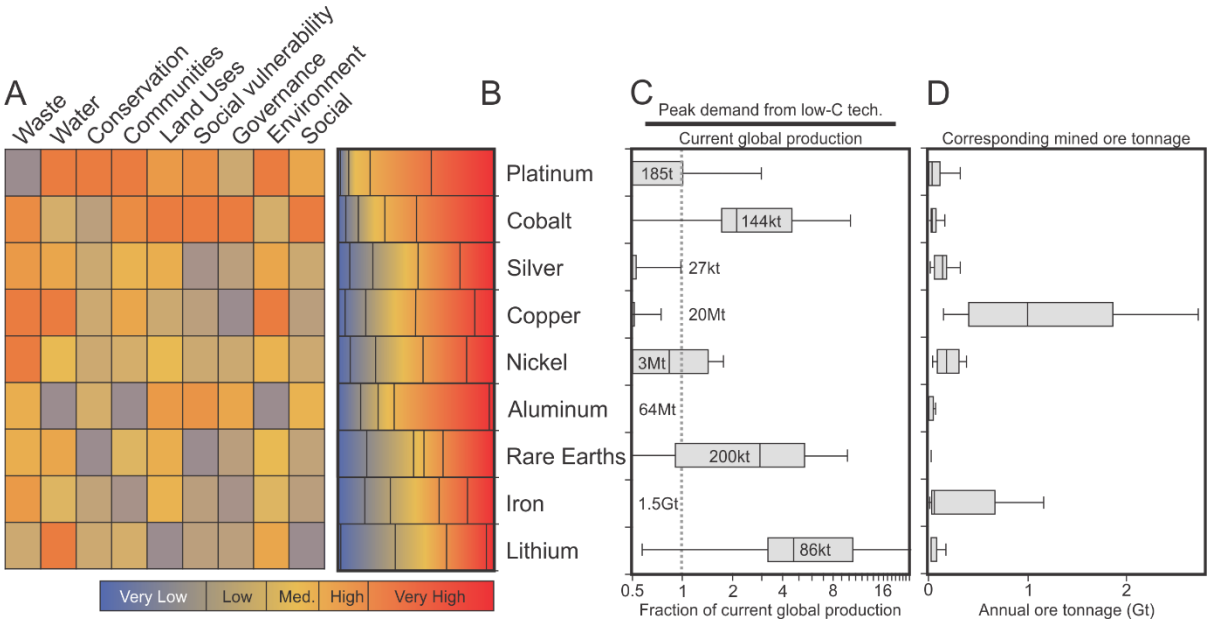


Figure 2.2 Risk profiles and demand projections for nine ETMs. A: Environmental, social and governance indicators ranked from very low to very high. B: Total risk scores based on resource tonnage. C: Prediced peak demand expected from low-carbon technologies as a part of current global production (dashed line). D: Estimated annual mined ore from predicted demand (modified from Lèbre et al., 2020).

As Co is almost entirely used in high energy technologies, high ESG scores translate into heightened mitigation complexities with managing future impact scenarios (Lèbre et al., 2019; Valenta et al., 2019). To address these complexities, major innovations are required in the development of resource projects that will ensure that the responsibility for solutions extends beyond governments and individual companies (Lèbre et al., 2019). This highlights the importance for future planning scenarios. The co-evolution and development of energy technologies enables the examination of the implications in a technologically-changing paradigm (Rockefeller Foundation, 2010). A Scenario Framework that examines technological, adaptability, economical and political aspects of modern societies (Rockefeller Foundation, 2010) identifies two critical uncertainties – political and economic alignment, and adaptive capacity – that predetermine contextual environment of scenarios including economic, environmental, technological, and socio-political trends. These two critical uncertainties define the relationship between technology and international development according to four scenarios

(Lock Step, Clever Together, Hack Attack, Smart Scramble) that are divergent, plausible, and challenging (Rockefeller Foundation, 2010). Global political and economic alignment addresses the intersections of capital, goods, people and ideas and the effectiveness of political structures in dealing with prospective global challenges (Rockefeller Foundation, 2010). Considering the political influences of ETM extraction and the global market, understanding how to foster improved global institutions, and international problem-solving networks (Rockefeller Foundation, 2010) is key to development within a precarious low-carbon economy. In addition, adaptive capacity is relevant in the discourse around using ETMs for a decarbonised economy and overall climate change mitigation, as it is concerned with assessing how different societies effectively adapt to change (Rockefeller Foundation, 2010). In whichever way the future pans out, the intersection of governance, policy, and energy technology is critical for facilitating development.

Chapter 3

3. Methods and Results

3.1 Tescan Integrated Mineral Analyser

Six ore block samples out of the 19 samples were selected for the Tescan Integrated Mineral Analyser (TIMA). The TIMA was used for qualitative mineralogical analysis in which phase maps, backscatter electron (BSE) images, and elemental maps were produced. The phase and elemental maps were generated via energy-dispersive x-ray spectroscopy (EDS) using the VEGA3 X64 instrument and TESCAN TIMA 1.70 software. The instrumentation is held in the School of Geosciences WAMLAB at the University of the Witwatersrand, Johannesburg. The beam conditions on the VEGA3 X64 TESCAN SEM for quantitative analysis were set at beam intensity of 17.68 nA, 25kV accelerating voltage, <1 pA adsorption current, and 43 pA emission current at a speed of 3 µs/pxl. Heating was 47 % with a gun pressure of 1.6×10^{-5} and 5.5×10^{-3} Pa column pressure. The scanning mode was set at resolution mode with a filament live time of 431 hours. The working distance was 15 mm with a spot size of 590.00 nm and a 597.2 µm field of view and produced high-resolution maps. The depth of focus was 241.000 µm. The TIMA method is selected as a verification method for the qualitative assessment which, through petrography, provides data on mineralogical association.

3.2 Mineral resource production forecast

Ongoing finite-resource consumption necessitates resource forecasting to determine the course of its future supply. Forecasting allows for strategic planning, such as scenario planning and therefore management of remaining resources (Nanzad et al., 2017). Forecasting Co production is vital for developing alternative and renewable energy policies that attempts to derive more sustainable development and minimise climate change. It is possible to examine the future supply and demand of Co semi-quantitatively through forecasting. The autoregressive integrated moving average (ARIMA) and the parametric Hubbert model are two methods for time series forecasts on a short-term and long-term basis. Although long-term forecasting of complex system behaviour is impossible, short-

term forecasts leveraging the statistical structure of the timeseries signal (e.g., through ARIMA) is possible and long-term, qualitative forecasts of the overall trend is possible through the Hubbert model, which makes specific assumptions such as the existence of a single production peak of a resource. The most up-to-date historical production data of 14 Co-producing countries from Brown et al., (2020) was used. In a few cases where production data for certain countries was unavailable for certain years, a linear, nearest-neighbour interpolation-based imputation was used.

3.2.1 Autoregressive Integrated Moving Average model

The ARIMA method provides seasonal patterns and a stable estimation of time-varying trends. The model has been used as a tool for mineral production forecasts on a short-term period through inspecting differences between reported production values instead of actual values (Jadhav et al., 2017). The ARIMA method can forecast a single commodity under production provided that that time series signal contains self-identical patterns in time, which then continue into the future (Mgaya, 2019; Fattah et al., 2018).

One approach to building an ARIMA model is the Box-Jenkins time series approach. The ARIMA model contains parameters *p*, *d*, and *q*, wherein *p* denotes the number of autoregressive terms; *d*, the number of differences; and *q*, the number of moving averages (Fattah et al., 2018). The model comprises three processes as expressed by Fattah et al. (2018) and Mgaya (2019):

a) The autoregressive (AR) process, which uses a 1st-order autoregressive model work under the assumption that the dependent variable, y_t, given by the equation:

$$y_t = \alpha_1 y_{t-1} + \varepsilon_t \quad (1)$$

is a linear function of the previous values. The parameter, α, represents a self-regression coefficient, y_{t-1} is a linear combination of previous observations i.e., lagged dependent variable, and ε, representing an unexplainable random shock.

b) An integrated (I) process, which represents the cumulative effect of selected processes/activities that may affect the time series behaviour. Short-term fluctuations have less of an effect on a long-term basis (Fattah et al., 2018). From a statistical perspective, a central characteristic is the stationarity of a series of differences. Since integrated processes are the prototype of nonstationary series, a differentiation of equation (1) assumes that there is a constant difference between two successive values of y_1, which is expressed as:

$$y_t = y_{t-1} + \varepsilon_1, \quad (2)$$

where the random perturbation, ε_1, is a white noise and y_{t-1} represents a lagged original series.

c) A moving average (MA) process that includes past and present forecast errors (previous observations of white noise processes) within the future observation forecasts, is defined by the equation:

$$y_t = \varepsilon_t - \theta_1 \varepsilon_{t-1}, \quad (3)$$

In which ε_t and ε_{t-1} are the forecast and the lagged forecast errors, respectively. Equation (3) expresses the number of previous perturbations embedded in the current value. The combination of the three 1st-order equations builds a time series model of the original signal, which can be used to predict future national Co production.

The Box-Jenkins time series approach for developing an ARIMA model is built through three stages, which include model identification, parameter estimation, and diagnostic checking steps (Fattah et al., 2018). This principle, founded on the input of Yule (1926) and Wold (1938), was adopted to develop a pragmatic approach in building ARIMA models. The main task in identifying a suitable ARIMA model is to make use of the data's autocorrelation properties, which can be assessed by the autocorrelation function (ACF) and the partial autocorrelation function (PACF) (Fattah et al., 2018). ACF is also used to assess the stationarity of the data, which measures the change in its unconditional joint probability distribution under time translation. This is a requirement for ARIMA modelling. Data that is non-stationary may generate false relationships (Mgaya, 2019). The ACF is applied to assess

stationarity, and a positive ACF signifies a very slow linear decay pattern, meaning that data are nonstationary (Nau, 2014; Mgaya, 2019). Non-stationarity is corrected by data differencing if caused by the mean or by model transformation if caused by variance (Nau, 2014, Mgaya, 2019). Following this procedure, the initial values for orders of seasonality (number of autoregressive terms, *p*) and non-seasonality (number of moving averages, *q*) are determined through the PACF analysis. These procedures are automated to identify the ARIMA model. Once the model is selected, its parameters can be determined through the method of least squares (Mgaya, 2019). In practice, the model identification and parameter estimation can be automated through a grid-search over (p, d, q) coupled with cross-validation by minimising an objective function that gauges the model's fit with the data.

3.2.2 Hubbert model

Hubbert's forecasting study of oil production in 1956 introduced a logistic curve that modelled production peak using historic data (Wang et al., 2017; Tilton, 2018). It predicted successfully that oil production would reach its peak in the early 1970s (Nanzad et al., 2017). The Hubbert model has since then been incorporated into the mineral resource industry for production forecasts of exhaustible non-fuel minerals (Calvo et al., 2017). These forecasts, influenced by the hypothesis of geological constraint, are expressed through a bell-shaped symmetrical curve showing annual production reaching a peak when half of the reserves have been produced (Giraud, 2012; Berk and Ediger, 2018). The Hubbert model in its simplest form is a parametric model that assumes a single peak-production behaviour for a resource and is suitable for 1st-order, qualitative projections (Saraiva et al., 2014; Berk and Ediger, 2016; Wang et al., 2017). The Hubbert model makes three basic assumptions: (1) a pure logistic curve represents cumulative discovery; (2) a constant mineral exploration effort over time; and (3) a constant time lag between discovery and production – hence the discovery rate is derived from a pure logistic curve of cumulative discoveries over (Giraud, 2012; Berk and Ediger, 2016). The Hubbert model needs to be applied with caution in the case of immature regions, where production has not passed peak production (Nanzad et al., 2017).

Mathematically, the Hubbert model is an example of a symmetric single-peak parametric function, whose family includes the Gaussian and Laplace functions. In comparison to many single-peak models, the Hubbert model exhibits a gentler rise and fall in the pre- and post-peak regions that are suited for resource supply forecasting. The Hubbert model features a production rate that is zero at zero time and when the resource is exhausted or becomes undesirable for further extraction (Calvo et al., 2017; Berk and Ediger, 2016). Since the model is parametric, it pre-supposes the behaviour of the data and therefore does not consider significant temporal changes of economic, technological, and political factors in mineral exploration, discovery, and production (Wang and Feng, 2016). Hubbert's curve is defined by three parameters: 1) the amount of ultimately recoverable reserves (URR), 2) date of production peak, and 3) a shape parameter.

The Hubbert curve represents cumulative production from an ultimately recoverable reserve over time which follows a logistic growth curve (Wang et al., 2017):

$$Q = \frac{N_R}{1+e^{-(a(t-t_m))}}, \tag{4}$$

$$P = \frac{a \cdot N_R \cdot e^{a(t-t_m)}}{1+e^{(a(t-t_m))^2}}, \tag{5}$$

$$e^{-(a(t-t_m))} = \frac{(N_R-Q)}{a}. \tag{6}$$

It is possible to solve for P and P/Q:

$$P = aQ - \frac{aQ^2}{N_R} = aQ(1 - \frac{Q}{N_R}), \tag{7}$$

$$\frac{P}{Q} = a\left(1 - \frac{Q}{N_R}\right) = \left(a - \frac{aQ}{N_R}\right) = a - mQ. \tag{8}$$

Here "***P***" denotes production; "***Q***" refers to cumulative production; "$\mathbf{N_R}$" to recoverable reserves; "$\mathbf{t_m}$" to the time of peak production; and "**m**" = $\boldsymbol{a}/\mathbf{N_R}$, which represents the production decay rate. The intrinsic growth rate, a, is the prediction parameter in the Hubbert model. Based on equation (5), "**P**" increases with an increase in "$\boldsymbol{a}$", given that other variables remain constant. The time of the peak and width of the Hubbert curve is determined by $\boldsymbol{a}$; the smaller the value, the wider

and shorter the curve is and the later the peak is reached and vice versa (Wang et al., 2017).

Chapter 4

4. Results

4.1 Qualitative mineralogy

Nineteen polished ore samples from the School of Geosciences mineral collection (University of the Witwatersrand) were collected for the study and a petrographical study was conducted. These samples were originally sourced from Kinservere, DRC. The DRC represents the Congolese Copperbelt portion of the Central African Copperbelt, which, is the world's biggest sediment-hosted stratiform Cu-Co province (Sillitoe et al. 2017; Twite et al., 2019). Samples from this region were selected to establish the ore composition of the ore to provide geological basis to the study, particularly as the DRC is one of the main focuses of the research.

Sulphide Cu-Co ores from Kinservere are mainly hosted in quartzose and dolomitic rock of a coarse-grained texture. Petrographic examination conducted through reflected microscopy revealed that the study samples are characterised by the presence of chalcopyrite as the main ore mineral. Its morphology is often anhedral and displays a medium-density fracture texture (Fig. 4.1B) when it is replaced by a carbonaceous mineral – often being ankerite (Fig. 4.1D). It also occurs in association with carrollite and both minerals usually show pitted textures (Fig 4.1B). It is common for chalcopyrite to alter to bornite and covellite (Fig 4.1C). Carrollite is the chief Co-bearing mineral in the sample set and its mineralisation shows a disseminated texture when it occurs cogenetically with chalcopyrite and quartz. The dominant texture observed was a massive sulphide texture, with a net-texture observed in a few instances. It is characteristic of carrollite to mineralise as a massive sulphide with high-fracture density (Fig. 4.1E), however, in some instances it occurs as perpendicular veins to bedding. Minimal pyritic mineralisation was observed but it tends to form rims around quartz and chalcopyrite (Fig 4.1A). Bornite was observed to either occur in relation to chalcopyrite and covellite as inclusions within the quarzitic or dolomitic matrix or as concentric bands adjacent to pyrite. It is often distinguished by its "basket-

weave" texture (Fig 4.1F). Numerous samples showed evidence of an iron oxide indicated by the platy blue-grey mineral (most likely haematite) which infills the chalcopyrite fractures. Small inclusions of covellite are common within Cu-Co ores and are spatially distributed within the quartz matrix and occur angular grains.

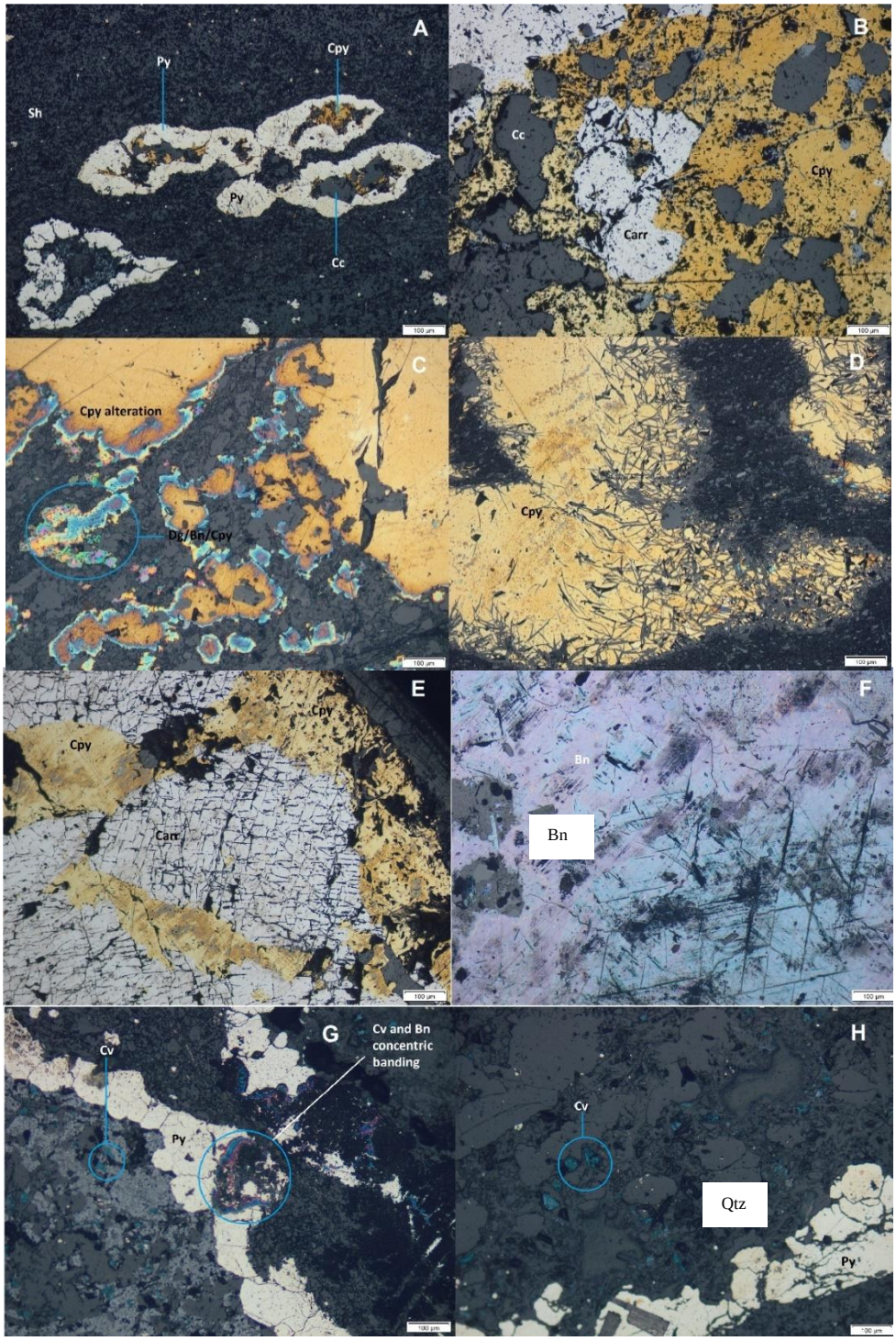
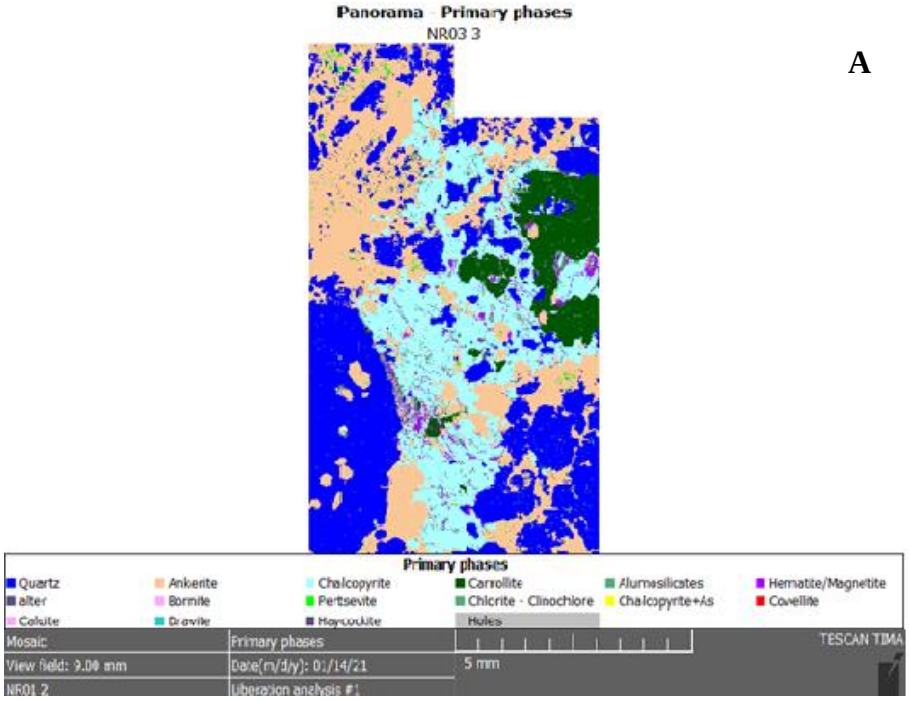


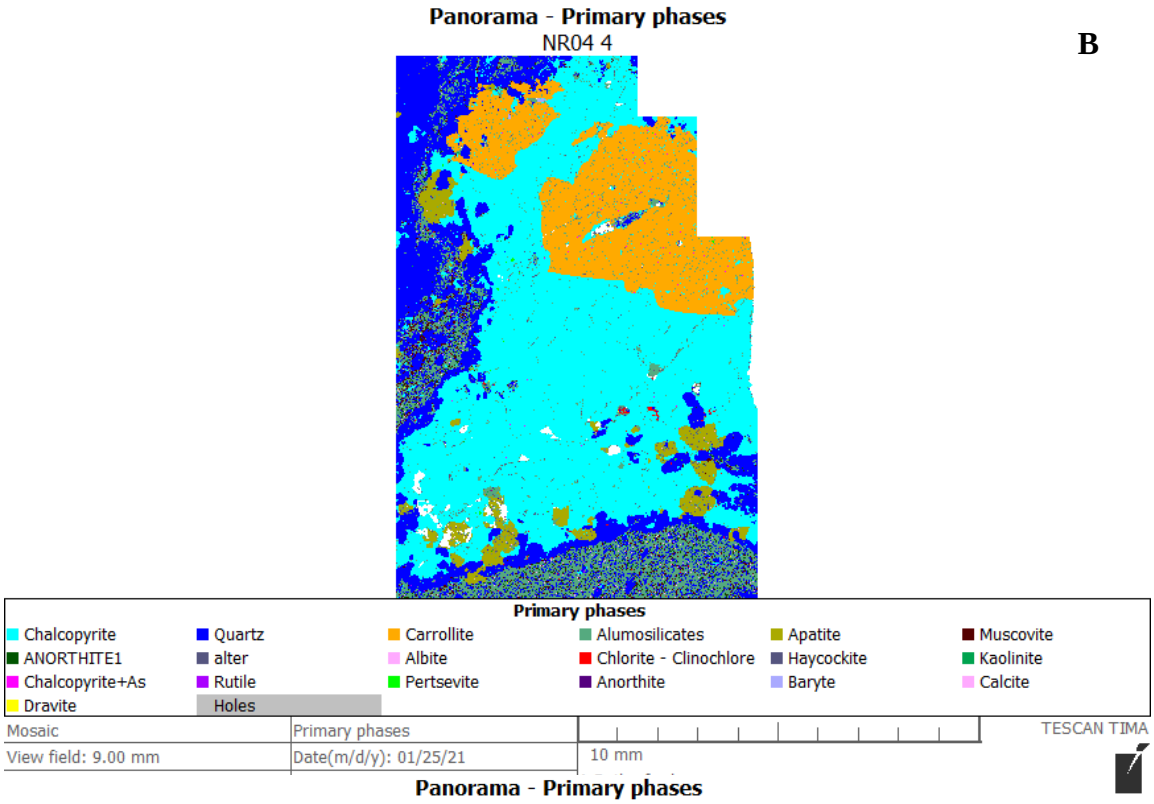
Figure 4.1 Photomicrographs of samples showing mineralisation features of the samples. A: pyrite rims around chalcopyrite and quartz. B: chalcopyrite-carrollite disseminated texture. C: chalcopyrite alteration. D: chalcopyrite replacement texture. E: intensely fractured carrollite. F: bornite with basket-weave texture. G: covellite and bornite concentric banding. H: covellite inclusion in quartz matrix. Cpy = chalcopyrite, Carr = carrollite, Py = pyrite, Cc = chalcocite, Bn = bornite, Qtz = quartz, Cv = covellite. Scale represents 100 µm.

4.2 Process Mineralogy

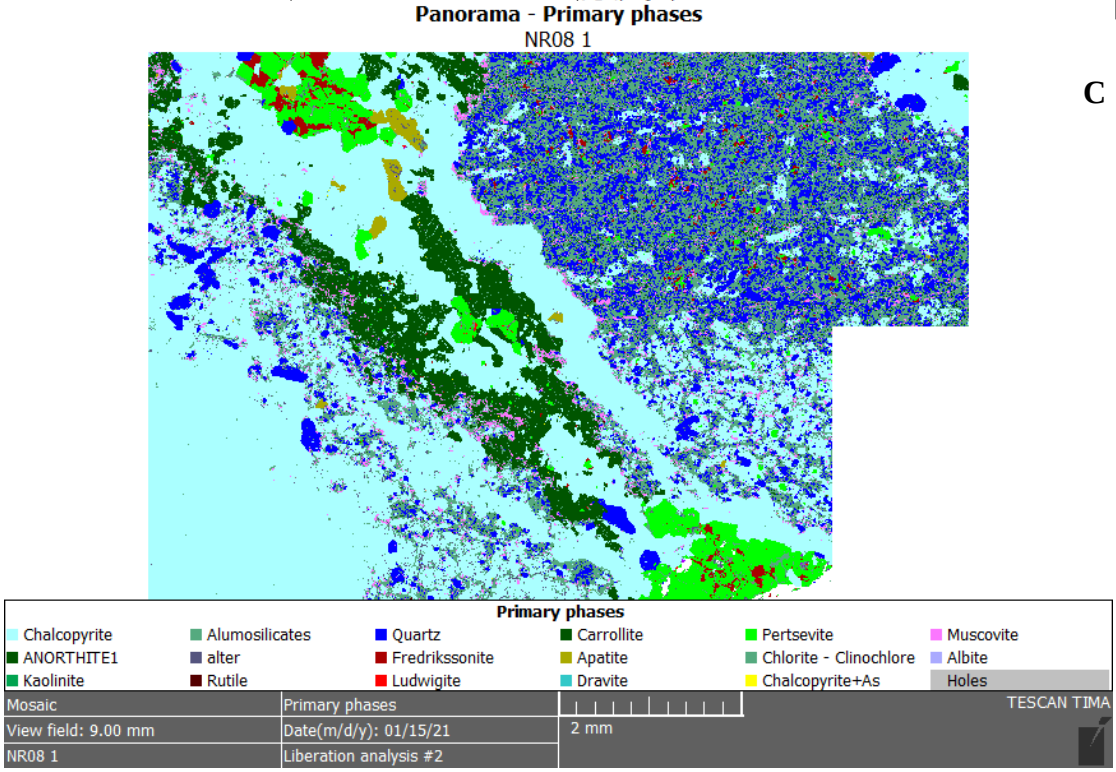
The TIMA, alongside petrography, allows for an understanding of the geological characteristics of known mineral reserves. Together with data from literature, this can then be use as a foundation for production trends. The TIMA, hence, detected the main primary phases to be chalcopyrite, ankerite, and quartz which agrees with what was revealed by the reflected microscopy. The distribution of these three minerals produces a disseminated texture which is observed to be the main sulphide texture. Overall, chalcopyrite is the most dominant mineral while ankerite and quartz distributed in almost equal proportions. The chief Co-bearing mineral is carrollite. Other ore minerals include pyrite, bornite, pyrrhotite and chalcocite. The primary phase maps show mineralisation of pyrite, pyrrhotite, chalcopyrite, bornite, covellite, and chalcocite which occurs amongst an array of gangue minerals. Common gangue minerals include apatite, fredrikssonite, ludwigite ($MgFe^{3+}BO_5$), pertsevite ($Mg_2(BO_3)(OH)$)and (unspecified) aluminosilicates.



B


Panorama - Primary phases
NR04 4
Primary phases
Chalcopyrite
Quartz
Carrollite
Alumosilicates
Apatite
Muscovite
ANORTHITE1
alter
Albite
Chlorite - Clinochlore
Haycockite
Kaolinite
Chalcopyrite+As
Rutile
Pertsevite
Anorthite
Baryte
Calcite
Dravite
Holes
Mosaic
Primary phases
View field: 9.00 mm
Date(m/d/y): 01/25/21
10 mm
TESCAN TIMA

C


Panorama - Primary phases
NR08 1
Primary phases
Chalcopyrite
Alumosilicates
Quartz
Carrollite
Pertsevite
Muscovite
ANORTHITE1
alter
Fredrikssonite
Apatite
Chlorite - Clinochlore
Albite
Kaolinite
Rutile
Ludwigite
Dravite
Chalcopyrite+As
Holes
Mosaic
Primary phases
View field: 9.00 mm
Date(m/d/y): 01/15/21
NR08 1
Liberation analysis #2
2 mm
TESCAN TIMA

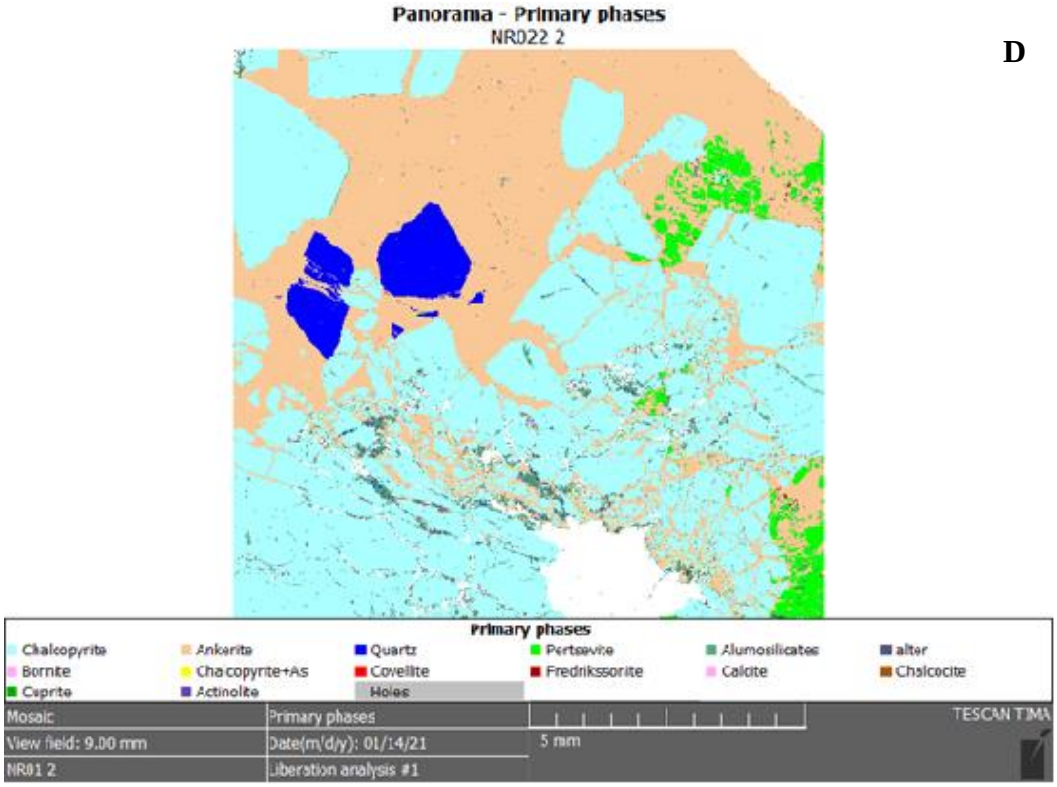


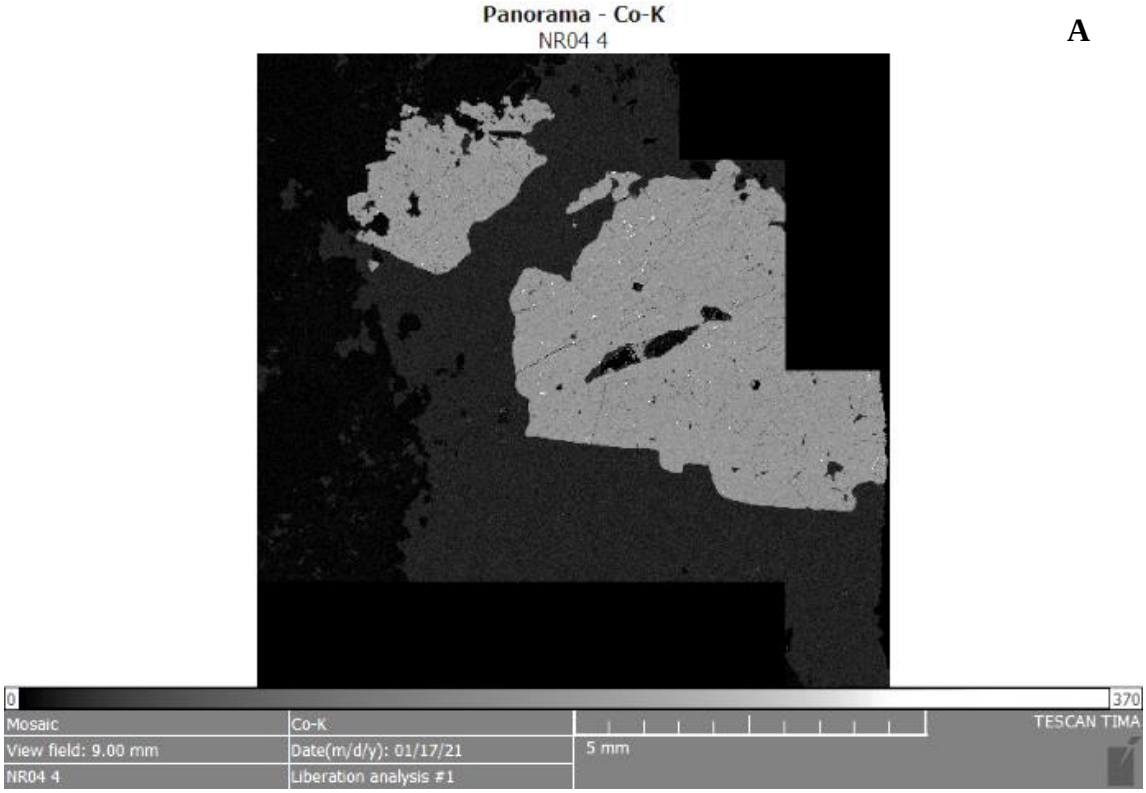
Figure 4.2 Primary phase maps showing the common minerals and disseminated sample texture as detected by the TIMA. Descriptions for each sample is provided in Appendix A1 of the research report.

4.2.2 Elemental composition

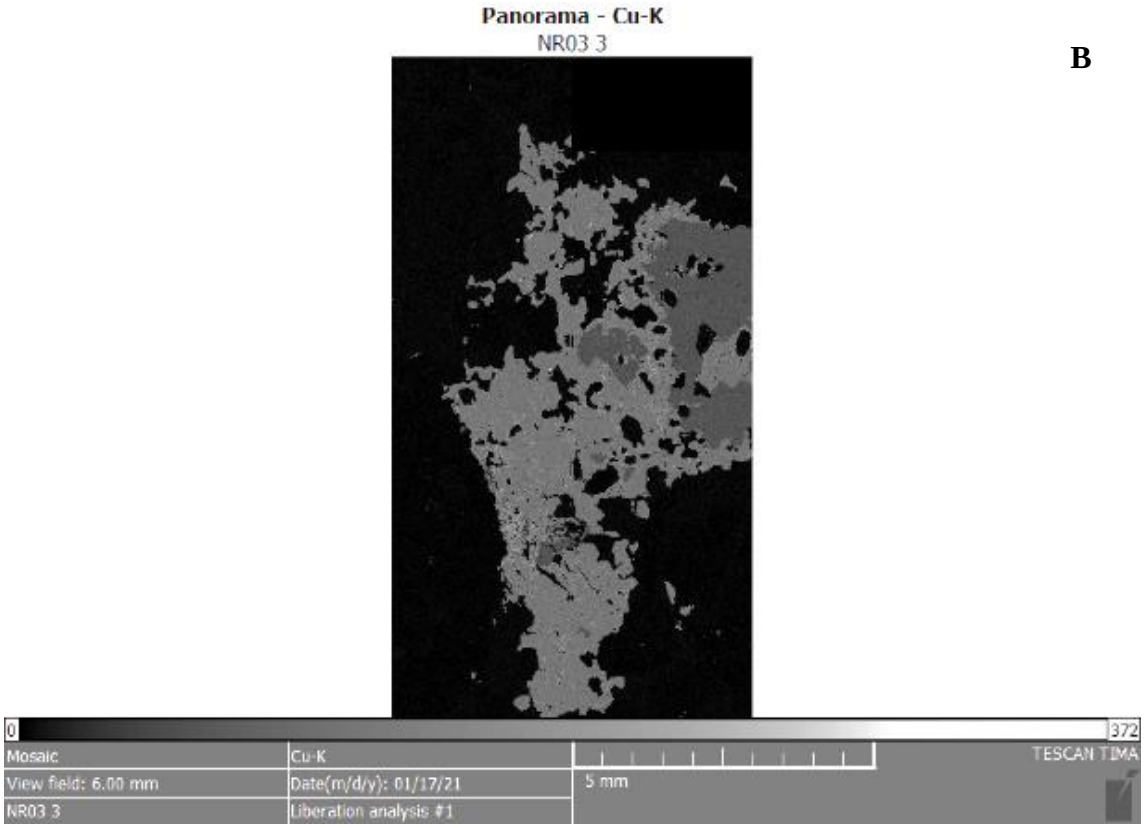
Table 4.1. Enrichment of elements in specific minerals.

Sample	Arsenic	Cobalt	Copper	Iron	Magnesium	Nickel	Antimony	Sulphur	Aluminium	Phosphorous
NR01	**X**	**X**		**X**	**X**					
NR03		**X**		**X**		**X**	**X**	**X**		
NR04		**X**	**X**			**X**		**X**		**X**
NR06		**X**	**X**					**X**		
NR08	**X**	**X**	**X**			**X**	**X**	**X**	**X**	
NR022						**X**	**X**	**X**		
NR064						**X**			**X**	

A


Panorama - Co-K
NR04 4
0
370
Mosaic
Co-K
TESCAN TIMA
View field: 9.00 mm
Date(m/d/y): 01/17/21
5 mm
NR04 4
Liberation analysis #1

B


Panorama - Cu-K
NR03 3
0
372
Mosaic
Cu-K
TESCAN TIMA
View field: 6.00 mm
Date(m/d/y): 01/17/21
5 mm
NR03 3
Liberation analysis #1

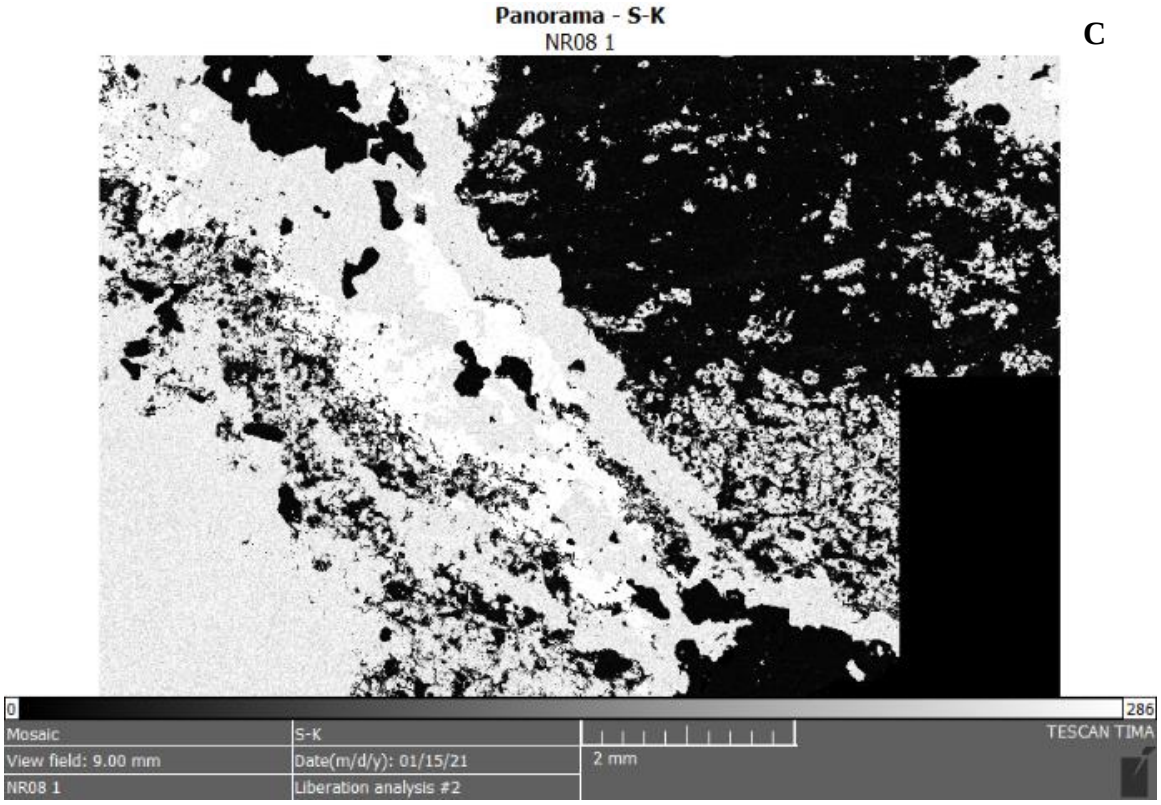


Figure 4.3 Elemental maps showing the distribution of the four most enriched elements (cobalt, sulphur, copper, and nickel) in the samples. Full set of elemental

maps and element distribution descriptions provided in Appendix B1 of this research report.

4.3 World cobalt production trends

The production capacity of Co is affected by the availability of reserves, technologies available for the discovery, exploration, mining, and processing of ore, the demand market, as well as numerous other socio-economic and/or environmental factors (Rosyid and Adachi, 2016). The world Co production, presented in Fig. 4.4 demonstrates the differential contribution of 14 countries to the world's supply of cobalt. The influence of reserves, governmental regulations on production, macroeconomics, amongst other reasons are responsible for the variances observed (Tisserant and Pauliuk, 2016). For the purpose of analysis and subsequent implications, production comparison is divided into production from southern and Global North countries[5]. Fig. 4.4 shows that 10 Global South countries are responsible for a vast majority (80 %; 1,738,630 of 2,106,166 metric tonnes) of world Co production. The three Global North countries produced the remaining 365,936 metric tonnes (Fig. 4.4). Throughout this period, the world compounded growth rate of production has increased at an average of 6.86 % per annum. Of the 14 countries, Botswana, Brazil, Canada, and Zambia have experienced a negative compounded growth rate (-1.75 %, -26.4 %, -2.84 % and -5.33 %, respectively). China displays a significantly higher positive compounded growth rate in comparison to the other producers at 21.28 %. China is a point of interest considering its high compounded growth rate and production peak in 2015, while production declines were observed in 2000, 2003, 2006, 2009, 2016, 2019 and 2020 (Fig. 4.4). The DRC, although being the largest producer of Co, has experienced the second largest compounded growth rate of 15.05 %. Production in the DRC has increased sharply but underwent its highest production decline in 2016, dropping by 14,707 metric tonnes compared to the previous year of production.

Key producers during the last two decades are countries from both the Global North and Global South. The DRC, Canada, China, Australia, and New Caledonia rank as

[5] Global South versus Global North is synchronous with the economic maturity of countries of so-called Developing versus Developed countries in which Global South countries are characterised by dependency on export revenues accrued from raw materials.

the top 5 key Co producers, producing ~79 % of the world total Co production (1,666,412 out of 2,106,166 metric tonnes) from 1998-2020. The majority of this production is by the DRC as it has produced 58 % (1,222,373 metric tonnes) of Co during the 22-year analysis period. Canada, China, Australia, and New Caledonia follow with a 6.09 %, 5.24 %, 4.8 %, and 4.7 % contribution, respectively. Crucial uncertainties arise where certain countries experience an explosion or implosion in production over a short period, which has implications for the validity of production forecasting. Countries like South Africa, Zimbabwe, Finland Brazil and Botswana that show these drastic production peaks and dips can be expected to express issues with objective accuracy of forecasts, especially in the future.

The mineral behavioural theory (Humphreys, 1982) categorises commodity development into four phases based on compounded annual growth rate namely, the youth, mature, gerontic, and declining phases. China, DRC, Finland, Morocco, South Africa, and Zimbabwe are in a youth phase of mineral development. This phase features a minimum compounded annual growth rate of 6 % per annum, indicating that commodity production is roughly limited and heavily driven by rapidly increasing consumption. A mature phase exhibits a compounded annual growth rate between 2 % and 5 % per annum, signifying that the commodity is more integrated into pre-existing economic processes. Australia, and Russia fall into this phase. The negative compounded annual growth rate of Botswana, Brazil, Canada, and Zambia are representative of the declining phase that follows the gerontic phase (experience fluctuations in growth rate). The declining phase is an erratic phase of production decline with a possible supply shortage. The production forecast suggests that the peak of world production occurred in 2015, which is the same year Co was classified as a high-risk market as per Herfindahl-Hirschmann Index[6]. This implies that a supply risk can be anticipated to intensify given the market concentration (in the DRC).

[6] The Herfindahl-Hirschman Index characterizes market concentration as either low-risk or high-risk based on susceptibility to supply chain disruptions.

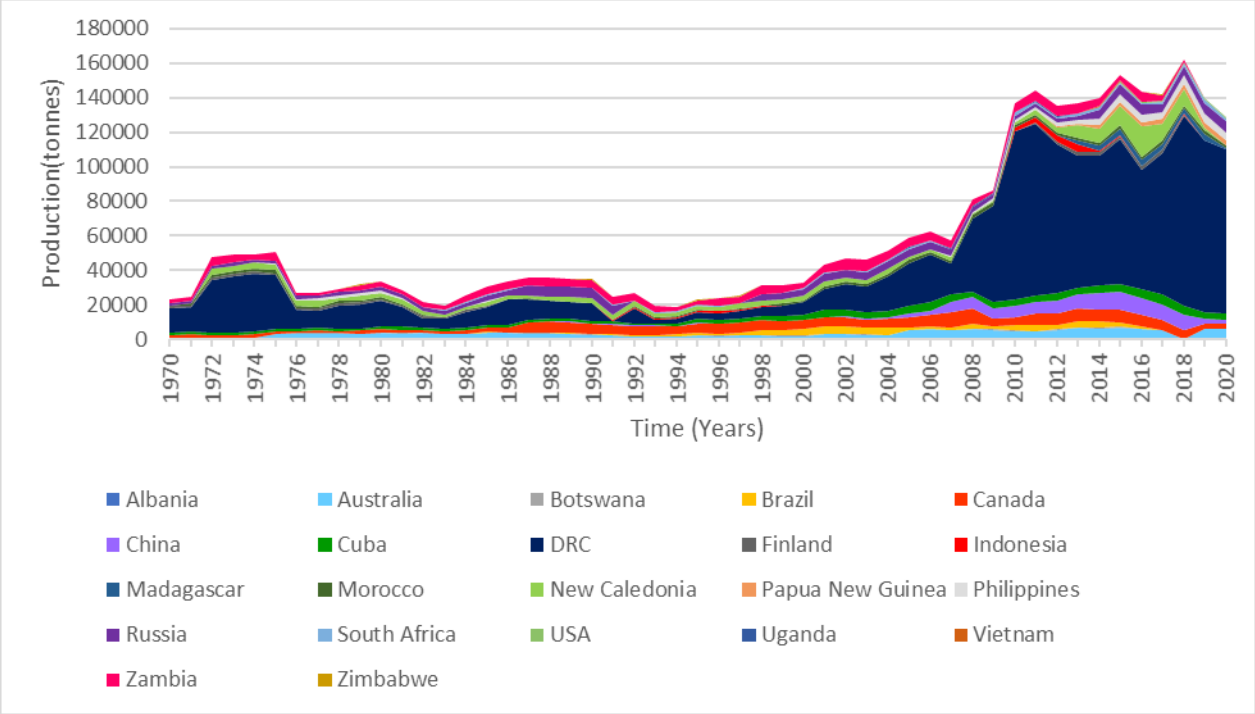


Figure 4.4 World Co production from 1970 to 2020. A full dataset for world production by country is provided in Appendix C1 to this research report (Brown et al., 2020)

4.4 Forecasting cobalt production

4.4.1 ARIMA model forecasting results

The production behaviour of Co based on an annual index from the 22-year analysis period, shows that the lowest production in the DRC occurred in 1998 and the highest production occurred in 2018 (Fig. 4.5E). Using the DRC as a time reference, its lowest production coincided with lowest productions in China and Morocco (Fig. 4.5C, F). Botswana, Brazil, Cuba, New Caledonia, South Africa, Zambia, Zimbabwe(Fig. 4.5A, B, D, G, H, I, J), Australia, Canada, and Russia, (Fig. 4.4A, B, D) experienced their lowest productions after the DRC. Except for South Africa (Fig. 4.4H) and Russia (Fig. 4.6D), all the other countries recorded their highest productions before 2018.

The production trend is decreasing for Australia (Fig. 4.6A), while China, Cuba, DRC, Morocco, New Caledonia, South Africa, Zimbabwe (Fig. 4.6C, D, E, F, G,

H, J), Canada, and Russia (Fig. 4.6B, D) showed an increasing trend. Botswana, Brazil (Fig. 4.5A, B), and Finland (Fig. 4.6C) are predicted to maintain a relatively constant production rate. Interestingly, Zambia (Fig. 4.5I) increases exponentially into a constant rate in 2028. A 95 % confidence interval is shown for each forecast and the greater the forecast into the future, the bigger the interval. Forecasts into negative production can be ignored because ARIMA modelling does not make any physical assumptions of the nature of the time series, but only its statistical characteristics. The shape of the confidence interval depends on the linearity of the forecasted region. For non-linear forecasts, such as that of Australia, the uncertainty in the forecast generally grows with time, whereas for linear forecasts, which the majority of the countries depict, the uncertainty range is constant. World production forecast shows that the supply of Co would likely continue to increase linearly in the short term and is dominated by the behaviour of the DRC's production frequency (Fig. 4.6E).

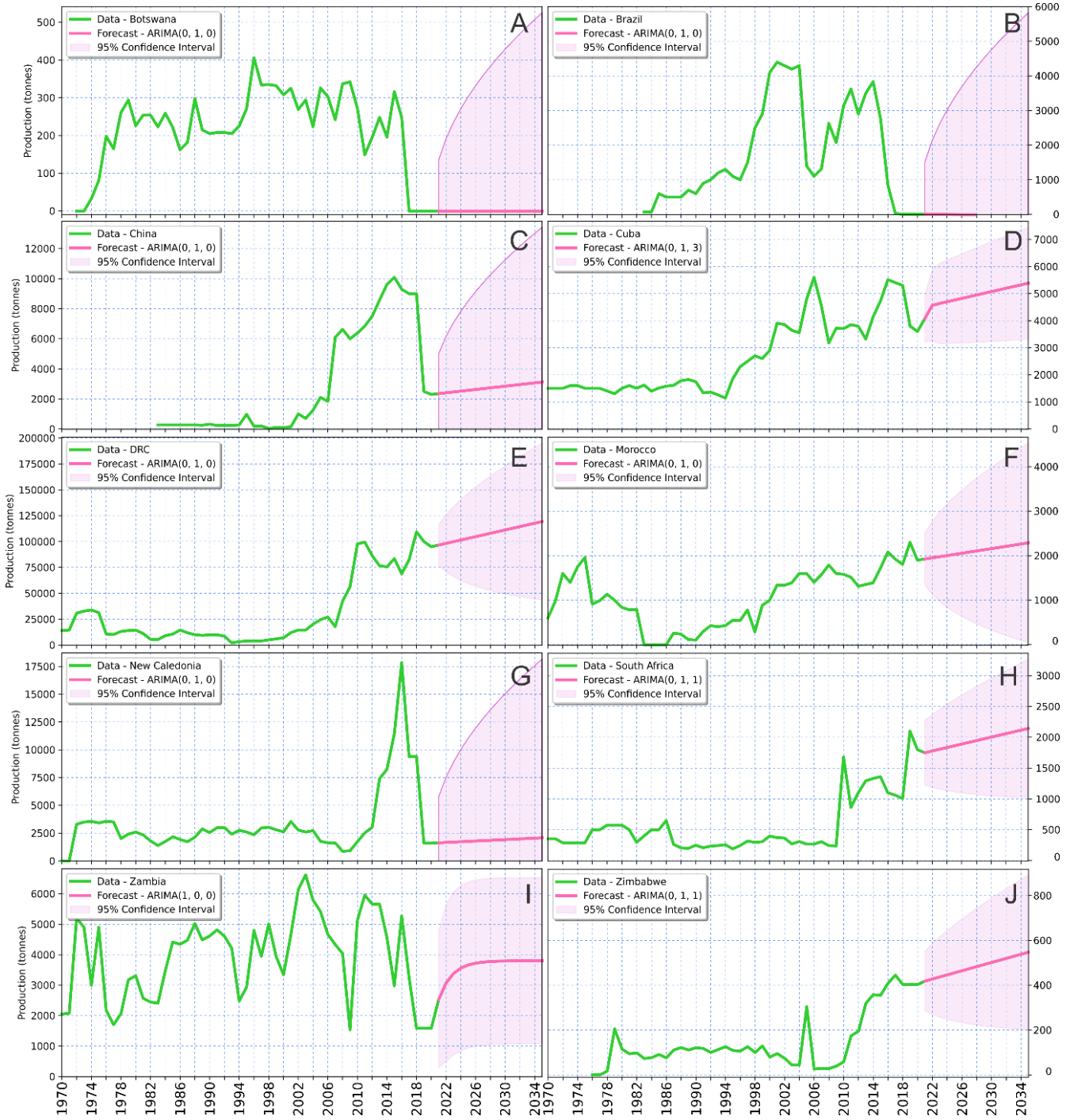


Figure. 4.5 ARIMA forecasts for Global South countries. Green lines represent production data. Pink lines correspond to the forecasted values and their respective 95 % confidence interval (pale pink). X-axis indicates time in years.

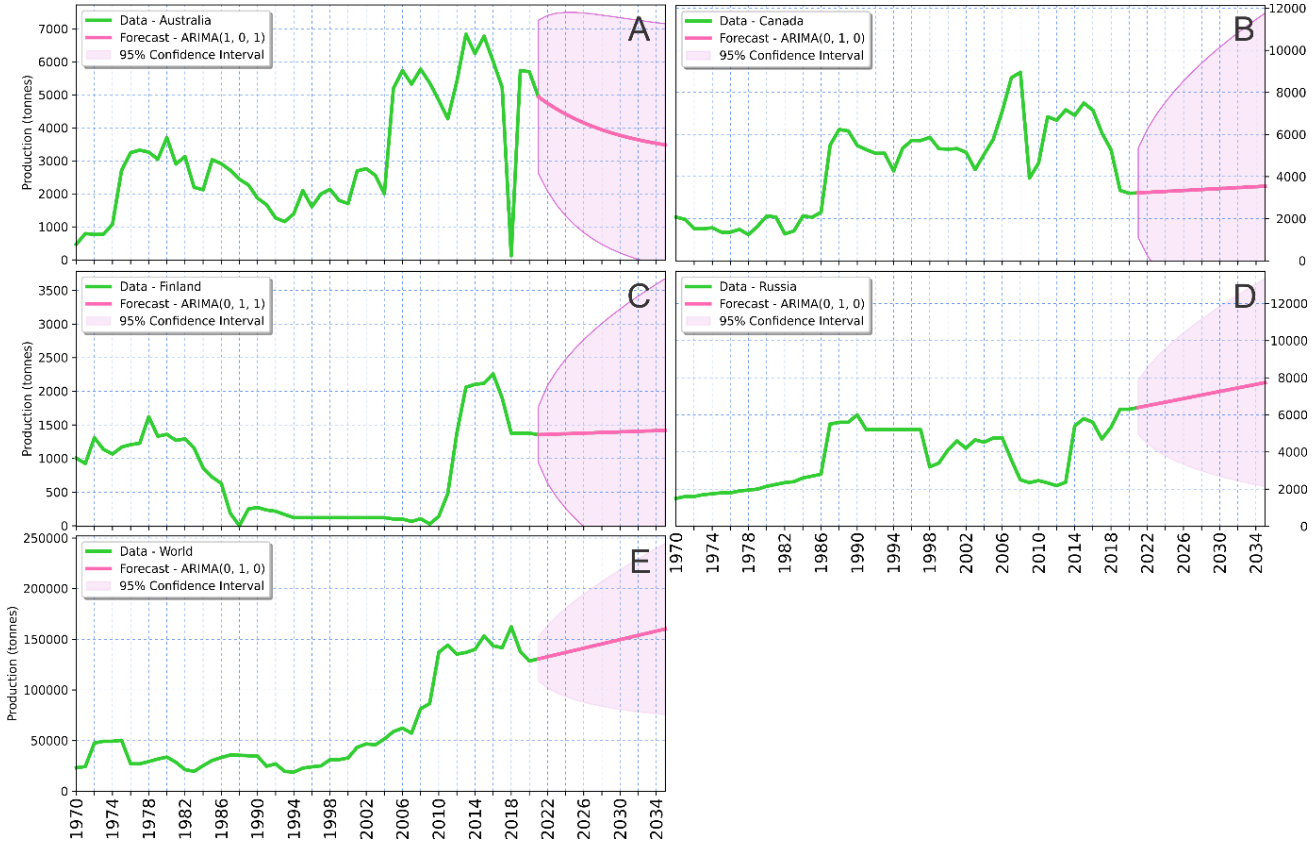


Figure. 4.6 ARIMA forecasts for Global North countries and the world. Green lines represent production data. Pink lines correspond to the forecasted values and their respective 95 % confidence interval (pale pink). X-axis indicates time in years.

4.4.2. Hubbert model forecasting results

The Hubbert model-based forecasts for the DRC and the world (Fig. 4.7) are displayed as conventional single-peak symmetric bell curves, which are best fits for the Hubbert models and our dataset of production. This comparison reveals data points are distributed in increasing and declining trends above and below the Hubbert curve. Both the apices of the DRC and the world logistic curves are placed where the cumulative production is 50 % of the total reserves. These apices do not coincide with the respective 2017 and 2015 peak production as the reported peaks exceed that of the prediction. However, as the Hubbert model is very sensitive to the location of the peak, and the amount of data in the peak region is sparse, the evidence of a peak is weak and therefore, whether the peak has actually been reached requires additional data to determine. If the peak in the DRC's production

was reached in 2017, then the DRC production peak is ~86,625 metric tonnes and that of the world's is ~127,695 metric tonnes. Assuming that the Hubbert models are correct, then a predicted 2080 production level would be similar to that of the late 1960s for both the DRC and world production. In contrast, Calvo et al. (2017) estimated a peak production occurring in 2142, which supports the conjecture that cobalt has resources that will last for more than 100 years. The critical uncertainty in the interpretation of the Hubbert model forecasts is whether or not the DRC's production peaked in 2017.

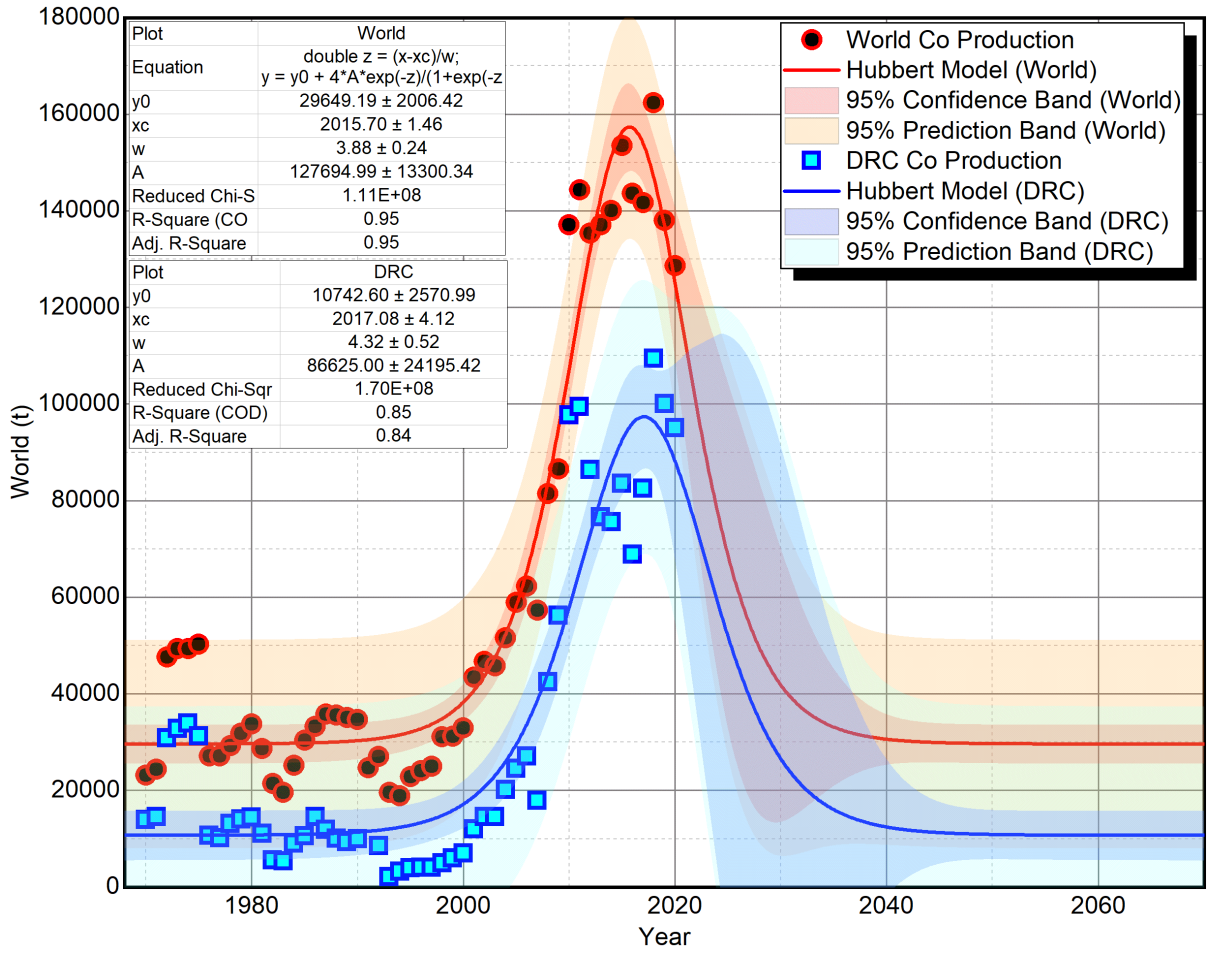


Figure. 4.7 Hubbert model fits for the DRC (blue line) and the world (red line). Blue and red shaded areas correspond to the 95 % confidence band for the DRC and the world, respectively.

According to Berk and Ediger (2016), the Hubbert curves can be classified into three categories that signify a relationship between production, remaining up-to-date reserves, and historic peaks (Berk and Ediger, 2016). The Definitely Declining

Phase (DDP) represents mineral production that has surpassed its historic peak hence revealing that cumulative production is much higher than remaining reserves. In contrast, the Definitely Increasing Phase (DIP) portrays cumulative production that is significantly less than remaining reserves meaning that production is yet to reach its peak. Lastly, the Plateau Phase (PP) presents difficulty in defining future production. This phase's cumulative production and remaining reserves are fairly similar to each other (Berk and Ediger, 2016). According to the United States Geological Survey (2020), world cobalt production is in its DIP given the vast remaining reserves (7,000,000 metric tonnes) compared to its cumulative production (140,000 metric tonnes). This presents a contrast to what is suggested by the Hubbert model fit (Table 4.2), which shows a historic peak in 2015, therefore, signifying that the DRC and therefore the world cobalt production is in a DDP. Extending Rutledge's (2011) terminology for coal production to cobalt production, the DRC and world can be referred to as mature regions indicating that production is declining as opposed to active regions, where production is tending towards its peak.

Table 4.2
Production data for the DRC and world based on Hubbert model.

Indicators / **DRC vs. World**	**Inflection point**	**Peak year**	**Peak production (metric tonnes)**
DRC	50 %	2015	86,625.00
World	50 %	2015	127,694.99

Chapter 5

5. Discussions

5.1 Mineralogical effects on recovery of cobalt

Mineralogical characterisation can define deposits and be linked to corresponsing metallurgical responses (Grammatikopoulos and Downing, 2020). Accurate mineralogical identification is, therefore, critical for process mineralogy, geometallurgy, and ore beneficiation because 1) metals have a variety of host minerals, 2) recovery methods are not standardised across minerals and, 3) certain elements may be deleterious (Grammatikopoulos and Downing, 2020).

5.1.1 Mineralogical limitations on separation

The main attributes important in optimising hydrometallurgical flow sheets include bulk modal mineralogy, element deportment on target minerals, mineral texture, grain size and association. These attributes affect the process mineralogy as they influence separation potential, size and liberation optimisation, and deleterious minerals and elements (Bradshaw, 2014). The mineralogical limit to separation can be determined using TIMA for mineralogical characterisation (Bradshaw, 2014; Kormos, 2014).

The study samples' modal abundance is dominated by sulphides with chalcopyrite being the most abundant sulphide mineral and carrollite being the target mineral as it the main Co-bearing mineral. Quartz, ankerite and aluminosilicates are the main gangue minerals. The textural characterisation of the samples is predominantly disseminated while massive sulphide textures are also common. In a few instances, a net-texture is observed. These two indicators – modal abundance and texture – can determine the "entitlement" of the ore which refers to the limit to separation through identifying which recovery process is most suitable for the minerals incolved based on mineral deportment (Bradshaw, 2014). The mineral association (ore versus gangue minerals) displayed by the primary phase maps hints at how the composition of the ore is a determinant of the (theoretical) grade recovery as modal abundance influences effective recovery. Considering that the sample lithologies are mostly quartzose sandstone and that the ore is comprised of disseminted,

massive and net-textured sulphides, recovery of target minerals will vary. A high recovery of the mineral of interest will also increase the recovery of gangue minerals which reduces the grade of the concentrate (Cropp et al., 2013; Bradshaw, 2014). This means that the net-textured ores will produce the lowest grades while the massive sulphide ores will have the highest grade as the degree of liberation is determined by the ore mineralogy and texture (Bradshaw, 2014).

In relation, the mineral grain size also has an effect on the recovery. Since coarse particles may contain multiple grains of ore versus gangue minerals (i.e., composite grains) coarser samples will increase the recovery however, will lower the grade of the concentrate due to recovery of gangue minerals. Liberated mineral grains are more associated with fine particles but they pose a lower chance of recovery because of the reduced probability of particle-bubble collision necessary for enhancing recovery during flotation stages (Bradshaw, 2014). The study samples are mainly coarse-grained, and hence the former scenario is the most feasible explanation for recovery and grade. However, considering the presence of fine-grained aluminosilicates and clays, understanding the mineral association in its entirety is vital for preempting challenges during ore beneciation (Grammatikopoulos and Downing, 2020) as these constituents are detrimental to the flotation process. Enhancing the recovery of Co from fine-grained particles would require increasing the agitating rate as it boosts the possibility of effective collision between the solid (mineral) and liquid (lixiviant/reagent) hence increasing the rate of leaching reaction (Pretorius, 2019).

5.1.2 Size and liberation optimisation

In mineral processing, the liberation of valuable minerals from gangue mineral is vital in attaining high recoveries from downstream processes such as gravity concentration and froth flotation. Quantification of mineral liberation is reliant on the parent rock ore texture in conjunction with properties of comminuted particles (Zhang and Subasinghe, 2013). Leaching is a hydrometallurgical process aimed at effectively and economically extracting valuable minerals from ore (Stuurman et al., 2014; Pretorius, 2019). Mineralogical texture is a limiting factor in size and liberation optimisation. This affects mineral processing as insufficient liberation

leads to poor performance. The relationship between ore texture and size of liberation of ore minerals is crucial to the flotation circuit design (Bradshaw, 2014).

Other prominent factors affecting leach efficiency include acid concentration, pH and temperature (Sibanda and Ndlovu, 2014). Considering that the samples consist of significant amount of chalcopyrite, the reagent and its concentration required to optimise recovery is one that can extract Co, even with the presence of the copper within the chalcopyrite. Seo et al., (2013) highlight sulphuric acid in conjunction with hydrogen peroxide or tartaric acid as effective reducing agents. When using inorganic acids, the recovery of Co (and Cu) is dependent on the concentration of the sulphuric acid, and the reducing agent, as well as temperature (Seo et al., 2013; Sibanda and Ndlovu, 2014). The use of sulphuric acid for extraction of Cu-Co ores provides higher Cu extraction percentages than Co, which is at its maximum at a sulphuric concentration of 0.8 M, then declines. The use of tartaric acid, however, results in higher Co extraction than Cu (~ 40 % and 5 %, respectively) as Co has a quicker reaction rate when interacting with an organic acid than Cu. The addition of a reducing agent, in this case, has a noteworthy effect on Co versus on Cu and increase the extraction efficiency from 40 % to 80 % Co (5 % to 10 % Cu). Similarly, temperature enhances extraction efficiency to ~ 60 % Co (Stuurman et al., 2014).

5.1.3 Deleterious minerals and elements

Different types and compositions of ores increase the likelihood of them containing deleterious minerals or elements to the flotation process (Cropp et al., 2013; Bradshaw, 2014). For this study, these minerals or elements were identified in both the ore and gangue mineral phases. The presence of aluminosilicates and clay minerals present possible problems to flotation and leaching because of their tendency to swell. The presence of arsenic detected in the samples is another potential issue for mineral processing as its separation is dependent on the texture and mineral deportment meaning that it could mix within the concentrate. The nickel detected in carrollite and chalcopyrite may also affect mineral processing especially considering that nickel and Co commonly occur as by-products. If these deleterious elements do not occur as isolated minerals, which is the case in this study, it means that they are a part of the crystal lattice of minerals which affects

the concentrate. This situation may affect the economics of the deposit and the final grades (Grammatikopoulos and Downing, 2020).

5.2 Validity of ARIMA forecasts

The cross validation technique was used to examine ARIMA production forecast objective accuracy and reliability by comparing forecasts made using pre-2010 data with actual post-2010 cobalt production data. This is an out-of-sample testing technique such that ARIMA models are trained using only pre-2010 data and the remainder is used for testing of model accuracy. Both Morocco and China represent cases where ARIMA forecasts are largely reliable to within 95 % confidence for predictions between 2010 and 2019 (Fig. 5.1A, C), in the sense that the forecasted ranges typically encapsulate the actual production data (pre-2010 testing set). More specifically, the data for China is predictable from 2010 to 2018 and unpredictable from 2018 onwards. This is clearly due to the sudden drop in production after 2018, which is a trend that is not exhibited by the data in the training interval (data up to 2010). This finding can be extended to forecasts of the world supply after 2020 (Fig. 4.5E), provided there are no sharp peaks or dips within the next 10 years. Therefore, for the world's supply of Co, I expect the ARIMA forecast will be relatively accurate, as the 95 % confidence interval has a high likelihood of covering all reasonable scenarios on the supply side. The effect of aggregating the production of various countries into a single forecast for the world is more reliable for two reasons: (1) fluctuations in the production of various producers are dampened, because they tend to occur at different times, and (2) the production of the dominant producer (DRC) dominates the world production (Fig. 4.5). However, ARIMA forecasts are unlikely to be as reliable at a country scale in general and especially for smaller producers of Co that feature relatively large and unpredictable fluctuations in their production behaviour, e.g., South Africa and Finland (Fig. 5.1B, D).

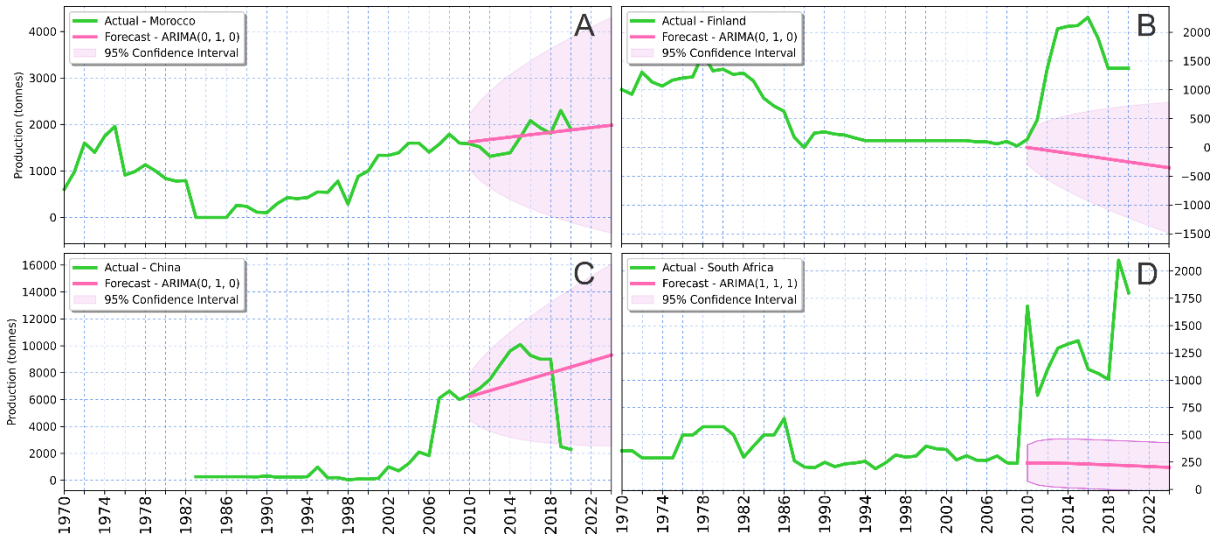


Figure 5.1 ARIMA cross validation forecasts of selected countries showing objective accuracy (A and C) and inaccuracy (B and D). A complete set of graphs is given in the Appendix D1 of this research report.

5.3 Importance of production forecasting on cobalt supply

The ARIMA- and Hubbert model-based forecasts paint a divergent picture of the future of Co production. The critical uncertainty of the Hubbert model-based forecasts rests on whether or not cobalt production has peaked. The slope of the bell curve of the Hubbert model is relatively constant near the full-width-half-maximum (FWHM) region and sharply changes near the peak, which renders the model insensitive to peaking behaviour that is exhibited by only a few data points, which are practically indistinguishable from noise. As our data does not contain a clear peak structure, the assumption of the existence of production peaks in 2015 (world) and 2017(DRC) is weak and therefore the Hubbert model-based forecasts are more likely to be wrong. There are other issues with the Hubbert model, for example, the concept of global peak oil (Hubbert, 1956) did not transpire as predicted. Although the Hubbert model did qualitatively predict the exhaustion of conventional crude and on a regional basis, it was unable to account for the development of non-conventional crude on a global scale. Similarly, peaking phenomenon for other materials such as phosphate (Edixhoven et al., 2014) and gold have not occurred to date. Nevertheless, the Hubbert model and its derivatives are useful to forecast the supply of commodities, which can become depleted and may exhibit an isolated

peak-like production behaviour. The assumptions behind the Hubbert model are generally not true or not explicitly demonstrable. Exploration for critical materials is hardly fixed in effort over time. Discovery to production lags is also variable. Therefore, the discovery rate is likely to be influenced by market conditions and geopolitical tension. Moreover, the Hubbert model's assumptions fail to acknowledge the possibility of an accelerated exploration pace, and the reduction of time lag between discovery and production given an increasing mineral price trend (Giraud, 2012; Berk and Ediger, 2016). Such a conceptual model has its shortcomings in forecasting global production considering that the production of resources is clearly affected by price variations (Wang et al., 2017).

The ARIMA-based forecasts are more accurate in comparison to the Hubbert model-based forecasts and in part due to their shorter-term nature, but also because they do not assume the structure of the production curve (e.g., a peak or plateau) and their validity is not contingent on a few critical data points. However, all of our ARIMA-based forecasts are relatively simple and are unable to replicate intrinsic variabilities in the parent data, such as isolated production dips or humps. This is due to the relatively short duration and low resolution of our dataset, which is only sampled on a yearly basis. However, this is not a problem for the forecasts, as they should reflect general trends at the same frequency of the data's sampling frequency and for strategic planning purposes, such as scenario planning and policymaking, the decadal behaviour is more relevant compared to yearly or monthly variability. By visual inspection, the forecasts for each country is satisfactory and in some cases, realistic, and the ability of the ARIMA method to calculate confidence intervals is highly useful for scenario planning, by providing a quantitative measure of the likelihood of outcomes. Our forecasts suggest that throughout the entire confidence interval, the world cobalt production in the next decade will most likely increase linearly.

5.4 Uncertainties for cobalt market future

The rising demand for metals and associated concerns regarding terrestrial metal availability has opened untraditional sources for consideration, such as deep-sea mining as an avenue for metal supply diversification (Petersen et al., 2016). The assumption that the demand for metals will increase and consequently, production

will peak then decline is a key driver in the growing interest for relying on deep-sea mining as a trajectory for global sustainable development (Kim, 2017). This is anticipated to unfold through non-discriminatory terms amongst all countries involved by the means of equitable distribution of economic benefits (Kim, 2017).

Deep-sea mining, particularly excavation of manganese nodules and Co -rich ferromanganese crusts could lead to key uncertainties regarding the supply of Co. The ~38 million km^2 extent of manganese nodules and 1.7 million km^2 for cobalt-rich crusts may potentially have a monumental impact on global cobalt markets (Petersen et al., 2016). Excavation from the Clarion-Clipperton Zone (CCZ), which hosts the greatest concentration of metal-rich nodules, can potentially boost the future production of cobalt due to an ever-growing demand for critical/strategic metals (Petersen et al., 2016; Mukhopadhyay et al., 2019). Deep sea mining is capable of producing more than 3,000 metric tonnes annually (Glasby, 2000; Mukhopadhyay et al., 2019). Cobalt production could also increase indirectly because of an increase in the demand for manganese to cater to the production of steel. This may secondhandedly lead to increased beneficiation of Co as a by-product, hence inserting more supply into the market, however since technology regarding deep-sea mining is in infancy (Dehaine et al., 2021), this may prove otherwise.

Despite this attraction towards deep-sea mining and its effect on cobalt production, non-governmental organisations and scientists have expressed apprehension because of the limited knowledge about environmental implications and practically non-exsistant regulatory frameworks (Petersen et al., 2016; Hoagland et al., 2010). Furthermore, deep-sea mining remains a questionable topic as critics believe that it will intensify unsustainable production and consumption patterns, widen the inequality gap in spatial and temporal dimensions, and divest from metals recycling (Kim, 2017). Not only will recycling be divested, but deep-sea mining will dissuade the goal of achieving a circular economy as it seeks to increase primary mineral supply with potentially long-term ecological risks. Even from a social perspective, the cost-benefit analysis remains questionable on a case-to-case basis (Wakefield and Myers, 2018).

Conclusion

6. Concluding Remarks

The global mineral resource supply chain has proven to be vulnerable due to the prioritisation of efficiency over resilience and redundancy. Despite the focus to ensure sufficiency and robustness, maintaining supply sustainability remains a moving target because of ever-increasing human population and development demands. More so for CRMs – which are crucial for contributing to socioeconomic development in the context of a sustainable and circular green economy – the need to ensure supply sustainability is vital. Through assessing Co's supply sustainability using production forecasts, supply risk is minimized by addressing unpredictability in the complex supply and demand system. Accurate mineralogical identification and characterisation is critical for production as process mineralogy, geometallurgy, and ore beneficiation are influencial metallurgical factors that enable the optimisation of mineral recovery to meet the market demand. The relationship between geology and metallurgy is, therefore, one of the most important criteria in ensuring cobalt supply sustainability. High-tech extractive metallurgy and mineral processing are essential for supplying critical raw materials (CRMs) for our modern society. The ability to effectively extract, process and beneficiate CRMs is dependent on understanding the mineralogical characteristics of ore deposits. Cobalt market adjustments in response to this complexity are, therefore, determinants for ensuring a supply-demand balance. Accurate production forecasting is indeed indispensable for not only mitigating potential supply-chain disruptions, but also for strategic planning and the implementation of green energy policies that are cognizant of ESG factors within the minerals industry, in alignment with climate change mitigation. Forecasting cobalt production using the Hubbert model alludes to the looming peak-like production behaviour while more importantly, the ARIMA forecasts, highlight how fluctuations in production and subsequent trends necessitate scenario planning and the implementation of policies that advance sustainable development contemporaneously with economic growth.

References

Adamas Intelligence, 2019. State of Charge: EVs, batteries and battery materials. Retrieved from https://www.adamasintel.com/state-of-charge-2019-h1/https://www.adamasintel.com/state-of-charge-2019-h1/. (Accessed 22 February 2021).

Ali, S., Giurco, D., Arndt, N., Nickless, E., Brown, G., Demetriades, A., Durrheim, R., Enriquez, M.A., Kinnaird, J., Littleboy, A., Meinert, L., Oberhansli, R., Salem, J., Schodde, R., Schneider, G., Vidal, O., Yakovleva, N., 2017. Mineral supply for sustainable development requires resource governance. Nat. 7645, 367–372. https://doi.org/10.1038/nature21359.

Alonso, E., Gregory, J., Field, F., Kirchain, R., 2007. Material availability and the supply chain: risks, effects, and responses. Env. Sci. Tech. 41 (19), 6649–6656. https://doi.org/10.1021/es070159c.

Berg, S.V., 2013. Regulatory functions affecting renewable energy in developing countries. Elec. J. 26 (6), 28–38. https://doi.org/10.1016/j.tej.2013.05.015.

Berk, I., Ediger, V.Ş., 2016. Forecasting the coal production: Hubbert curve application on Turkey's lignite fields. Resour. Pol. 50, 193–203. https://doi.org/10.1016/j.resourpol.2016.10.002.

Blengini, G.A., Nuss, P., Dewulf, J., Nita, V., Peiro, L.T., Vidal-Legaz, B., Latunussa, C., Mancini, L., Blagoeva, D., Pennington, D., Pellegrini, M., Van Maercke, A., Solar, S., Grohol, M., Ciupagea, C., 2017. EU methodology for critical raw materials assessment: Policy needs and proposed solutions for incremental improvements. Resour. Pol. 53, 12–19. https://doi.org/http://dx.doi.org/10.1016/j.resourpol.2017.05.008.

Bradshaw, D., 2014. The role of process mineralogy in improving the process performance of complex sulphide ores: *Proceedings of the XXVII International Mineral Processing Congress, January, Santiageo, Chile.*

Brown, T., Idoine, N., Wrighton, C., Raycraft, R., Hobbs, S., Shaw, R., Everett, P., Kresse, C., Deady, E., Bide, T. 2020. World mineral production 2014-2018. British Geological Survey, Keyworth. Retrieved from

https://www.bgs.ac.uk/mineralsUK/statistics/worldStatistics.html (Accesssed 06 April 2021).

Calvo, G., Valero, A., Valero, A., 2017. Assessing maximum production peak and resource availability of non-fuel mineral resources: Analyzing the influence of extractable global resources. Resour. Conserv. Recy. 125, 208–217. https://doi.org/http://dx.doi.org/10.1016/j.resconrec.2017.06.009.

Campbell, G., 2020. The cobalt market revisited. Min. Econ. *33*, 21–28. https://doi.org/https://doi.org/10.1007/s13563-019-00173-8.

Church, C., Crawford, A., 2018. Green Conflict Minerals, the Fuels of Conflict in the Transition to a Low-carbon Economy: IISD Report, 56. International Institute for Sustainable Development.

Cobalt Institute, 2021. Ores Containing Cobalt. Retrieved from https://www.cobaltinstitute.org/ores-containing-cobalt.html. (Accessed 9 February 2021).

Coetzee, L., Theron, S., Martin, G., van de Merwe, J.,Stanek, T., 2011. Modern gold deportments and its application to industry. *Minerals Engineering*, 24(6), pp.565-575. https://doi.org/10.1016/j.mineng.2010.09.001

Cropp, A.F, Goodall, W.R., Bradshaw, D.J. 2013.The Influence of Textural Variation and Gangue Mineralogy on Recovery of Copper by Flotation from Porphyry Ore – a Review: AusIMM GeoMet 2013 Proceedings, October, Australia. pp.

Crundwell, F.K., du Preez, N.B., Knights, B.D.H., 2020. Production of cobalt from copper-cobalt ores on the African Copperbelt–An overview. Miner. Eng. 156, p.106450. https://doi.org/10.1016/j.mineng.2020.106450

Dehaine, Q., Tijsseling, L., Glass, H., Tormanen, T., and Butcher, A., 2021. Geometallurgy of cobalt ores: a review. Miner. Eng. 160, 1–28. https://doi.org/https://doi.org/10.1016/j.mineng.2020.106656.

DeCarlo, S., Matthews, D., 2019. More than a pretty color: the renaissance of the cobalt Industry. J. Int. Commer. Econ. Policy. 1–23. https://doi.org/http://www.usitc.gov/journals.

European Commission, 2010. Critical raw materials for the EU: Report of the Ad-hoc Working Group on defining critical raw materials. Retrieved from https://eplca.jrc.ec.europa.eu/uploads/rawmat-Nowakowska-Defining-Critical-Raw-Materials-in-the-EU-Information-Gaps-and-Available-Solutions.pdf . (Accessed 10 January 2022)

European Commission, 2011. Tackling the challenges in commodity markets and on raw materials, Brussels, Belgium.

European Commission, 2014. Report on critical raw materials for the EU, report of the Ad-hoc working group on defining critical raw materials, Brussels, Belgium.

European Commission, 2017. On the 2017 list of Critical Raw Materials for the EU, 2017. Retrieved from https://ec.europa.eu/transparency/regdoc/rep/1/2017/EN/COM-2017-490-F1-EN-MAIN-PART-1.PDF. (Accessed 5 January 2021).

European Commission, 2020. Critical Raw Materials Resilience: Charting a Path towards greater Security and Sustainability. Retrieved from https://ec.europa.eu/docsroom/documents/42849. (Accessed 5 January 2021).

Edixhoven, J.D., Gupta, J., Savenije, H.G., 2014. Recent revisions of phosphate rock reserves and resources: a critique. Earth Syst. Dyn. 5, 491–507. https://doi.org/10.5194/esd-5-491-2014.

Elshkaki, A., Graedel, T.E., Ciacci, L., Reck, B.K., 2016. Copper demand, supply, and associated energy use to 2050. Glob. Environ. Change. 39, 305–315. https://doi.org/10.1016/j.gloenvcha.2016.06.006.

Fattah, J., Ezzine, L., Aman, Z., El Moussami, H., Lachlab, A., 2018. Forecasting of demand using ARIMA model. Int. J. Eng. Bus. Manag. 10, 1–9. https://doi.org/10.1177/1847979018808673.

Ghorbani, Y., 2018. Gaining access to high-tech and critical raw materials: A driving factor in developing future concept and methods in mineral

processing and extractive metallurgy. Conference: III Congress of Industrial Engineering of the North of Chile, 22-24 August, 2018, Antofagasta-Chile.

Ghorbani, Y., Nwaila, G.T., Zhang, S.E., Rosenkranz, J., 2021. Rethinking mineral processing and extractive metallurgy approaches to ensure a sustainable supply of high-tech and critical raw materials, in Azimi, G., Ouchi, T., Forsberg, K., Kim, H., Alam, S., Abdullahi Baba, A., Neelameggham, N.R. (Eds.), Rare Metal Technology 2021. Springer international publishing, pp. 173–186.

Giraud, P.N., 2012. A note on Hubbert's thesis on mineral commodities production peaks and derived forecasting techniques. Procedia Eng. 46, 22–26. https://doi.org/10.1016/j.proeng.2012.09.441.

Glasby, G.P., 2000. Lessons learned from deep-sea mining. Sci. 289 (5479), 551–553. https://doi.org/10.1126/science.289.5479.551.

Graedel, T.E. Reck, B.K., 2016. Six years of criticality assessments: what have we learned so far?. J. Ind. Ecol. 20 (4), 692-699. https://doi.org/10.1111/jiec.12305.

Grammatikopoulos, T., Downing, S., 2020. The disruptive role of process mineralogy in geology and mineral processing industry. *Asp. Min. Miner. Sci*, *5*, 571-579. https://doi.org/10.31031/AMMS.2020.05.000609

GRD Minproc, 2007. Tenke Fungurume Feasibility Study, Report no. 99.1, Lundin Mining Corporation.

Krishnamurthy, N., Gupta, C.K., 2015. Extractive metallurgy of rare earths, 2nd edition, CRC Press, Taylor & Francis Group, USA.

Haraguchi, N., Cheng, C. F. C., Smeets, E., 2017. The importance of manufacturing in economic development: has this changed? World Dev. *93*, 293–315. https://doi.org/http://dx.doi.org/10.1016/j.worlddev.2016.12.013.

Heredia, F., Martinez, A.L., Urtubey, V.S., 2020. The importance of lithium for achieving a lowcarbon future: overview of the lithium extraction in the 'Lithium Triangle.' J. Energy Nat. Res. Law. 38 (3), 213–236. https://doi.org/10.1080/02646811.2020.1784565.

Hoagland, P., Beaulieu, S., Maurice, A.T., Roderick E.G., Christopher, G., Lyle, G., and Jian, L. 2010. Deep-sea mining of seafloor massive sulfides. Mar. Policy. 34,728–732. doi: 10.1016/j.marpol.2009.12.001

Hofmann, M., Hofmann, H., Hagelüken, C., Hool, A., 2018. Critical raw materials: A perspective from the materials science community. SM&T. 17, 1–10. https://doi.org/10.1016/j.susmat.2018.e00074.

Horn, S., Gunn, A.G., Petavratzi, E., Shaw, R., Eilu, P., Törmänen, T., Bjerkgård, T., Sandstad, J.S., Jonsson, E., Kountourelis, S., Wall, F., 2021. Cobalt resources in Europe and the potential for new discoveries. Ore Geol. Rev. 130, 1–25. https://doi.org/10.1016/j.oregeorev.2020.103915.

Hostettler, S., 2015. Energy challenges in the Global South, in: Hostettler S., Gadgil A., Hazboun E. (Eds.) Sustainable access to energy in the Global South. Springer, Cham. https://doi.org/10.1007/978-3-319-20209-9_1.

Hitzman, M.W., Bookstrom, A.A., Slack, J.F., Zientek, M.L., 2017. Cobalt – Styles of deposits and the search for primary deposits: U.S. Geological Survey, Open-File Report 2017–1155, 47. https://doi.org/10.3133/ofr20171155.

Hubbert, M.K., 1956. Nuclear Energy and the fossil fuels, in: Drilling and production practice (API-56-007), American Petroleum Institute. https://www.resilience.org/stories/2006-03-08/nuclear-energy-and-fossil-fuels/.

Humphreys, D., 1982. A mineral commodity life-cycle?: Relationships between production, price and economic resources. Resour. Policy. 8 (3), 215–229. https://doi.org/0301-4207/82/030215-1!$03.00.

Humphries, M., 2019. Critical Minerals and U.S. Public Policy, Report no. R45810, Congressional Research Service.

Jadhav, V., Chinnappa, R.B., Gaddi, G.M., 2017. Application of ARIMA model for forecasting agricultural prices. *J. Agric. Sci. Technol. 19 (*4), 981–992. https://www.sid.ir/en/journal/ViewPaper.aspx?id=539819.

Johnson, R.D. 2014. *Orebody characterisation and structural features that govern copper and cobalt mineralisation in the eastern limb of the Lufilian Arc,*

Democratic Republic of Congo (Master of Science dissertation, Braamfontein: University of the Witwatersrand).

Kalenga, J.N., 2014. Production of nonferrous metals in the Katanga region of the Democratic Republic of Congo: 1906-2012. *Int J Econ and Manage*, *3*(2), 1-7.https://doi.org/0301-4207/82/030215-1!$03.0010.4172/2162-6359.1000181.

Kariuki, D., 2018. Barriers to renewable energy technologies development. Energy Today. Retrieved from https://www.energytoday.net/economics-policy/barriers-renewable-energy-technologies-development/. (Accessed 26 February 2021).

Kim, R., 2017. Should deep seabed mining be allowed? Mar. Policy. 82, 134–137. https://doi.org/http://dx.doi.org/10.1016/j.marpol.2017.05.010.

Kochtcheeva, L.V., 2016. Renewable Energy: Global Challenges. E-International Relations. Retrieved from https://www.e-ir.info/2016/05/27/renewable-energy-global-challenges/. (Accessed 22 February 2021).

Kormos, L., Sliwinski, J., Oliveira, J. and Hill, G. 2013. . Geometallurgical characterisation and representative metallurgical sampling at Xstrata process support: In The Annual Canadian Mineral Processors Operators Conference, January, CIM: Montreal, QC, Canada

Lèbre, E., Owen, J., Corder, G., Kemp, D., Stringer, M., Valenta, R., 2019. Source Risks As Constraints to Future Metal Supply. Environ. Sci. Tech. 53, 10571–10579. https://doi.org/:10.1021/acs.est.9b02808.

Lèbre, É., Stringer, M., Svobodova, K., Owen, J., Kemp, D., Côte, C., Arratia-Solar, A., Valenta, R., 2020. The social and environmental complexities of extracting energy transition metals. Nat. Commun. 11, 4823. https://doi.org/https://doi.org/10.1038/s41467-020-18661-9.

Lusty, P.A.J., Gunn, A.G., 2015. Challenges to global mineral resource security and options for future supply. Geol. Soc. Lond. Special Pub. 393 (1), 265–276. https://doi.org/10.1144/SP393.13.

MacLeod, J.M., Rosei, F., 2015. Supporting the development and deployment of sustainable energy technologies through targeted scientific training, in: Hostettler S., Gadgil A., Hazboun E. (Eds.), Sustainable access to energy in the Global South, Springer, Cham. https://doi.org/10.1007/978-3-319-20209-9_20.

Mathieux, F., Ardente, F., Bobba, S., Nuss, P., Blengini, G. A., Dias, P. A., Blagoeva, D., de Matos, C. T., Wittmer, D., Pavel, C., Hamor, T., Saveyn, H., Gawlik, B., Orveillon, G., Huygens, D., Garbarino, E., Tzimas, E., Bouraoui, F., Solar, S., 2017. *Critical Raw Materials and the Circular Economy*, Report no. JRC108710, JRC Science-for-Policy Report, Publications Office of the European Union.

Mgaya, J.F., 2019. Application of ARIMA models in forecasting livestock products consumption in Tanzania, in: Yildiz, F. (Ed.), Cogent Food and Agriculture, 5 (1), 1–29. https://doi.org/https://doi.org/10.1080/23311932.2019.1607430.

Mukhopadhyay, R., Naik, S., De Souza, S., Dias, O., Iyer, S., Ghosh, A., 2019. The economics of mining seabed manganese nodules: A case study of the Indian Ocean nodule field. *Mar. Georesources Geotechnol. 37* (7), 845–851. https://doi.org/10.1080/1064119X.2018.1504149.

Nanzad, B., Anderson, K., Conder, J., 2017. Evaluation of the logit/probit transform method to modeling historical resource production and forecasting compared to conventional Hubbert modeling. Int. J. Coal Geol. 182, 42–51. https://doi.org/http://dx.doi.org/10.1016/j.coal.2017.08.016.

National Research Council (2008). Managing materials for a twenty-first century military, National Academies Press.

Nau, R., 2014. Lecture notes on forecasting – introduction to ARIMA models. Duke University.

Nurmi, P., 2017. Green mining – a holistic concept for sustainable and acceptable mineral production. Ann. Geophys. 60. https://doi.org/10.4401/ag-7420.

Overland, I., 2019. The geopolitics of renewable energy: Debunking four emerging myths. Energy Res. Soc. Sci. 49, 36–40. https://doi.org/10.1016/j.erss.2018.10.018.

Petersen, S., Krätschell, A., Augustin, N., Jamieson, J., Hein, J.R., Hannington, M.D., 2016. News from the seabed – Geological characteristics and resource potential of deep-sea mineral resources. Mar. Policy, 70, 175–187. http://dx.doi.org/10.1016/j.marpol.2016.03.012.

Pommeret, A., Ricci, F. and Schubert, K., 2022. Critical raw materials for the energy transition. Eur. Econ. Rev, 141, p.103991, https://doi.org/10.1016/j.euroecorev.2021.103991

Pretorius, P.J., 2019. *Atmospheric acid leaching of oxidised and mixed copper cobalt ores mined in the Democratic Republic of the Congo* (Doctoral dissertation, Stellenbosch: Stellenbosch University).

Rissman, J., Bataille, C., Masanet, E., Aden, N., Morrow III, W.R., Zhou, N., Elliott, N., Dell, R., Heeren, N., Huckestein, B., Cresko, J., 2020. Technologies and policies to decarbonize global industry: Review and assessment of mitigation drivers through 2070. Appl. Energy. 266, https://doi.org/10.1016/j.apenergy.2020.114848.

Rockefeller Foundation, 2010. Scenarios for the Future of Technology and International Development, 1–51, The Rockefeller Foundation and Global Business Network.

Rosyid, F.A. Adachi, T., 2016. Forecasting on Indonesian coal production and future extraction cost: A tool for formulating policy on coal marketing. Nat. Resour. 7 (12), 677–696. http://dx.doi.org/10.4236/nr.2016.712054.

Rutledge, D., 2011. Estimating long-term world coal production with logit and probit transforms. Int. J. Coal Geol. 85, 23–33. http://dx.doi.org/10.1016/j.coal.2010.10. 012.

SAMREC, 2016. The South African code for the reporting of exploration results, mineral resources and mineral reserves. Prepared by the South African Mineral Resource Committee (SAMREC), pp. 95.

Santoro, L., Tshipeng, S., Pirard, E., Bouzahzah, H., Kaniki, A., Herrington, R., 2019. Mineralogical reconciliation of cobalt recovery from the acid leaching of oxide ores from five deposits in Katanga (DRC). Miner. Eng.,137, 277-289. https://doi.org/10.1016/j.mineng.2019.02.011

Saraiva, T.A., Szklo, A., Lucena, A.F.P., Chavez-Rodriguez, M.F., 2014. Forecasting Brazil's crude oil production using a multi-Hubbert model variant. *Fuel*. *115*, 24–31. https://doi.org/10.1016/j.fuel.2013.07.006.

Scholz, R.W. Wellmer, F.W., 2013. Approaching a dynamic view on the availability of mineral resources: what we may learn from the case of phosphorus? Glob. Environ. Change. 23 (1), 11–27. http://dx.doi.org/10.1016/j.gloenvcha.2012.10.013.

Selley, D., Scott, R., Emsbo, P., Koziy, L., Hitzman, M.W., Bull, S.W., Duffett, M., Sabagenzi, S., Halpin, J., Broughton, D.W., 2018. Structural configuration of the Central African Copperbelt: roles of evaporites in structural evolution, basin hydrology, and ore location. JOM, Society of Economic Geologists Special Publication, 21, 115–156. https://doi.org/https://doi.org/10.5382/sp.21.07.

Seo, S.Y., Choi, W.S., Kim, M.J., Tran, T., 2013. Leaching of a Cu-Co ore from Congo using sulphuric acidhydrogen peroxide leachants. J Min. Metall. Sect. B-Metall. 49(1), 1-7. https://doi.org/https://doi.org/10.2298/JMMB120103035S.

Shedd, K.B., McCullough, E.A., Bleiwas, D.I., 2017. Global trends affecting the supply security of cobalt. Miner. Eng. 69 (12), 37-42. https://dx.doi.org/10.1021/acs.est.9b04975

Shengo, M., Kime, M., Mambwe, M. and Nyembo, T., 2019. A review of the beneficiation of copper-cobalt-bearing minerals in the Democratic Republic of Congo. *Journal of Sustainable Mining*, 18(4), 226-246. https://doi.org/10.1016/j.jsm.2019.08.001

Slack, J.F., Kimball, B.E., and Shedd, K.B. Critical mineral resources of the United States—Economic and environmental geology and prospects for future

supply, in: Schulz, K.J., DeYoung, J.H., Jr., Seal, R.R., Bradley, D.C. (Eds.). U.S. Geological Survey, pp. 1–39. https://pubs.er.usgs.gov/publication/pp1802

Sillitoe, R.H., Perello, J., Creaser, R.A. and Wilson, A., 2017. Age of the Zambian Copperbelt: Mineralium Deposita, 52, 1245-1268. http://doi/10.1007/s00126-017-0726-8

Statista, 2021. Global cobalt reserves by country 2020. Statista. Retrieved from https://www.statista.com/statistics/264930/global-cobalt-reserves/. (Accessed 20 February 2021).

Stuurman, S., Sibanda, V., Ndlovu, S., 2014. Comparing the extent of the dissolution of copper-cobalt ores from the DRC Region. J South Afr Inst Min Metall , 114, 347-353. https://doi.org/10.1007/s40831-017-0149-x

Sykes, J.P., Wright, J.P., Trench, A., Miller, P., 2016. An assessment of the potential for transformational market growth amongst the critical metals. App. Earth Sci. 125 (1), 21-56. https://doi.org/10.1080/03717453.2015.1104055.

Thiam, D.R., 2011. An energy pricing scheme for the diffusion of decentralized renewable technology investment in developing countries. Energy Policy. 39 (7), 4284–4297. https://doi.org/10.1016/j.enpol.2011.04.046.

Tilton, J.E., 2018. The Hubbert peak model and assessing the threat of mineral depletion. Resour. Conserv. Recycl. 139. https://doi.org/https://doi.org/10.1016/j.resconrec.2018.08.026.

Tisserant, A., Pauliuk, S., 2016. Matching global cobalt demand under different scenarios for co-production and mining attractivenes. J. Econ. Struct. 5 (4), 2–19. https://doi.org/10.1186/s40008-016-0035-x.

Twite, F., Broughton, D., Nex, P., Kinnaird, J., Gilchrist, G., Edwards, D., 2019. Lithostratigraphic and structural controls on sulphide mineralisation at the Kamoa copper deposit, Democratic Republic of Congo. J. Afr. Earth Sci. 151, 212–224. https://doi.org/https://doi.org/10.1016/j.jafrearsci.2018.12.016.

United States Geological Survey, 2020. *Cobalt Statistics and Information*. Retrieved from https://www.usgs.gov/centers/nmic/cobalt-statistics-and-information. (Accessed 14 January 2021).

United Nations, 2020. Sustainability Development Goals. Retrieved from https://www.un.org/sustainabledevelopment/sustainable-development-goals/. (Accessed 15 February 2021)

UNEP, 2007. United Nations Environmental Programme Annual Report. Retrieved from https://www.iri.edu.ar/publicaciones_iri/anuario/CD%20Anuario%202008/Mayd/PNUMA.pdf. (Accessed 9 February 2021).

UNEP, 2009. United Nations Environment Annual Programme. Retrieved from https://www.oeko.de/oekodoc/1070/2009-129-en.pdf (Accessed 11 February 2021).

UNEP, 2013. Metal Recycling: Opportunities, Limits, Infrastructure, A Report of the Working Group on the Global Metal Flows to the International Resource Panel. Retrieved from https://wedocs.unep.org/handle/20.500.11822/8423. (Accessed 21 December 2020).

Valenta, R.K., Kemp, D., Owen, J.R., Corder, G.D. Lèbre, É., 2019. Re-thinking c complex orebodies: Consequences for the future world supply of copper. J. Clean. Prod. 220, 816–826. https://doi.org/10.1016/j.jclepro.2019.02.146.

Vanbrabant, Y., Burlet, C. and Louis, P., 2013. Mineralogical characterization of cobaltic oxides from the democratic republic of congo., 243-254. Springer, Cham.

Wakefield, J.R., Myers, K., 2018. Social cost benefit analysis for deep sea minerals mining. Mar. Policy. 95, 346–355. http://dx.doi.org/10.1016/j.marpol.2016.06.018.

Wang, X., Yao, M., Li, J., Zhang, K., Zhu, H., Zheng, M., 2017. China's rare earths production forecasting and sustainable development policy implications. *Sustainability*. *9* (6), 1–14. https://doi.org/doi:10.3390/su9061003.

Wang, J., Feng, L., 2016. Curve-fitting models for fossil fuel production forecasting: Key influence factors. J Nat Gas Sci Eng. 32, 138–149. http://dx.doi.org/10.1016/j.jngse.2016.04.013.

Wilburn, D.R., 2012. Cobalt mineral exploration and supply from 1995 through 2013: U.S. Geological Survey Scientific Investigations, Report no. 2011–5084, pp. 16.

Wills B, A, Napier-Munn T. In: Mineral processing technology: an introduction to the practical aspects of ore treatment and mineral recovery. 7th Edition. Oxford: Elsevier Science and Technology Books; 2006. p. 4332.

Wold, H., 1939. A study in analysis of stationary time series, a review. J. Royal Stat. Soc. 102 (2), 295–298. http://dx.doi.org/doi:10.2307/2980009.

Woollacott, L., Eric, R. 1994. Mineral and Metal Extraction: An Overview. Johannesburg, South Africa: Southern African Institute for Mining and Metallurgy. 108 (8), http://dx.doi.org/10.17159/2411-9717/2018/v118n8a5 .

World Commission on Environment and Development, 1987. Report of the World Commission on environment and development: our common future.

Yule, G.U., 1926. Why do we sometimes get nonsense-correlations between Time-Series?-a study in sampling and the nature of time-series. J. Royal Stat. Soc. 89 (1), 1–63. https://doi.org/10.2307/2341482.

Zhang, J., Subasinghe, N., 2013. Prediction of mineral liberation characteristics of comminuted particles of high grade ores. *Miner. Eng. 49*, 68-76. https://doi.org/10.1016/j.mineng.2013.05.005

Zuo, L., Wang, C., Corder, G.D., 2019. Strategic evaluation of recycling high-tech metals from urban mines in China: An emerging industrial perspective. J. Clean. Prod. 208, 697–708. https://doi.org/10.1016/j.jclepro.2018.10.030.

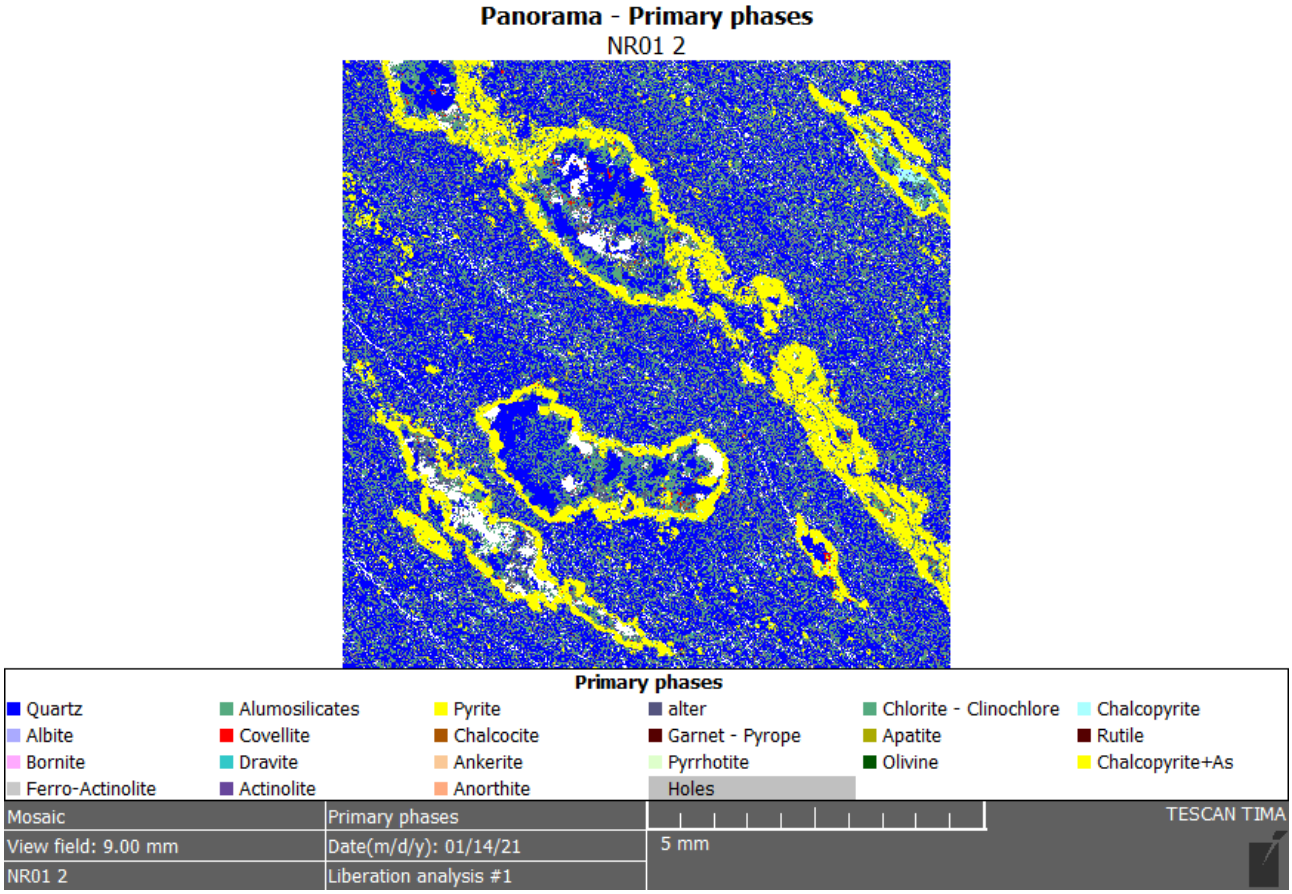
Appendices

Appendix A:TIMA primary phase map descriptions

4.1.1.1 Sample NR01

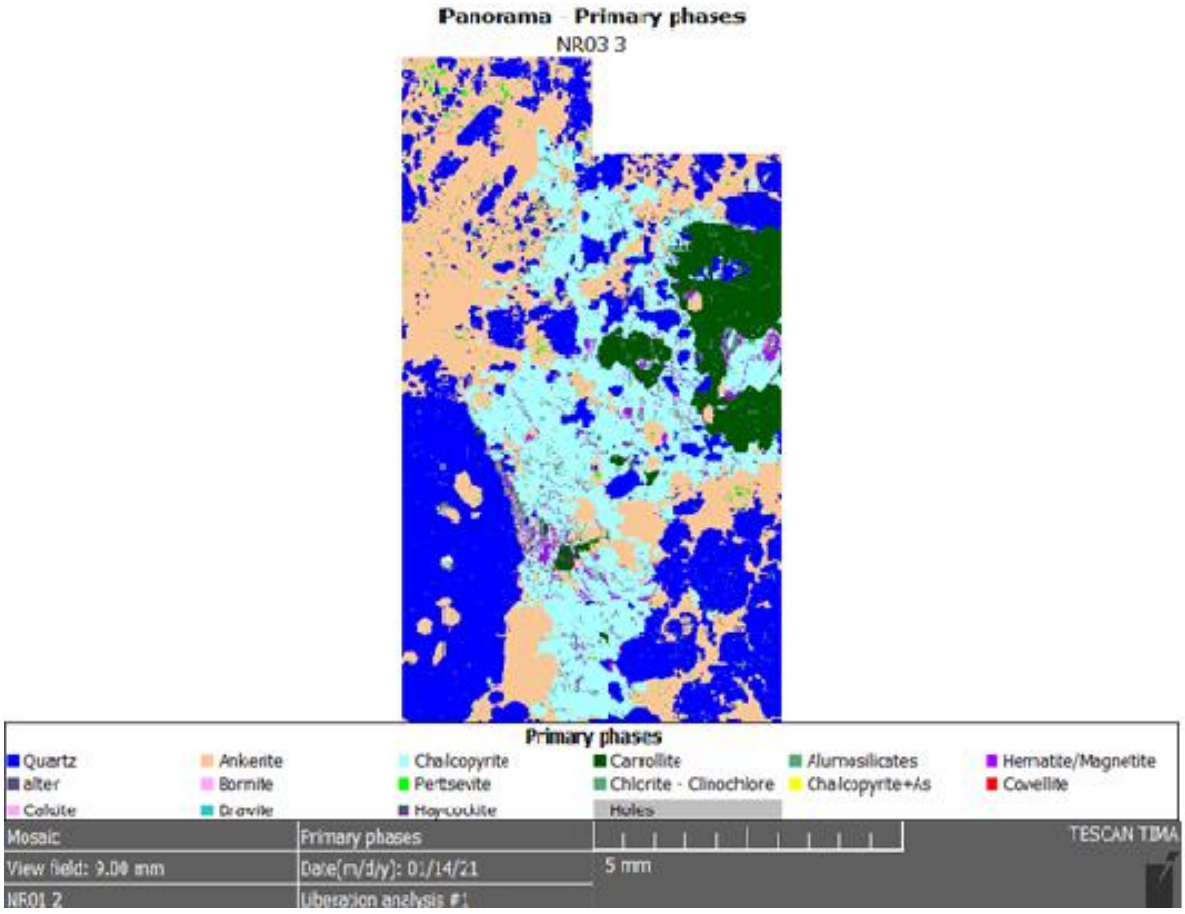
Sample 01 is a Co-mineralised quartzose sandstone. It is medium-grained and chiefly consists of foliated quartz, and laminated pyrite accompanied by minor amounts of (unspecified) aluminosilicates, actinolite, chlorite-clinochlore, and chalcopyrite. The principal ore minerals consist of pyrite and chalcopyrite (~ 1.5 mm thick) with trace amounts of pyrrhotite, bornite, covellite (0.75mm) and chalcocite.

Both quartz and pyrite crystals are elongate and define a foliation. Pyrite occurs as elongated rims (~ 1.5 - 3 mm thick) around quartz and the aluminosilicates, covellite, and chalcopyrite. Pyrite shows a preferential orientation that is parallel to the foliation.



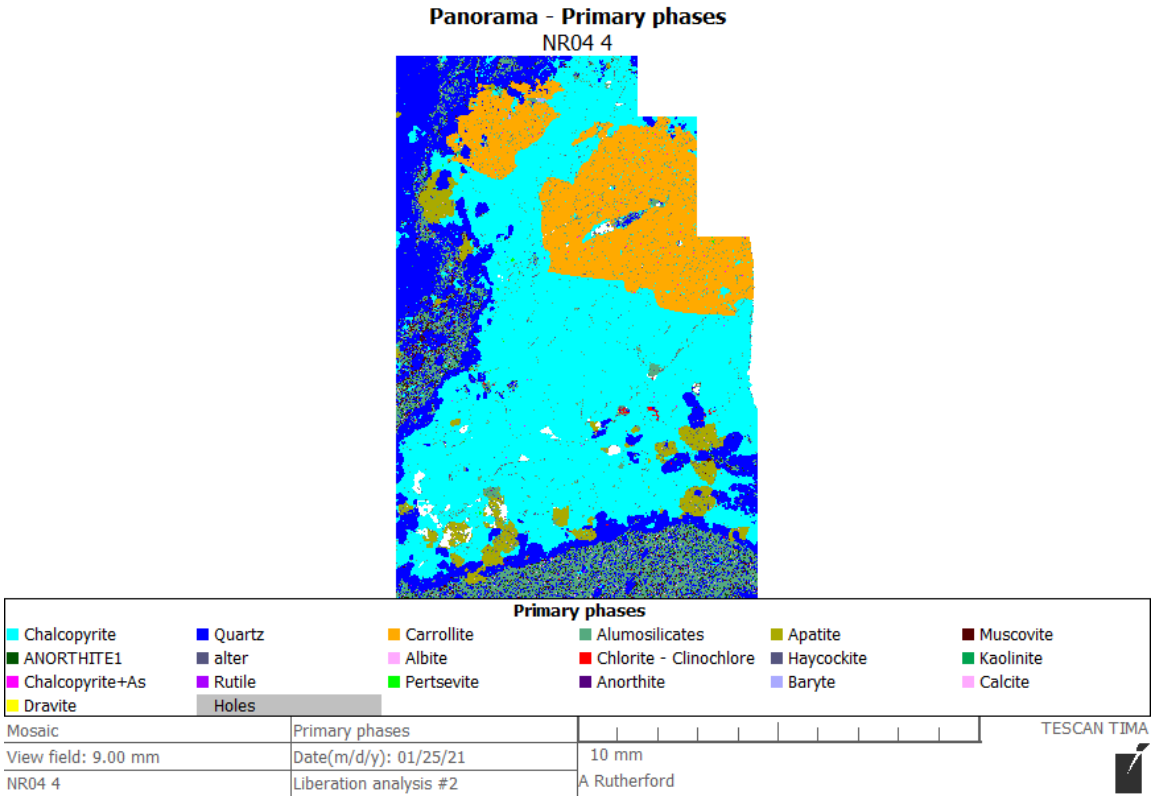
4.1.1.2 Sample NR03: Co-bearing ore sample

Sample NR03 is a Co-mineralised dolomite. It is coarse-grained and primarily consists of chalcopyrite, ankerite, and quartz accompanied by minor amounts haematite/magnetite and pertsevite, and trace amounts of covellite, arsenic-chalcopyrite, and bornite are the accessory ore minerals that are present alongside calcite, dravite, haycockite, chlorite-clinochlore, and aluminosilicates. Principal ore minerals consist of chalcopyrite and carrollite. Chalcopyrite, ankerite and quartz are disseminated with pertsevite occurring as. inclusions within it is indicative of its affinity for copper, arsenic, and iron sulphide minerals.



4.1.1.3 Sample NR04: Co-bearing ore sample

Sample NR04 is a Co-mineralised sandstone. It is coarse-grained and chiefly consists of euhedral carrollite, chalcopyrite, and anhedral quartz, accompanied by minor amounts of apatite and aluminosilicates, and trace amounts of chlorite-clinochlore, muscovite, calcite, dravite, anorthite, rutile, albite, barite, kaolinite, and haycockite. The main ore minerals consist of carrollite (~ 5 mm) and chalcopyrite (~ 8 mm). Pyrite shows a preferential distribution as rims around chalcopyrite. Chalcopyrite, carrollite and quartz display a disseminated texture with carrollite consisting of pertsevite inclusions.

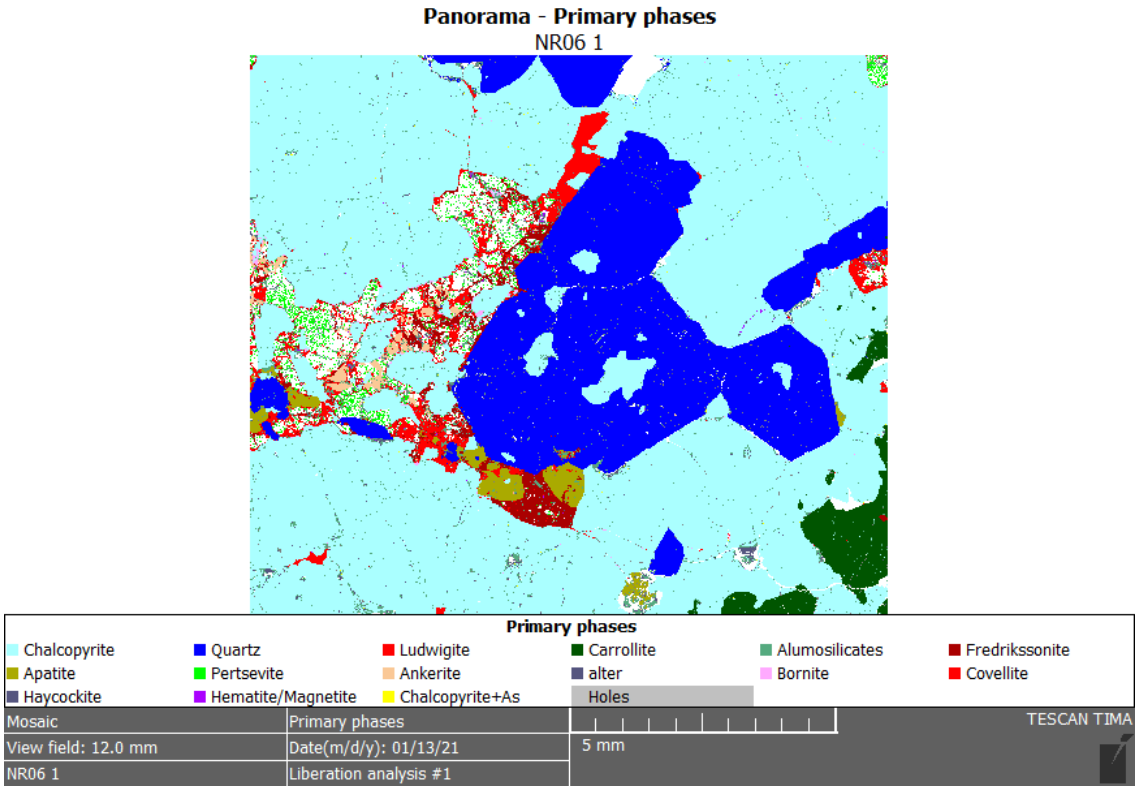


4.1.1.1.3 Sample NR06: Co-bearing ore sample

Sample NR06 is a Co-mineralised quartzose sandstone. It is coarse-grained and chiefly consists of chalcopyrite, quartz, and covellite accompanied by minor amounts of apatite, ankerite, fredrikssonite, ludwigite and pertsevite, and trace

amounts of haycockite, aluminosilicates, and haematite/magnetite. Principal ore minerals consist of chalcopyrite (~ 11mm) and carrollite (~ 2.5 mm) with trace amounts of covellite and bornite.

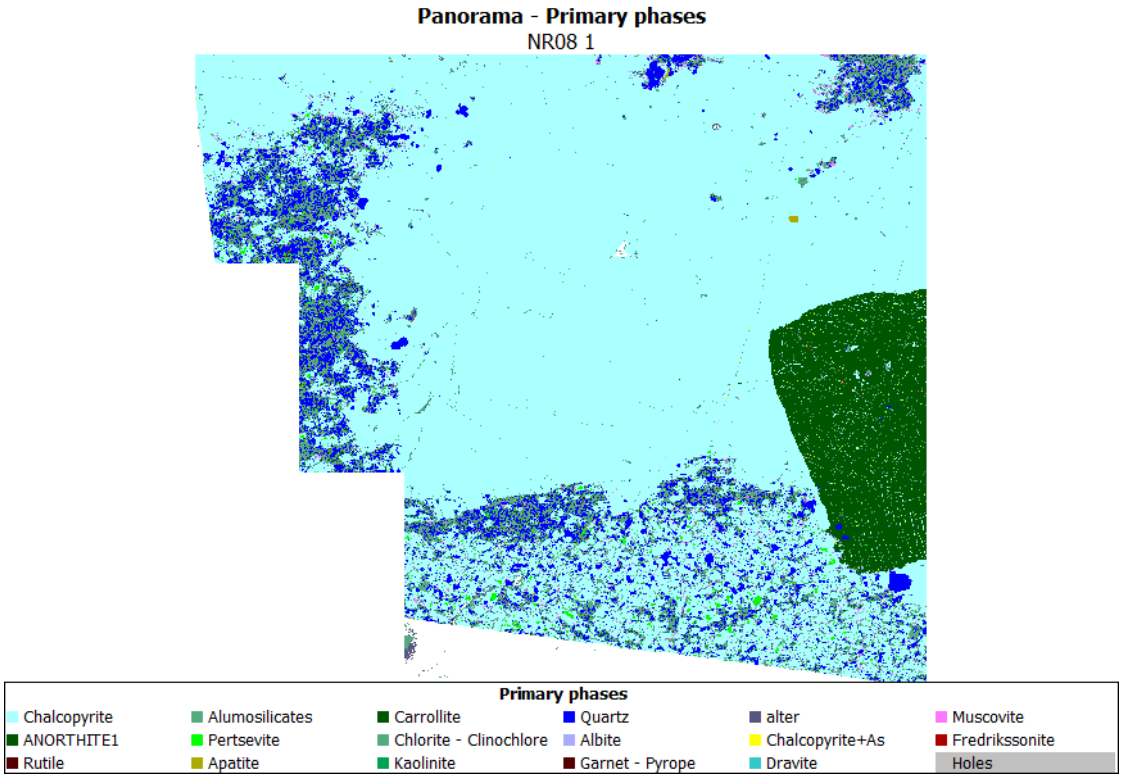
Quartz and chalcopyrite are euhedral and define a disseminated texture. Carrollite also occurs as euhedral grains. Apatite, pertsevite, and fredrikssonite also as a disseminated texture between the quartz and chalcopyrite grain boundaries.

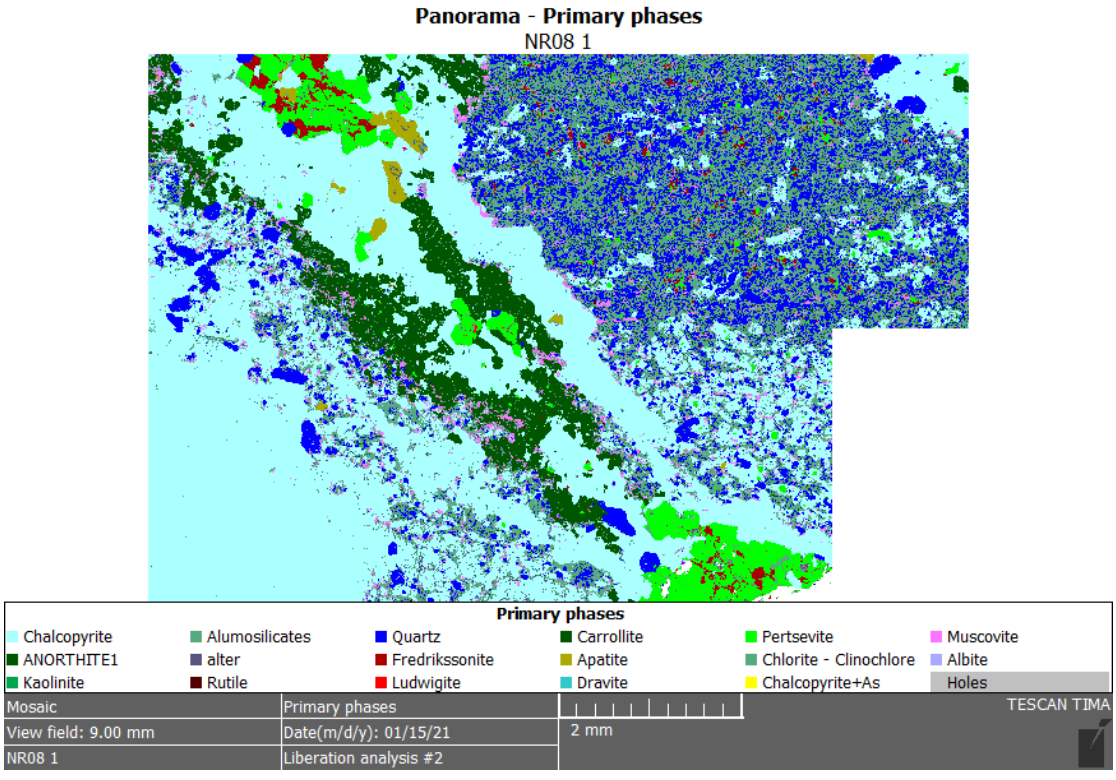


4.1.1.1.4 Sample NR08: Co-bearing ore sample

Sample NR08 is a Co-mineralised quartzose sandstone. It is medium to coarse-grained and mainly consists of chalcopyrite, carrollite, and the aluminosilicates, accompanied by minor amounts of pertsevite, and trace amounts of kaolinite, anorthite, rutile, muscovite, ludwigite, dravite, albite and chlorite-clinochlore. Principal ore minerals are chalcopyrite (~ 4 mm – 9 mm) and carrollite (3 mm). Carrollite displays two morphologies – euhedral grains and elongated crystals that define a foliation. The relationship between the principal ore and gangue minerals

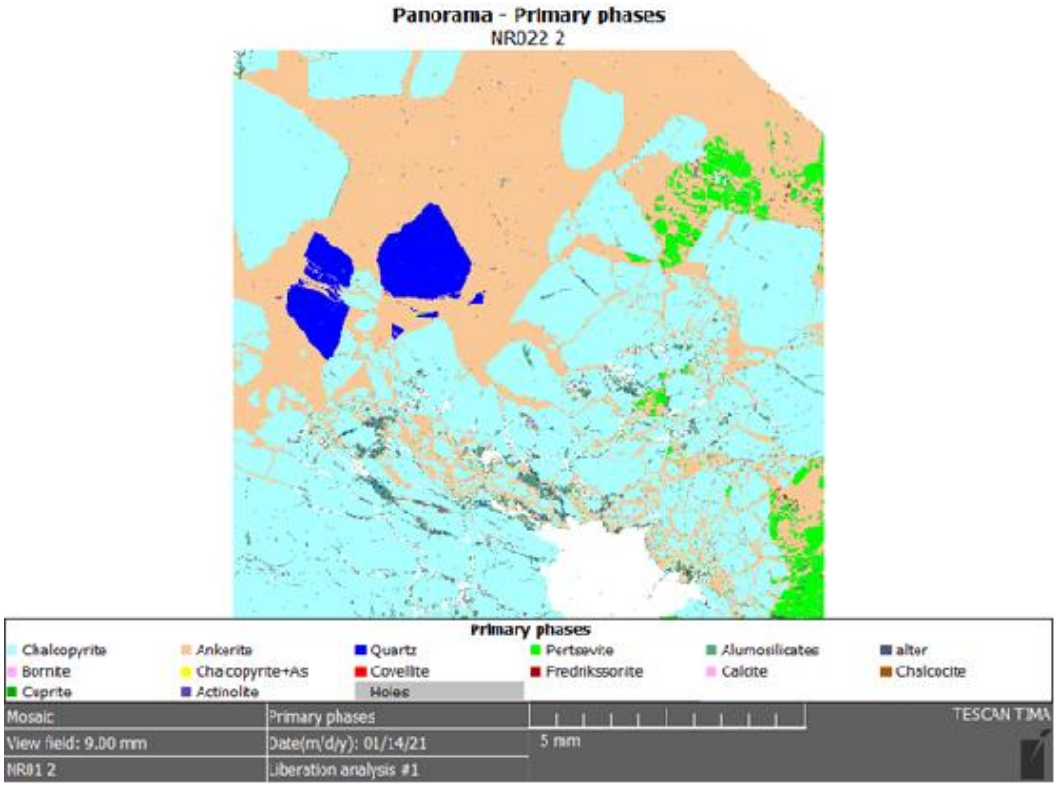
indicates both a massive and disseminated texture. The gangue minerals show a direction-preferred preferential orientation included in the chalcopyrite as a vein-like occurrence.





4.1.1.1.5 Sample NR022

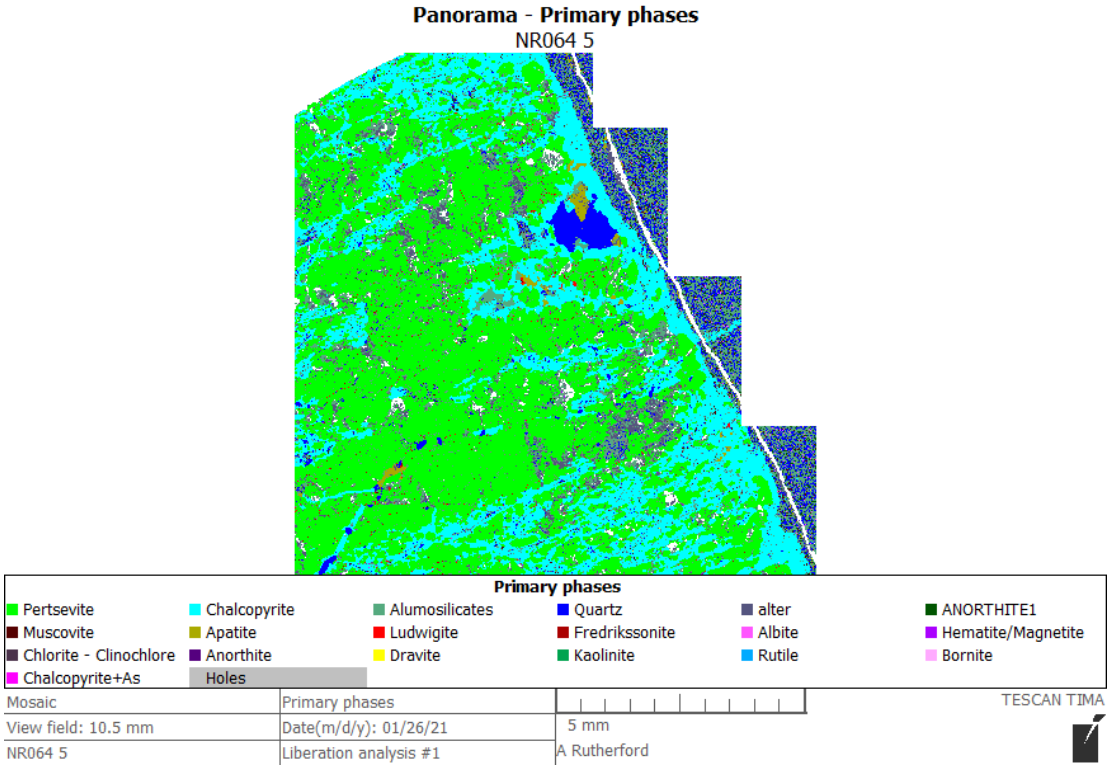
Sample NR022 is a coarse-grained dolomite and chiefly consists of ankerite, chalcopyrite and quartz. These minerals are accompanied with trace amounts of aluminosilicates, actinolite, calcite, and fredrikssonite. The principal ore mineral is chalcopyrite (3 mm- 9 mm), with trace amounts of bornite, cuprite, chalcocite, covellite. The overall texture is disseminated with pertsevite included within ankerite and chalcopyrite. The ankerite is replacing chalcopyrite as shown by the replacement texture and the angular morphology of the chalcopyrite crystals.



4.1.1.1.6 Sample NR064

Sample NR064 is a medium-grained quartzose sandstone and mainly consists of pertsevite and chalcopyrite, with minor haematite/magnetite, quartz, aluminosilicates, and chlorite-clinochlore. It is accompanied with trace amounts of dravite, albite, rutile, fredrikssonite, kaolinite, anorthite and muscovite and

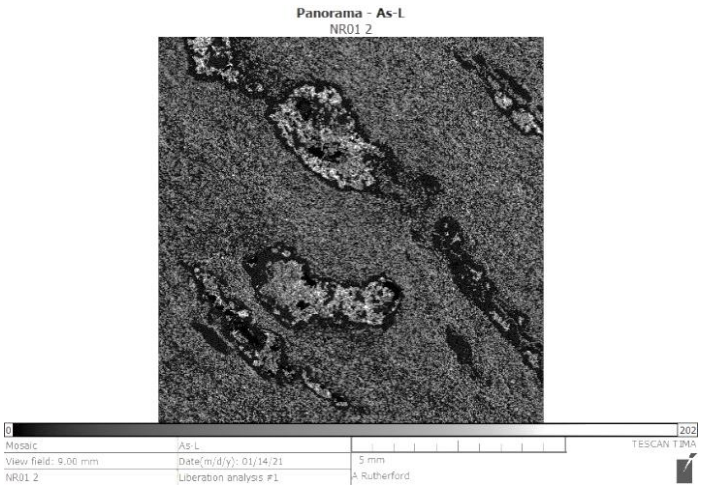
ludwigite. The principal ore is chalcopyrite, with trace amounts of bornite. A disseminated sulphide “toothbrush” texture is observed, where the tendrils of chalcopyrite occur perpendicular to the sedimentary lamination.

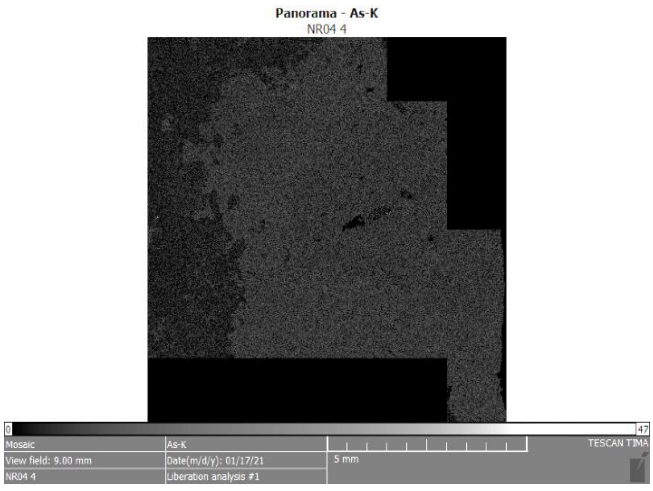


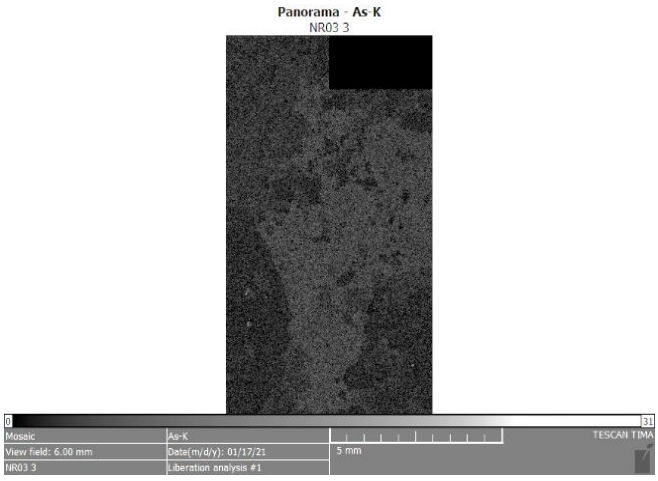
Appendix B: TIMA elemental distribution through 6mm, 9mm, 10.5mm and 12mm fields of view

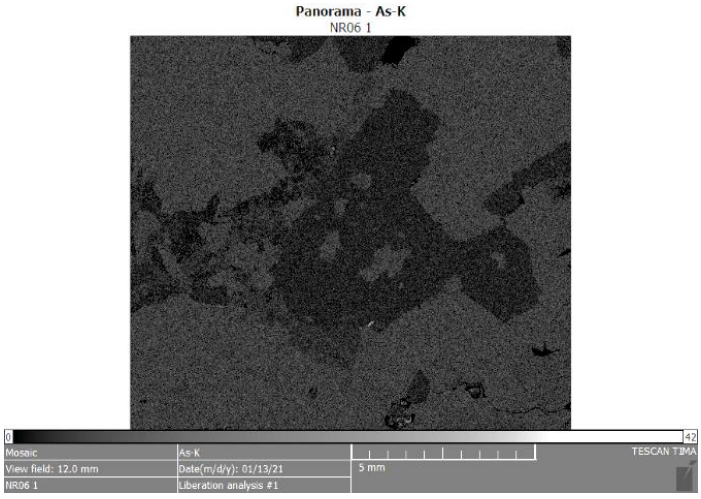
4.1.2.1 Arsenic

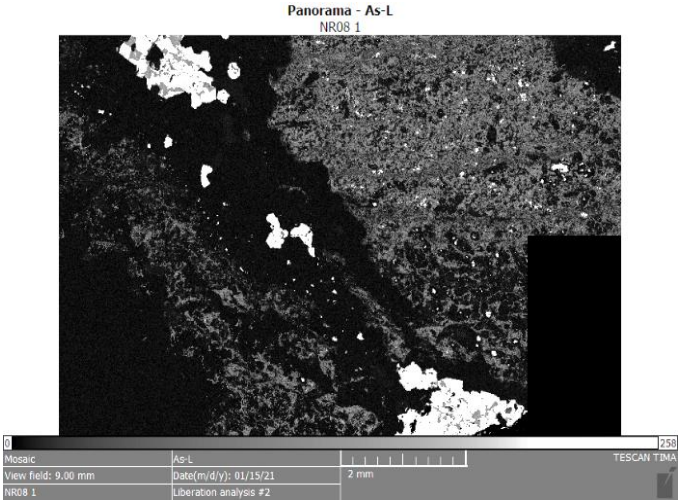
Samples NR01 and NR08 show enrichment of arsenic while samples NR03, NR04, NR06, NR022 and NR064 are depleted in arsenic. Arsenic in enriched sample NR01 is spatially evenly spread, however, the pyrite rims is depleted in arsenic which is a contrast to the arsenic present by the minerals rimmed by the pyrite. The minerals rimmed by pyrite hold the highest arsenic enrichment within the sample. Arsenic in enriched sample NR08 shows a varied spatial association of enrichment with the highest proportion corresponding to pertsevite and a depletion zone occurring with chalcopyrite. The fine-grained gangue minerals (quartz, chlorite-clinochlore, kaolinite, and fredrikssonite) all contain a significant amount of arsenic.

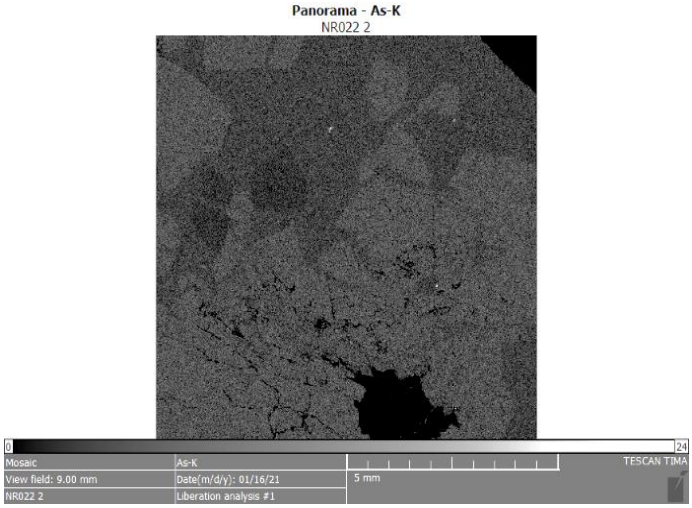


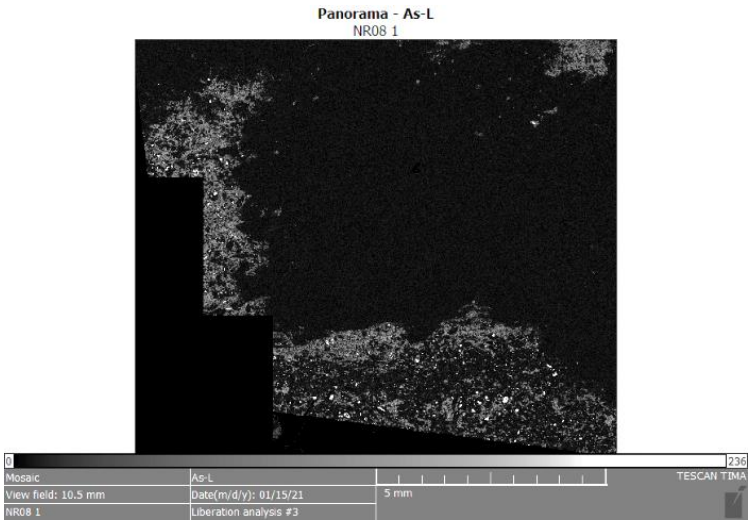


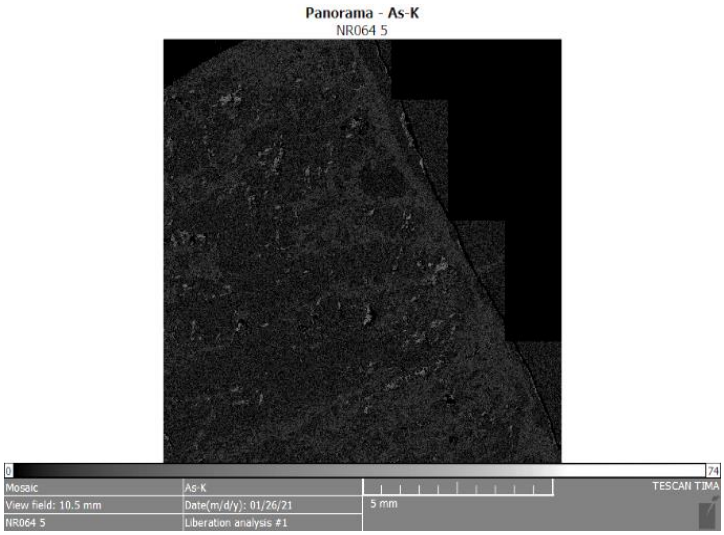






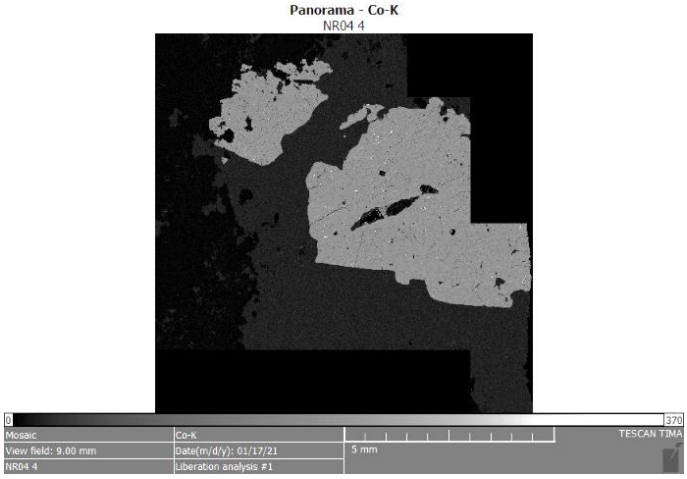


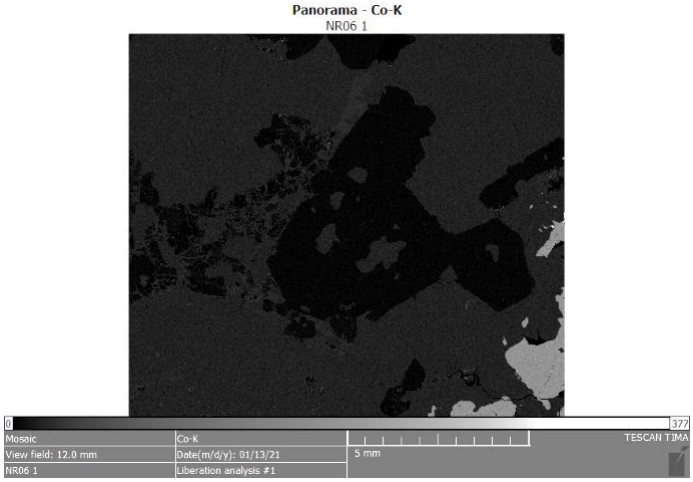


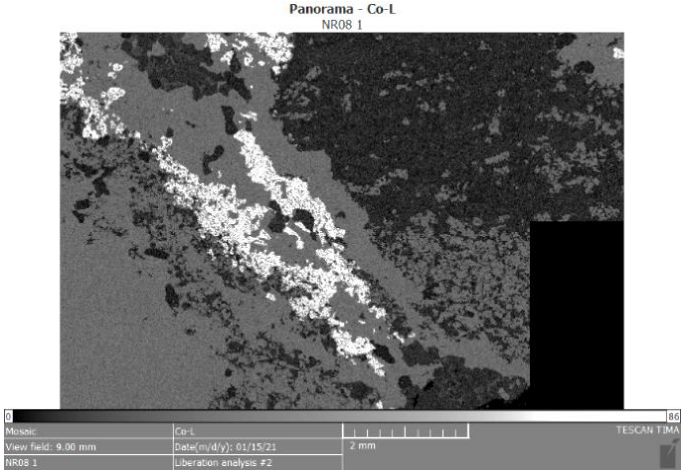


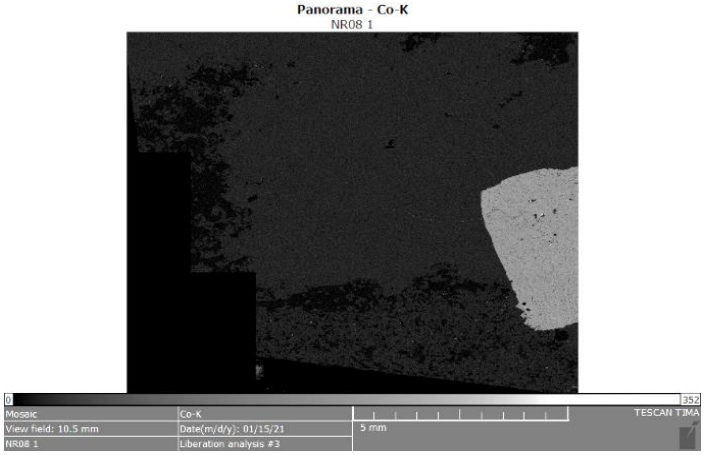
4.1.2.2 Cobalt

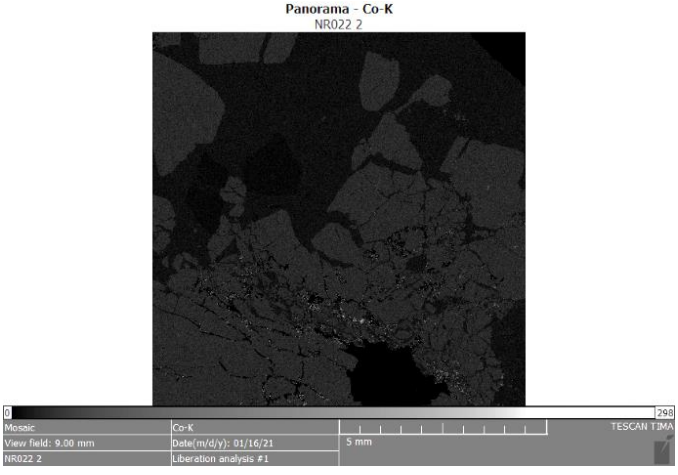
Samples NR03, NR04, NR06 and NR08 show the clear occurrence of carrollite as the main cobalt-bearing mineral. A notable amount of cobalt also exits in association with pyrite (NR01). Zones of cobalt depletion are associated with the gangue minerals, predominantly quartz, ankerite. In the case where cobalt-bearing minerals are not present, cobalt can be detected in the aluminosilicates as shown in NR022. The enrichment of cobalt in pyrite and depletion in chalcopyrite is indicative of cobalt's preferential distribution in iron sulphides over copper sulphides.

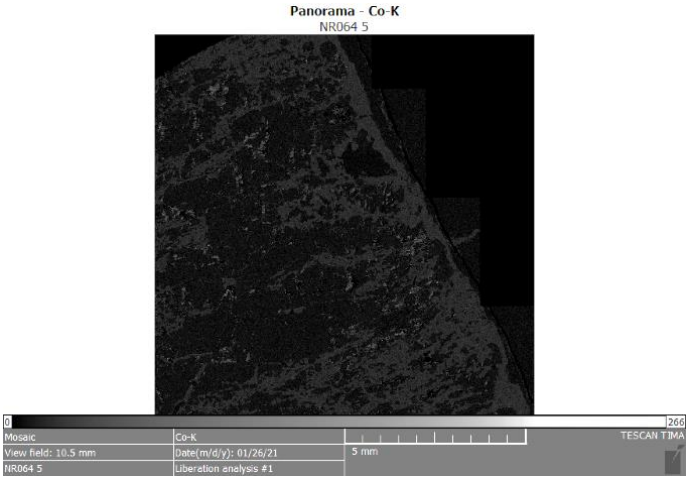






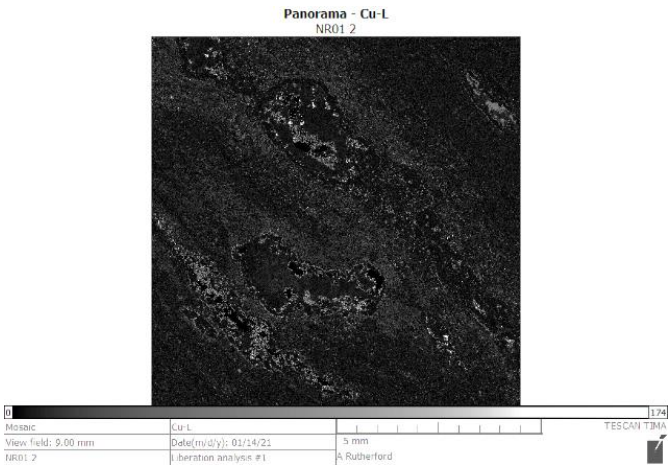


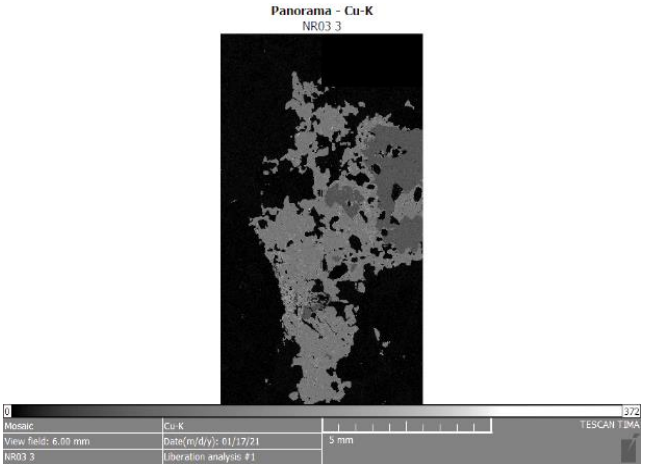


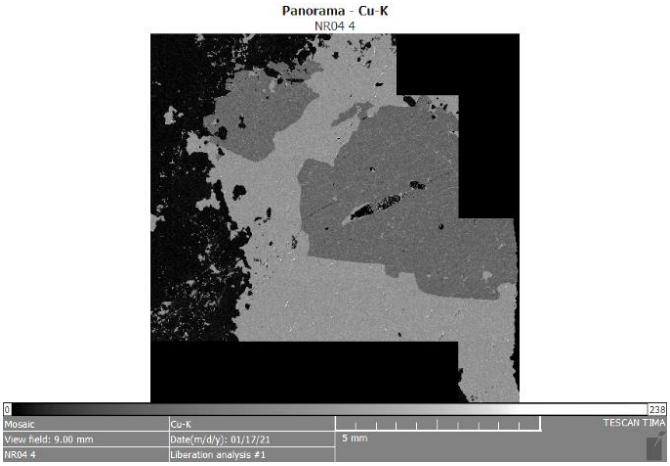


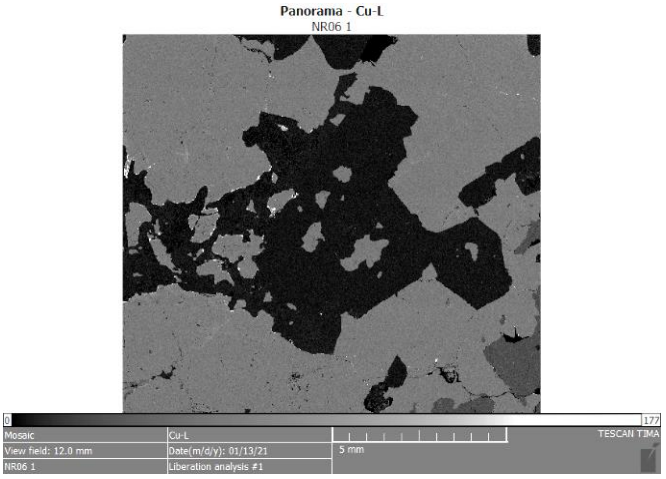
4.1.2.3 Copper

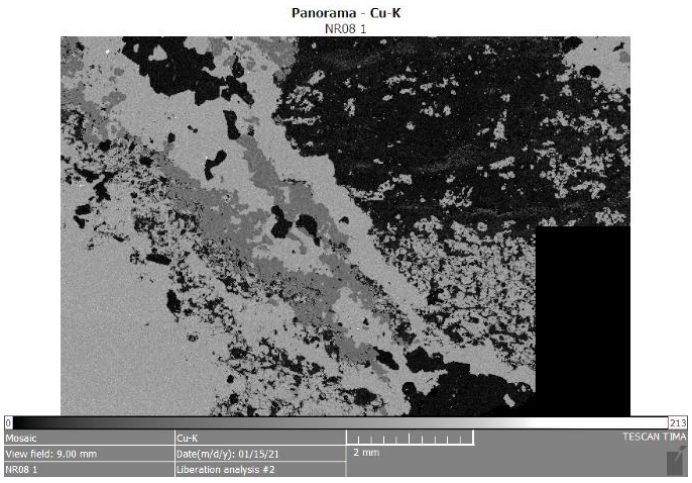
A notable amount of copper exists throughout the sample set as chalcopyrite is one of the main Cu-bearing sulphides. Pyrite and the gangue minerals represent zones of copper depletion.

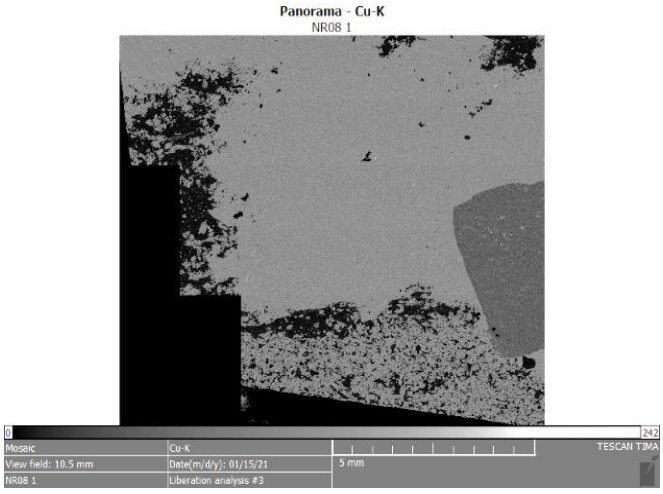

Panorama - Cu-L
NR01 2
0
174
Mosaic
Cu-L
TESCAN TIMA
View field: 9.00 mm
Date(m/d/y): 01/14/21
5 mm
NR01 2
Liberation analysis #1
A Rutherford

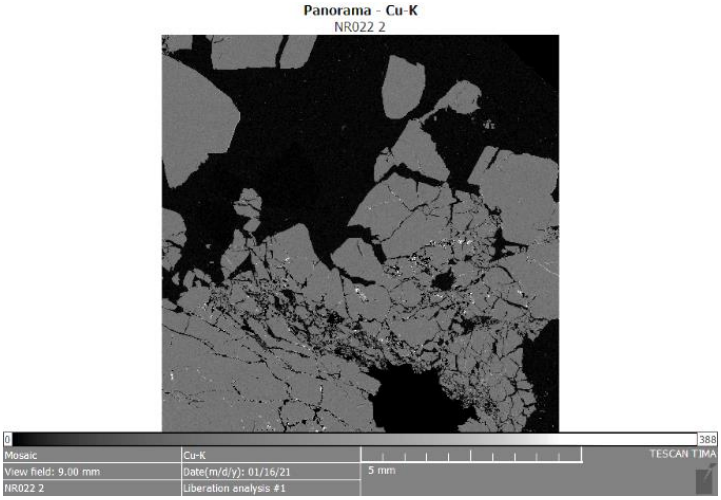

Panorama - Cu-K
NR03 3
0
372
Mosaic
Cu-K
TESCAN TIMA
View field: 6.00 mm
Date(m/d/y): 01/17/21
5 mm
NR03 3
Liberation analysis #1

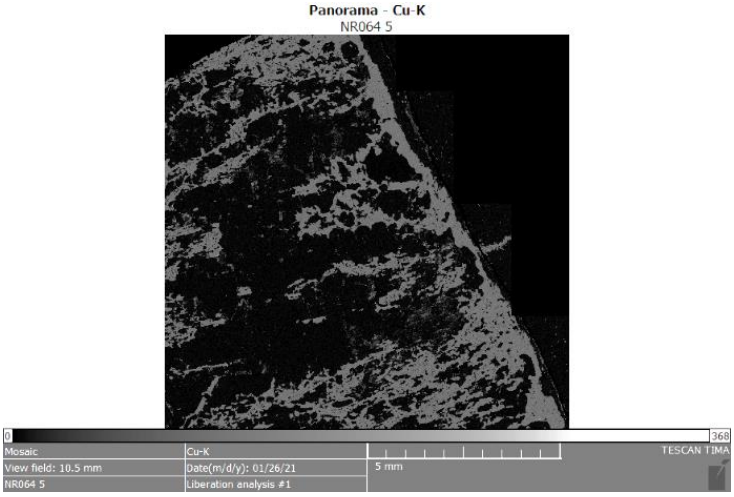

Panorama - Cu-K
NR04 4
0
238
Mosaic
Cu-K
TESCAN TIMA
View field: 9.00 mm
Date(m/d/y): 01/17/21
5 mm
NR04 4
Liberation analysis #1


Panorama - Cu-L
NR06 1
0
177
Mosaic
Cu-L
TESCAN TIMA
View field: 12.0 mm
Date(m/d/y): 01/13/21
5 mm
NR06 1
Liberation analysis #1


Panorama - Cu-K
NR08 1
0
213
Mosaic
Cu-K
TESCAN TIMA
View field: 9.00 mm
Date(m/d/y): 01/15/21
2 mm
NR08 1
Liberation analysis #2

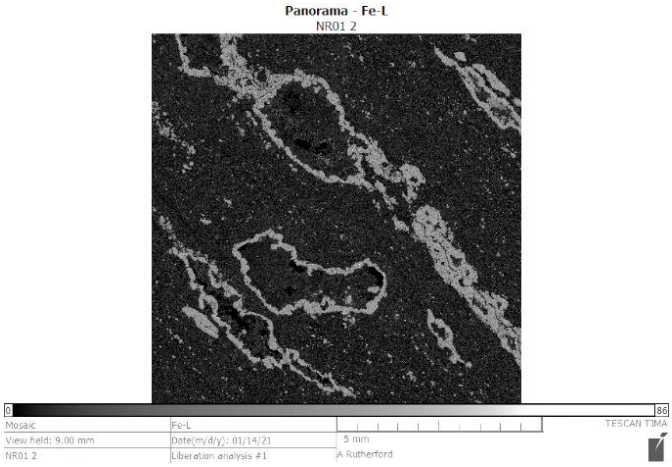

Panorama - Cu-K
NR08 1
0
242
Mosaic
Cu-K
TESCAN TIMA
View field: 10.5 mm
Date(m/d/y): 01/15/21
5 mm
NR08 1
Liberation analysis #3

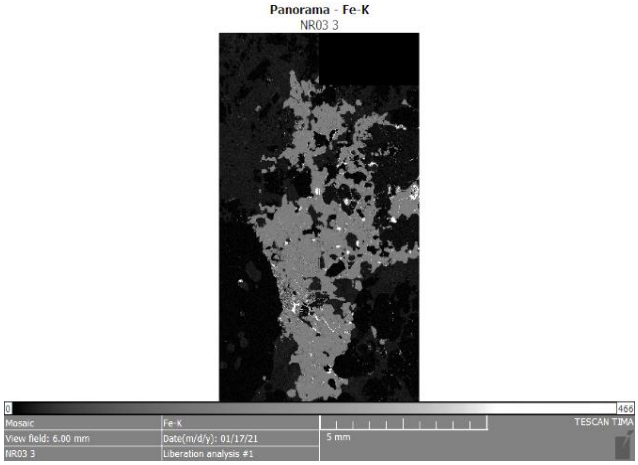




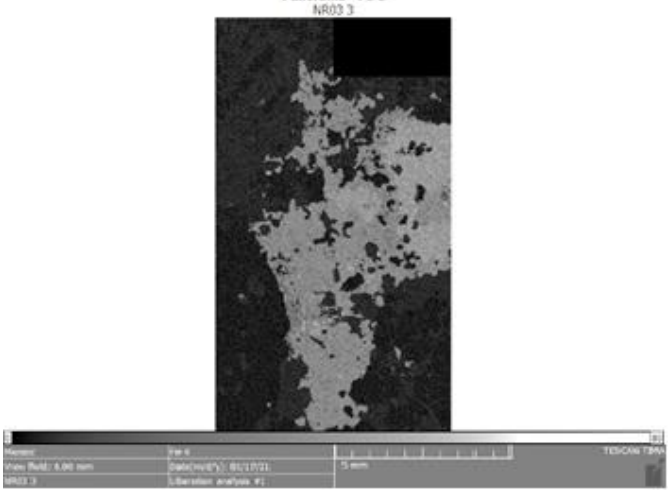
4.1.2.4 Iron

Iron is a common element within the sample set and is characteristically found in the most abundant sulphide mineral, chalcopyrite. Sample NR03 contains the highest proportions of iron due to the presence of haematite/magnetite. The main gangue minerals – quartz and ankerite – represent zones of depletion together with pertsevite as seen in sample NR03 Iron shows an affinity for copper as the two correspond to the siderophile and chalcophile nature of the ore.

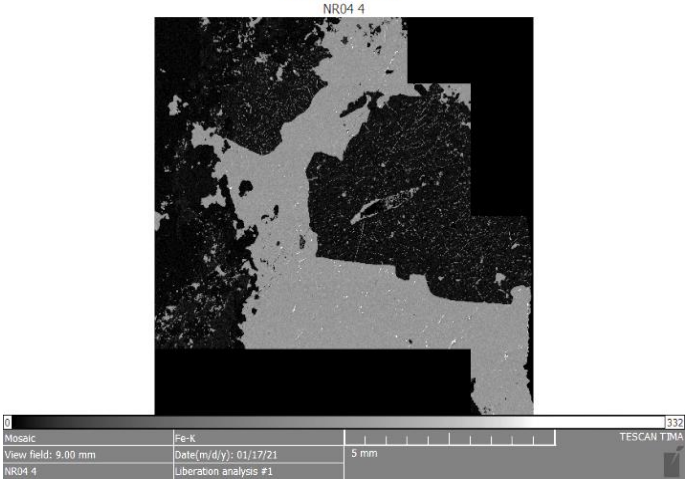




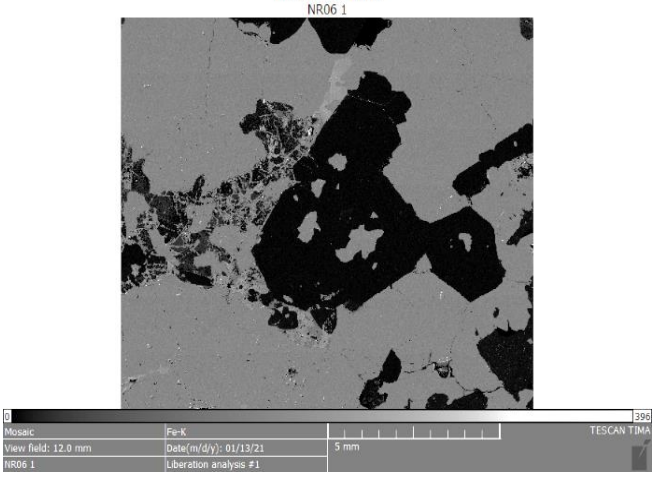
Panorama - Fe-L
NR03 3



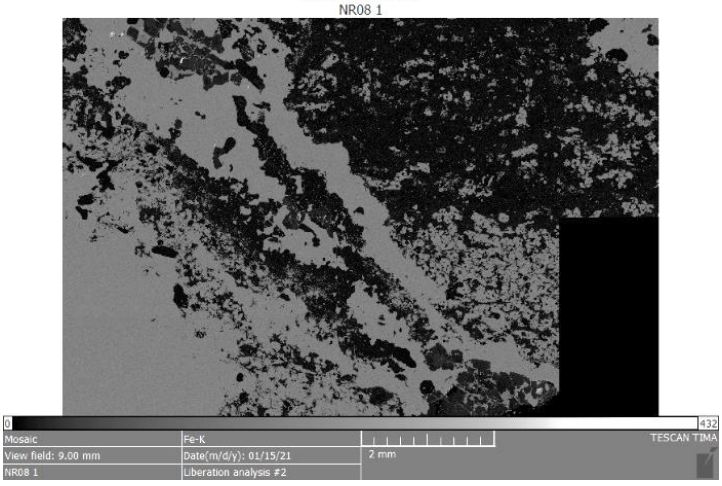
Panorama - Fe-K
NR04 4



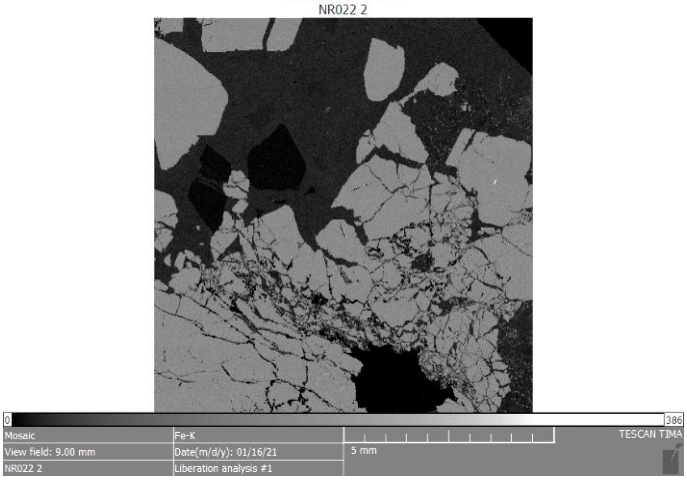
Panorama - Fe-K
NR06 1



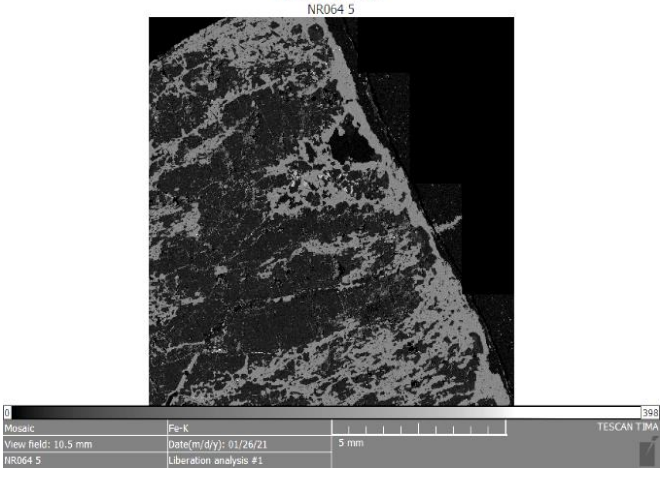
Panorama - Fe-K
NR08 1



Panorama - Fe-K
NR022 2

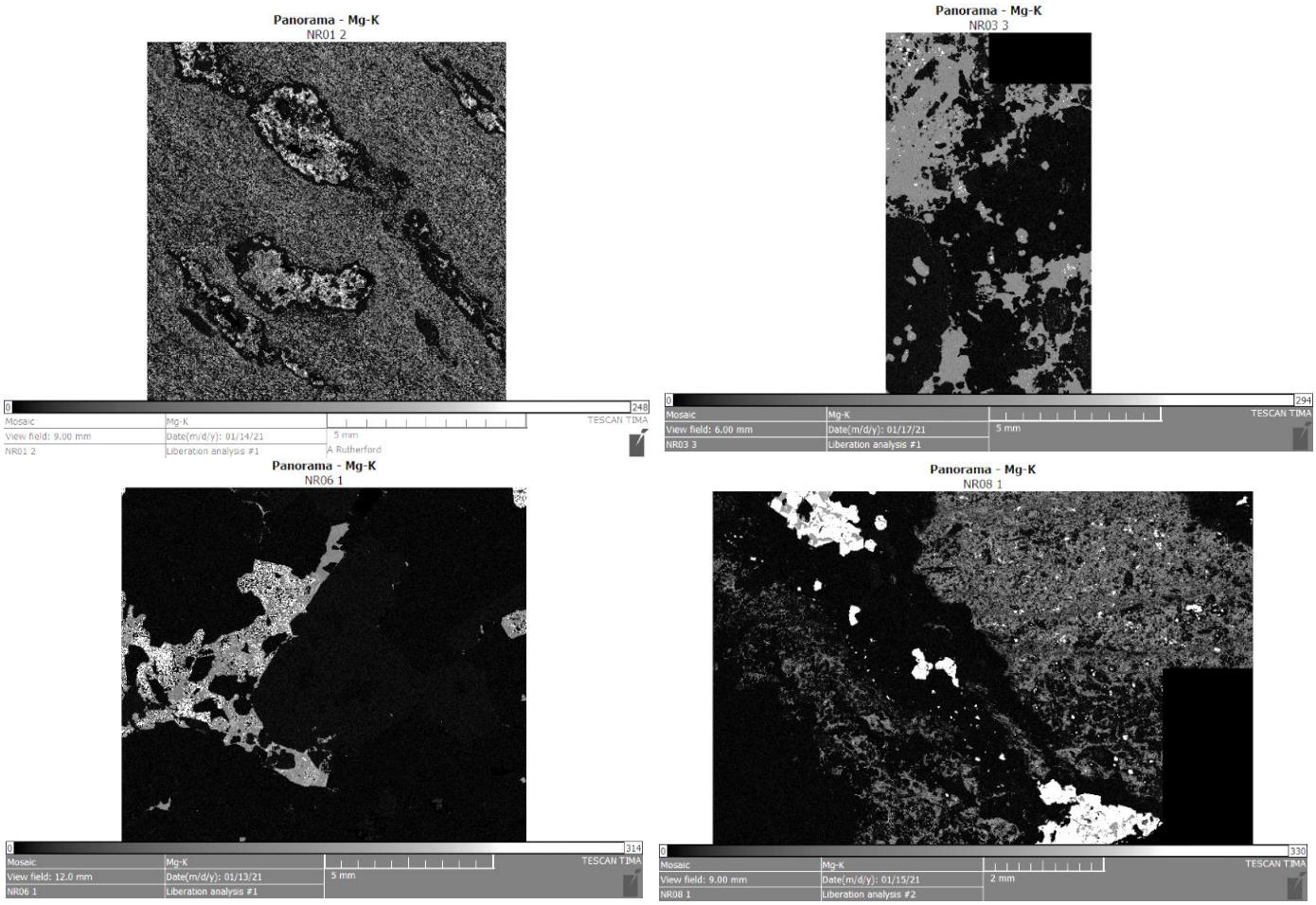


Panorama - Fe-K
NR064 5



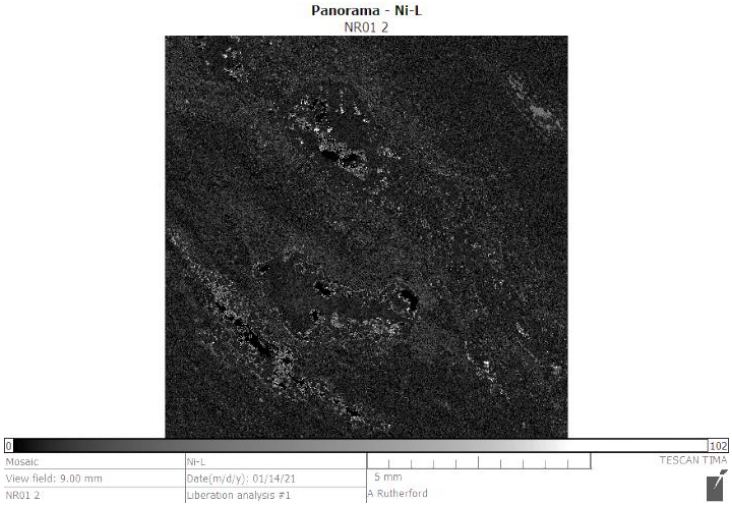
4.1.2.5 Magnesium

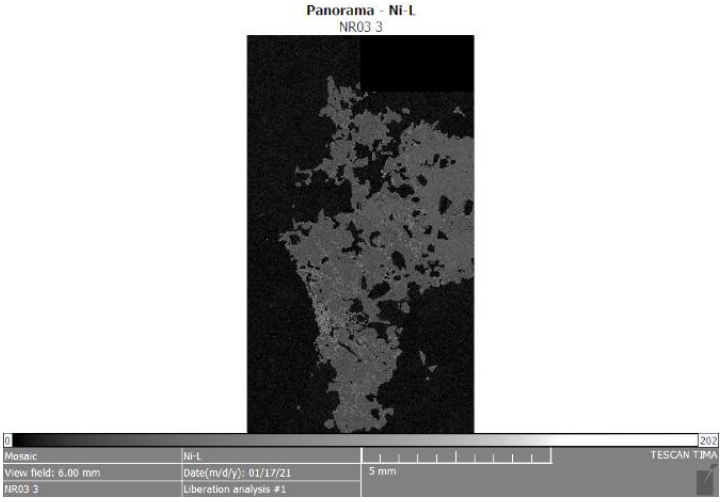
Magnesium commonly occurs within the ore and gangue minerals. The main magnesium-bearing mineral is pertsevite which shows significant enrichment. Magnesium is also found in ferro-actinolite and actinolite indicated in sample NR01. Quartz, chalcopyrite and ankerite represent zones of magnesium depletion.

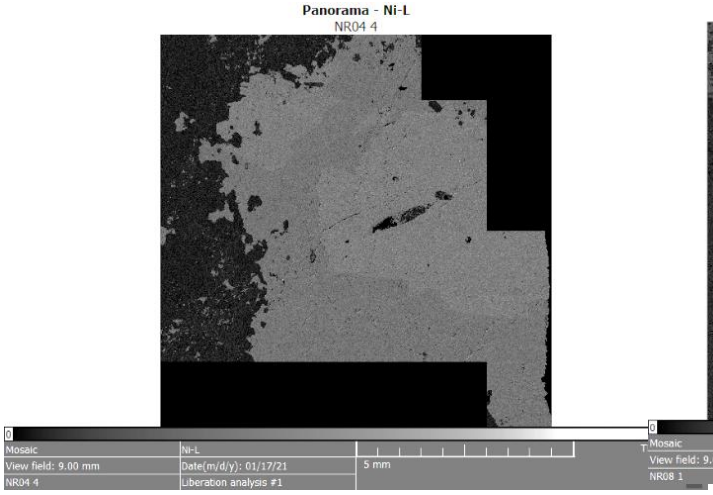


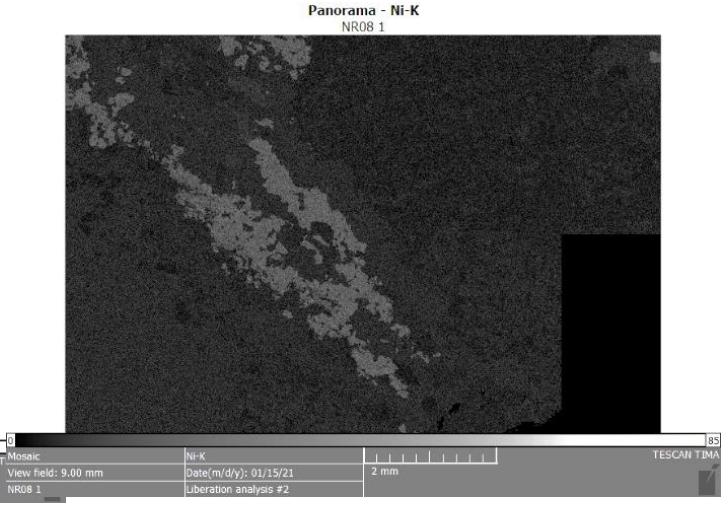
4.1.2.6 Nickel

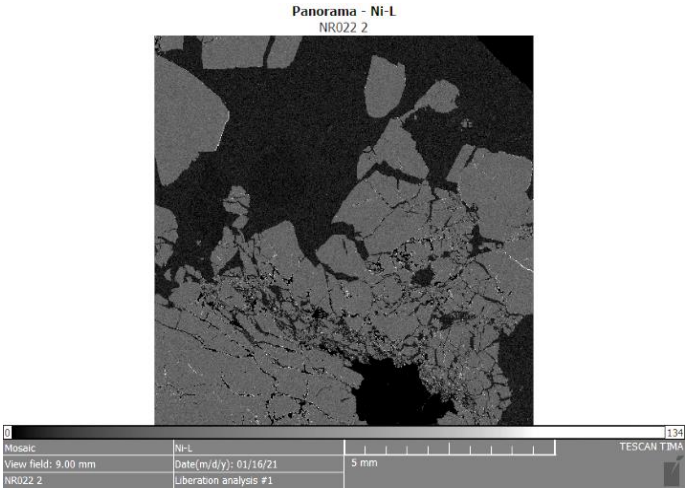
Samples NR03, NR04, NR08, NR022, and NR064 contain nickel. It is mainly hosted in carrollite (NR04 and NR08) as well as in chalcopyrite. The by-product nature of nickel and cobalt is shown by nickel's occurrence in carrollite. The haematisation in sample NR01 represents the highest proportion of nickel which contrasts with quartz as a zone of depletion.

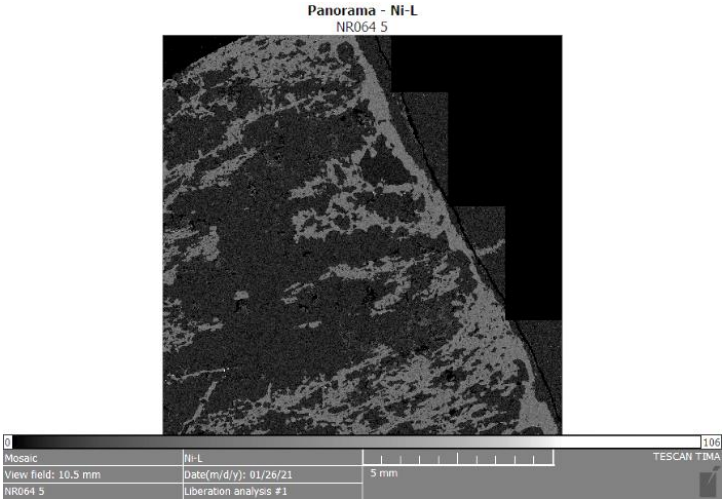






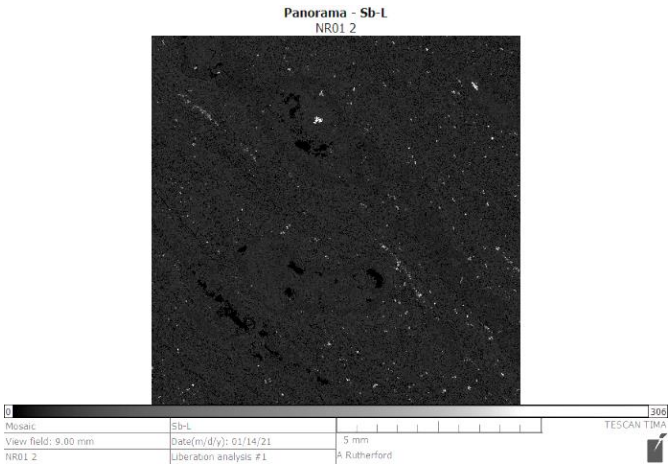


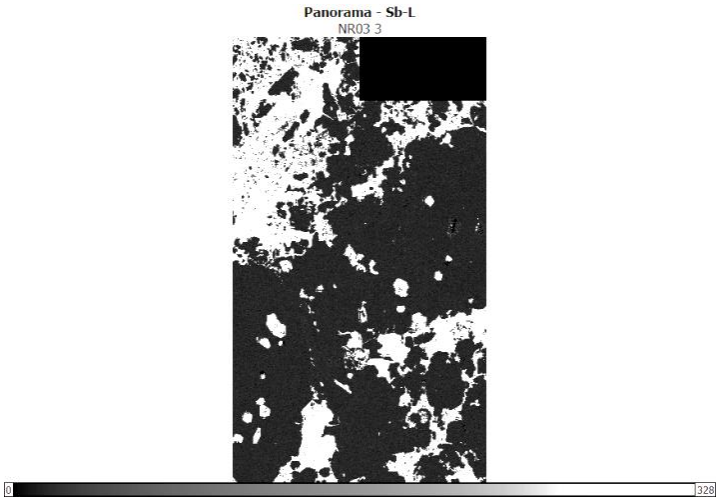




4.1.2.7 Antimony

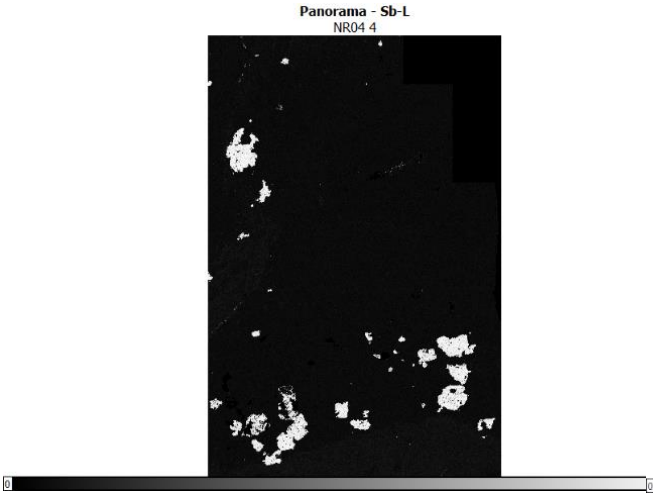
Antimony shows a preferential distribution for gangue minerals as its highest proportions are found in ankerite and apatite (NR03, NR08 and NR022). However, other gangue minerals such as quartz are sites of depletion (NR06). Antimony is also enriched in ore minerals however carrollite and chalcopyrite are depleted in antimony.

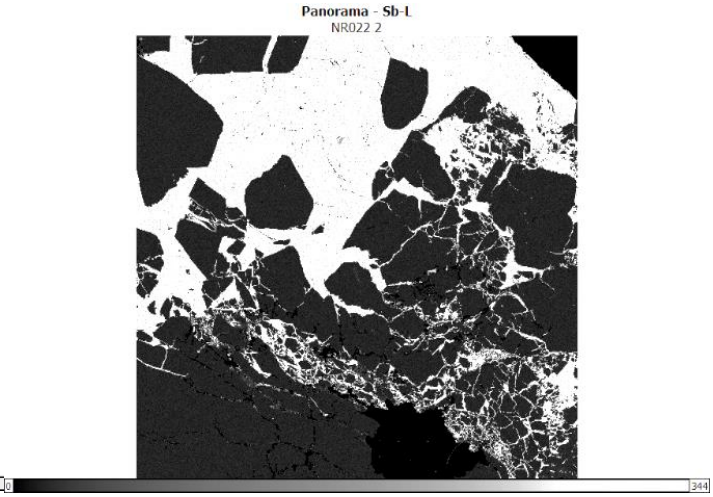




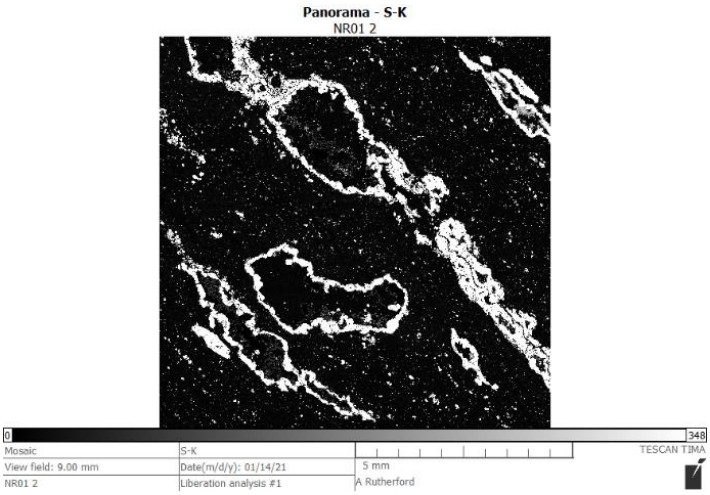
4.1.2.7 Sulphur

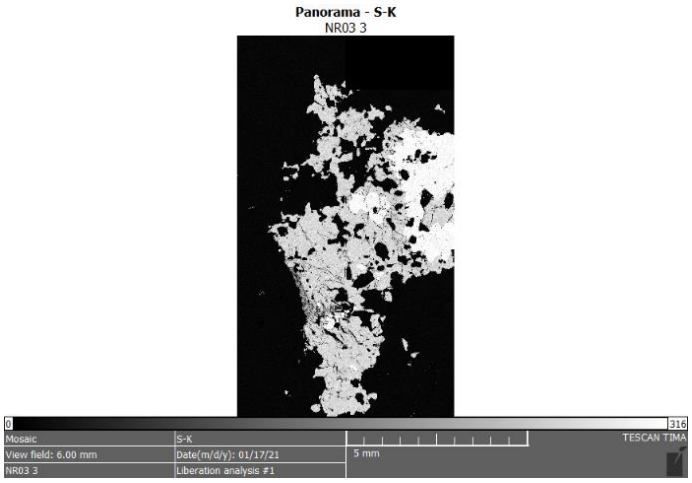
The sample set is highly enriched with sulphur which reflects the redox state of the ore (i.e., sulphide ore). The enrichment is associated with pyrite, chalcopyrite and carrollite. Carrollite presents the most enrichment of sulphur (NR06 and NR08) which corresponds

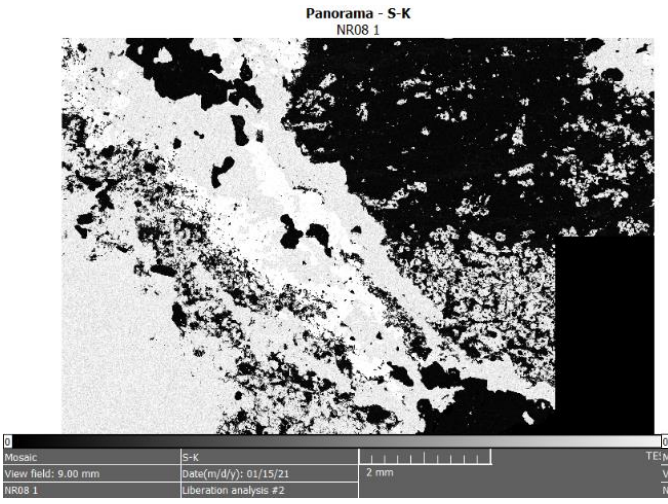


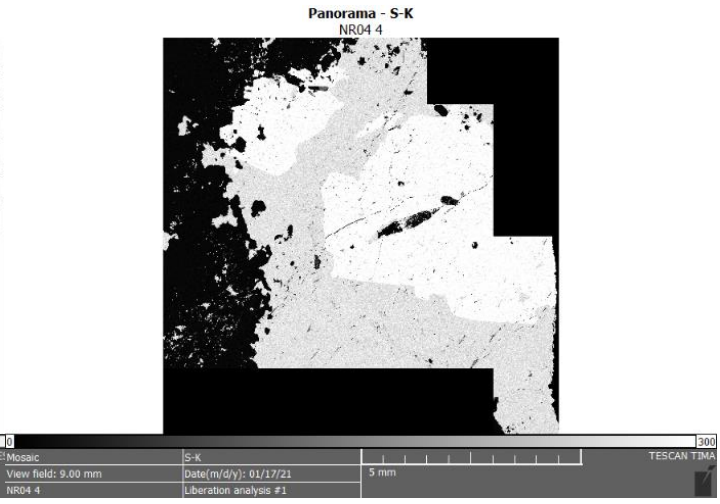


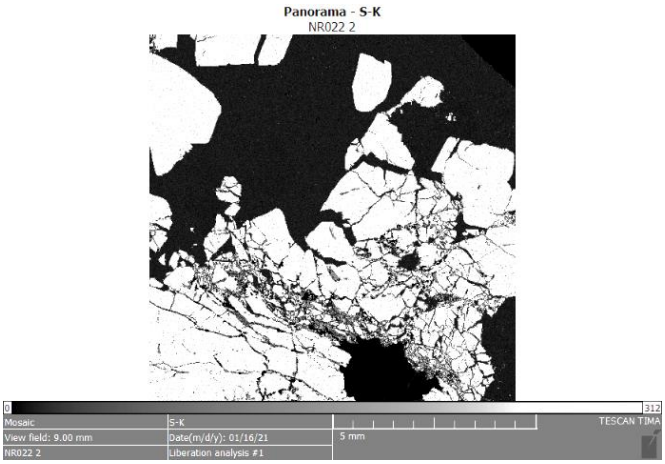
with the enhanced enrichment of cobalt and nickel in carrollite. The zones of depletion are predominantly in quartz, aluminosilicates and ankerite (NR03, NR08 and NR022).

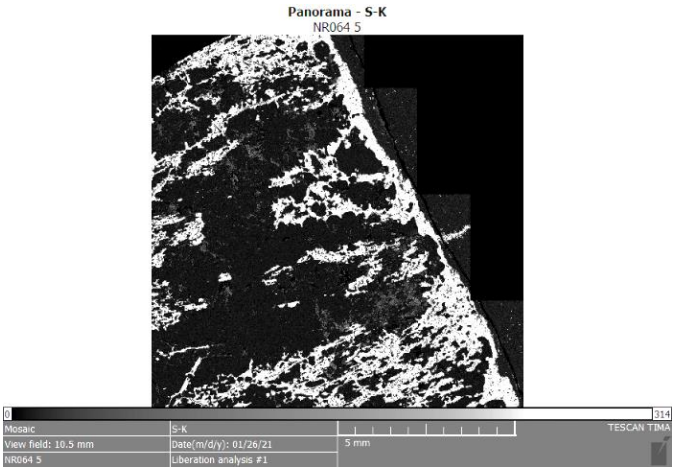


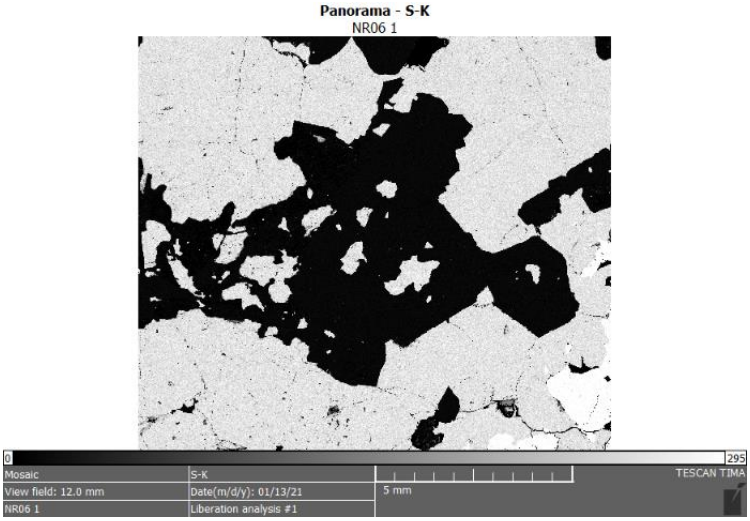


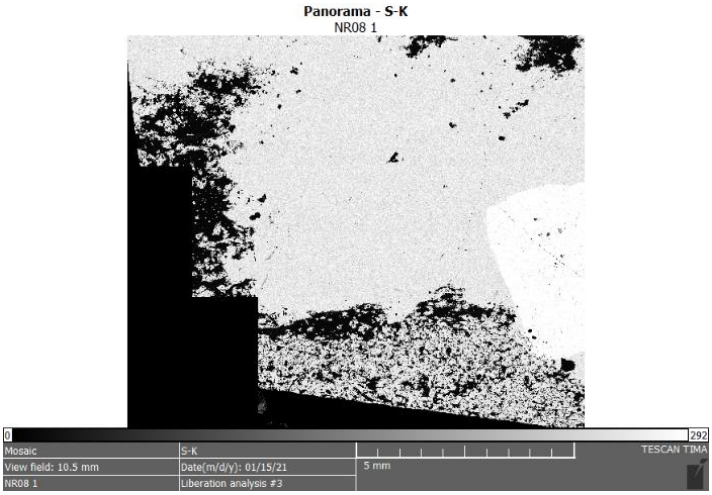












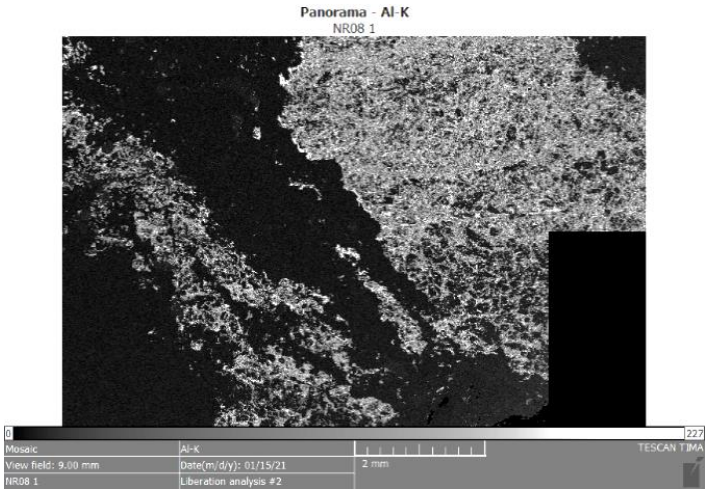
4.1.2.8 Aluminium

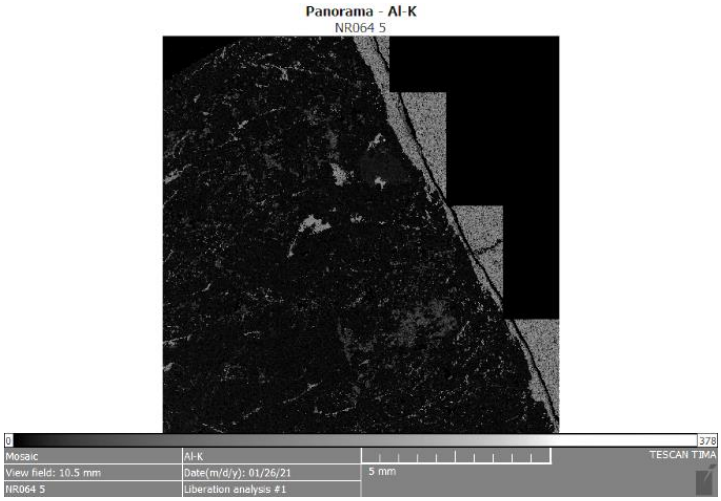
Aluminium is an uncommon element within the ore as it is depleted in most minerals. The occurrence of aluminium is attributable to the presence of aluminosilicates (NR08 and NR064).

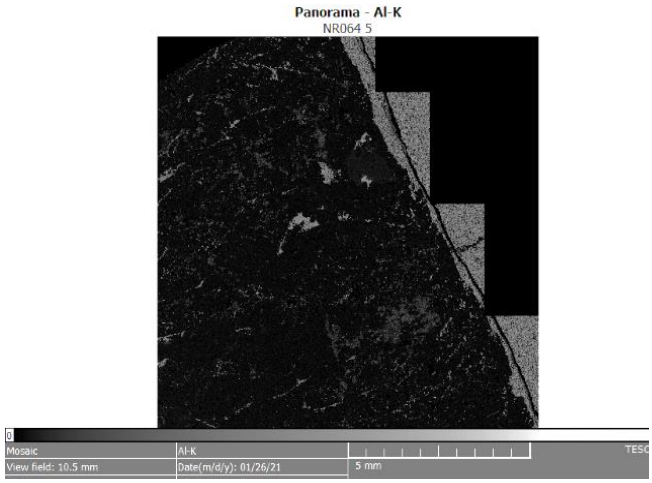
4.1.2.9 Phosphorous

Apatite is the main phosphorous-bearing mineral and is present in sample NR04.

.


Panorama - Al-K
NR08 1
0
227
Mosaic
Al-K
TESCAN TIMA
View field: 9.00 mm
Date(m/d/y): 01/15/21
2 mm
NR08 1
Liberation analysis #2


Panorama - Al-K
NR064 5
0
378
Mosaic
Al-K
TESCAN TIMA
View field: 10.5 mm
Date(m/d/y): 01/26/21
5 mm
NR064 5
Liberation analysis #1


Panorama - Al-K
NR064 5
0
Mosaic
Al-K
View field: 10.5 mm
Date(m/d/y): 01/26/21
5 mm

Appendix C: Cobalt world productin from 1970 to 2020 in metric tonnes (Brown et al., 2020)

Year	Albania	Australia	Botswana	Brazil	Canada	China	Cuba	DRC
1970		469			2069		1500	13958
1971		796			1961		1500	14518
1972		770	0		1520		1500	30800
1973		776	0		1517		1600	32800
1974		1078	33		1564		1600	33900
1975		2709	81		1354		1500	31300
1976		3250	198		1356		1500	10686
1977		3324	165		1485		1500	10208
1978		3265	261		1233		1400	13146
1979		3046	294		1640		1300	14029
1980		3704	226		2118		1500	14482
1981	345	2902	254		2080		1600	11124
1982	400	3132	254		1274		1500	5573
1983	450	2196	223	70	1410	270	1621	5370
1984	600	2125	259	70	2123	270	1393	9075
1985	600	3036	222	600	2067	270	1513	10571
1986	522	2914	162	500	2297	270	1578	14518
1987	612	2715	182	500	5490	270	1613	11871
1988	673	2443	298	500	6234	270	1783	10026
1989	643	2270	215	700	6167	255	1827	9311
1990	586	1870	205	600	5470	325	1743	9981
1991	500	1670	208	900	5274	233	1331	
1992		1270	208	1000	5102	255	1360	8547
1993		1159	205	1200	5108	240	1258	2092
1994		1394	225	1300	4265	270	1141	3274
1995		2100	271	1100	5339	981	1854	3967
1996		1609	406	1000	5714	192	2300	4041
1997		1996	334	1500	5709	200	2500	4000
1998		2138	335	2500	5861	40	2700	5000
1999		1802	332	2900	5323	100	2600	6000
2000		1704	308	4100	5298	91	2900	7000
2001		2696	325	4400	5326	150	3908	12000
2002		2763	269	4300	5148	1004	3856	14500

2003		2562	294	4200	4327	707	3643	14500
2004		2004	223	4300	5060	1253	3554	20200
2005		5198	326	1400	5767	2104	4798	24500
2006		5736	303	1100	7115	1840	5602	27100
2007		5325	242	1311	8692	6100	4549	17886
2008		5779	337	2631	8953	6630	3175	42461
2009		5365	342	2075	3919	6003	3721	56258
2010		4838	272	3139	4636	6382	3706	97693
2011		4275	149	3623	6836	6843	3853	99475
2012		5411	195	2900	6676	7498	3792	86433
2013		6837	248	3500	7168	8580	3319	76593
2014		6252	196	3838	6907	9619	4143	75560
2015		6777	316	2771	7489	10093	4729	83529
2016		6020	248	852	7148	9293	5514	68822
2017		5221	0	28	6058	9000	5407	82461
2018		125	0	4	5268	9000	5300	109402
2019		5740			3340	2500	3800	100000
2020		5700			3200	2300	3600	95000

Year	Finland	Indonesia	Madagascar	Morocco	New Caledonia	Papua New Guinea	Philippines	Russia
1970	1008			604	0			1500
1971	925			978	0			1600
1972	1309			1602	3300		0	1600
1973	1137			1400	3500		0	1700
1974	1067			1750	3560		30	1750
1975	1170			1960	3420		106	1800
1976	1207			911	3568		492	1800
1977	1227			990	3504		1084	1900
1978	1623			1133	2015		1192	1950
1979	1332			1001	2414		1370	2000
1980	1360			838	2598		1331	2150
1981	1270			783	2343		997	2250
1982	1293			792	1803		466	2350
1983	1157			0	1385		165	2400
1984	860			0	1750		64	2600
1985	724			0	2171		911	2700
1986	631			0	1936		92	2800
1987	187			259	1724			5500
1988	0			238	2137			5600

1989	250			114	2885			5600
1990	273			103	2551			6000
1991	234	700		295	2990			5200
1992	216	700		425	3000			
1993	167	800		405	2407			
1994	121	800		427	2756			
1995		814		548	2601			
1996		800		540	2356			
1997		650		780	2964			
1998		650		287	3036			3200
1999		650		882	2803			3400
2000				1001	2620			4100
2001				1337	3540			4600
2002				1335	2780			4200
2003				1391	2602			4654
2004				1600	2726			4527
2005	100			1600	1769			4748
2006	100			1405	1629			4759
2007	64		0	1573	1620		1000	3587
2008	105		0	1791	869	0	1200	2502
2009	27		0	1600	913	0	1500	2352
2010	140	1600	0	1582	1735	0	1500	2460
2011	480	3200	0	1518	2520	0	1500	2337
2012	1381	3600	718	1314	3026	469	2269	2186
2013	2061	4700	2340	1353	7414	1013	2126	2368
2014	2104	329	3221	1391	8239	2134	4094	5400
2015	2119	350	3920	1722	11444	2505	4140	5800
2016	2260	350	3370	2081	17844	2191	4400	5600
2017	1900	350	2840	1924	9397	3308	3700	4700
2018	1377	350	2655	1806	9400	3275	5400	5330
2019			3400	2300	1600	2910	5100	6300
2020			700	1900		2800	4700	6300

Year	Finland	Indonesia	Madagascar	Morocco	New Caledonia	Papua New Guinea	Philippines	Russia
1970	1008			604	0			1500
1971	925			978	0			1600
1972	1309			1602	3300		0	1600
1973	1137			1400	3500		0	1700
1974	1067			1750	3560		30	1750

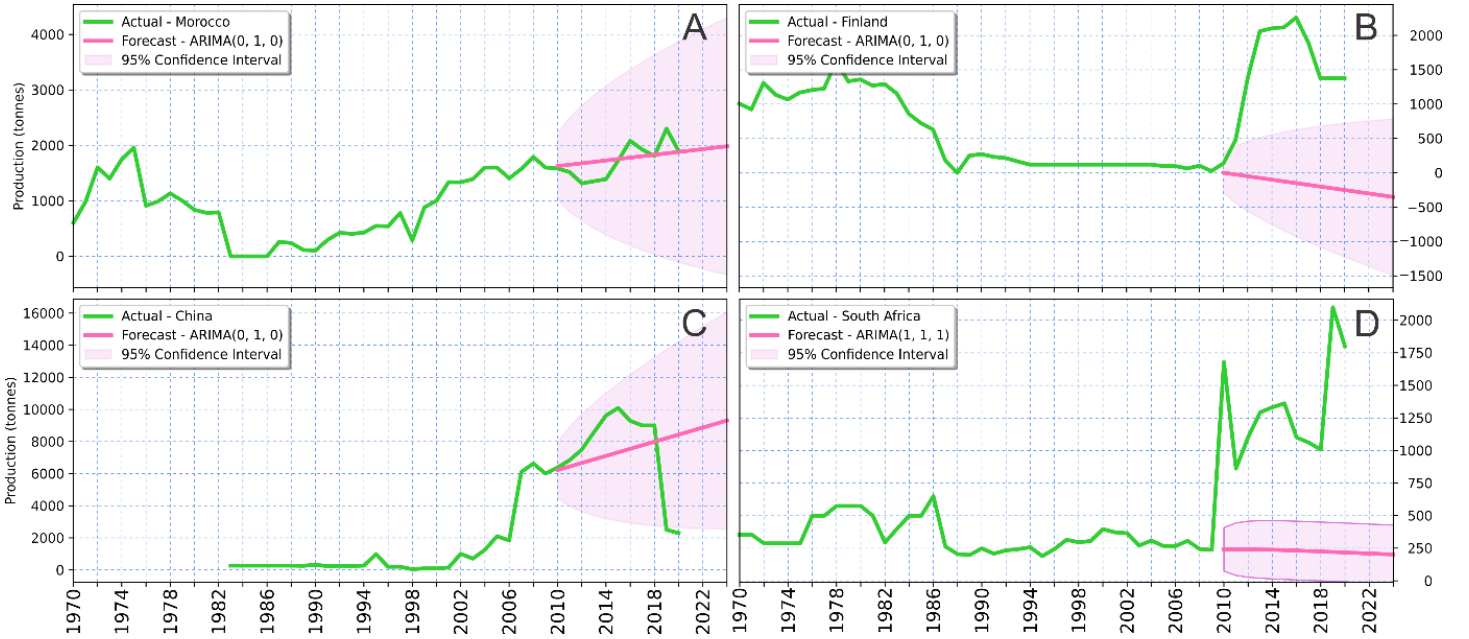
1975	1170			1960	3420		106	1800
1976	1207			911	3568		492	1800
1977	1227			990	3504		1084	1900
1978	1623			1133	2015		1192	1950
1979	1332			1001	2414		1370	2000
1980	1360			838	2598		1331	2150
1981	1270			783	2343		997	2250
1982	1293			792	1803		466	2350
1983	1157			0	1385		165	2400
1984	860			0	1750		64	2600
1985	724			0	2171		911	2700
1986	631			0	1936		92	2800
1987	187			259	1724			5500
1988	0			238	2137			5600
1989	250			114	2885			5600
1990	273			103	2551			6000
1991	234	700		295	2990			5200
1992	216	700		425	3000			
1993	167	800		405	2407			
1994	121	800		427	2756			
1995		814		548	2601			
1996		800		540	2356			
1997		650		780	2964			
1998		650		287	3036			3200
1999		650		882	2803			3400
2000				1001	2620			4100
2001				1337	3540			4600
2002				1335	2780			4200
2003				1391	2602			4654
2004				1600	2726			4527
2005	100			1600	1769			4748
2006	100			1405	1629			4759
2007	64		0	1573	1620		1000	3587
2008	105		0	1791	869	0	1200	2502
2009	27		0	1600	913	0	1500	2352
2010	140	1600	0	1582	1735	0	1500	2460
2011	480	3200	0	1518	2520	0	1500	2337
2012	1381	3600	718	1314	3026	469	2269	2186
2013	2061	4700	2340	1353	7414	1013	2126	2368
2014	2104	329	3221	1391	8239	2134	4094	5400

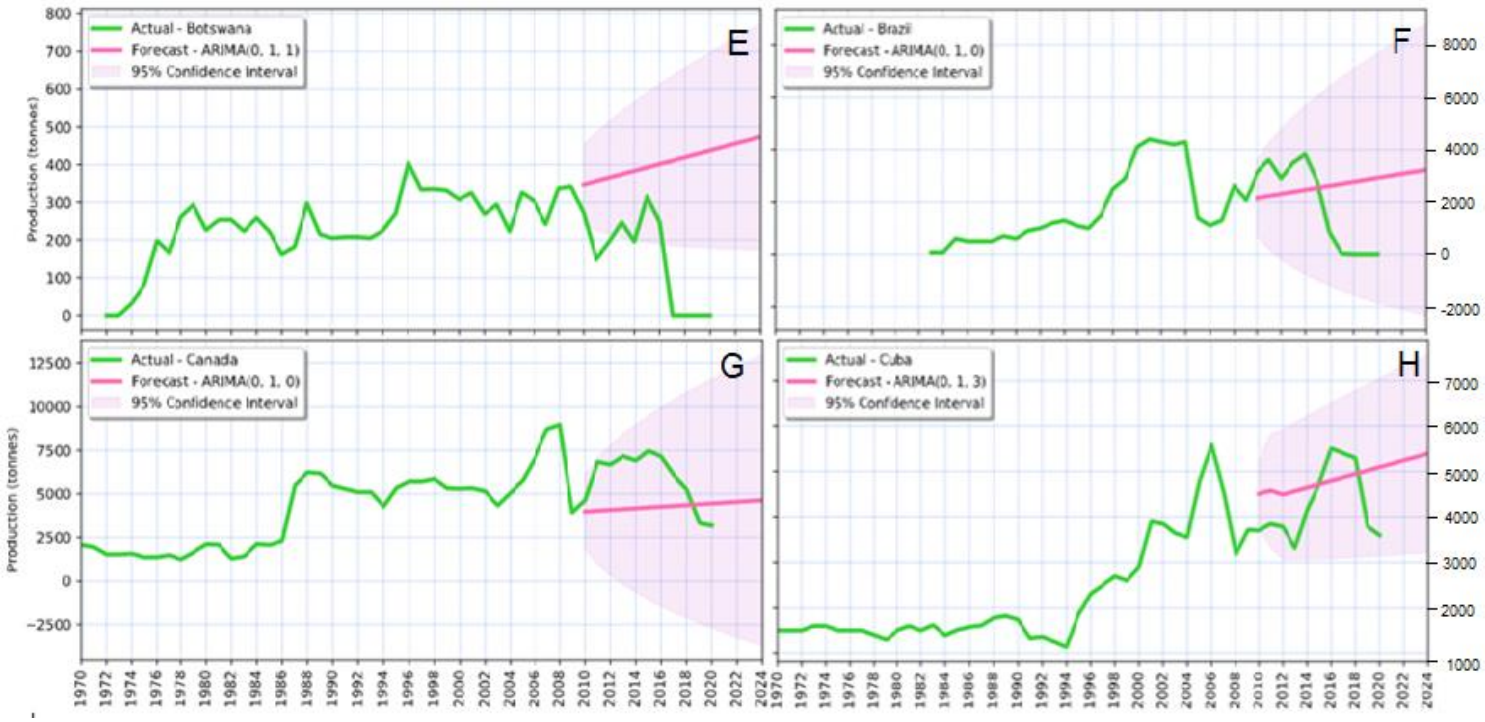
2015	2119	350	3920	1722	11444	2505	4140	5800
2016	2260	350	3370	2081	17844	2191	4400	5600
2017	1900	350	2840	1924	9397	3308	3700	4700
2018	1377	350	2655	1806	9400	3275	5400	5330
2019			3400	2300	1600	2910	5100	6300
2020			700	1900		2800	4700	6300

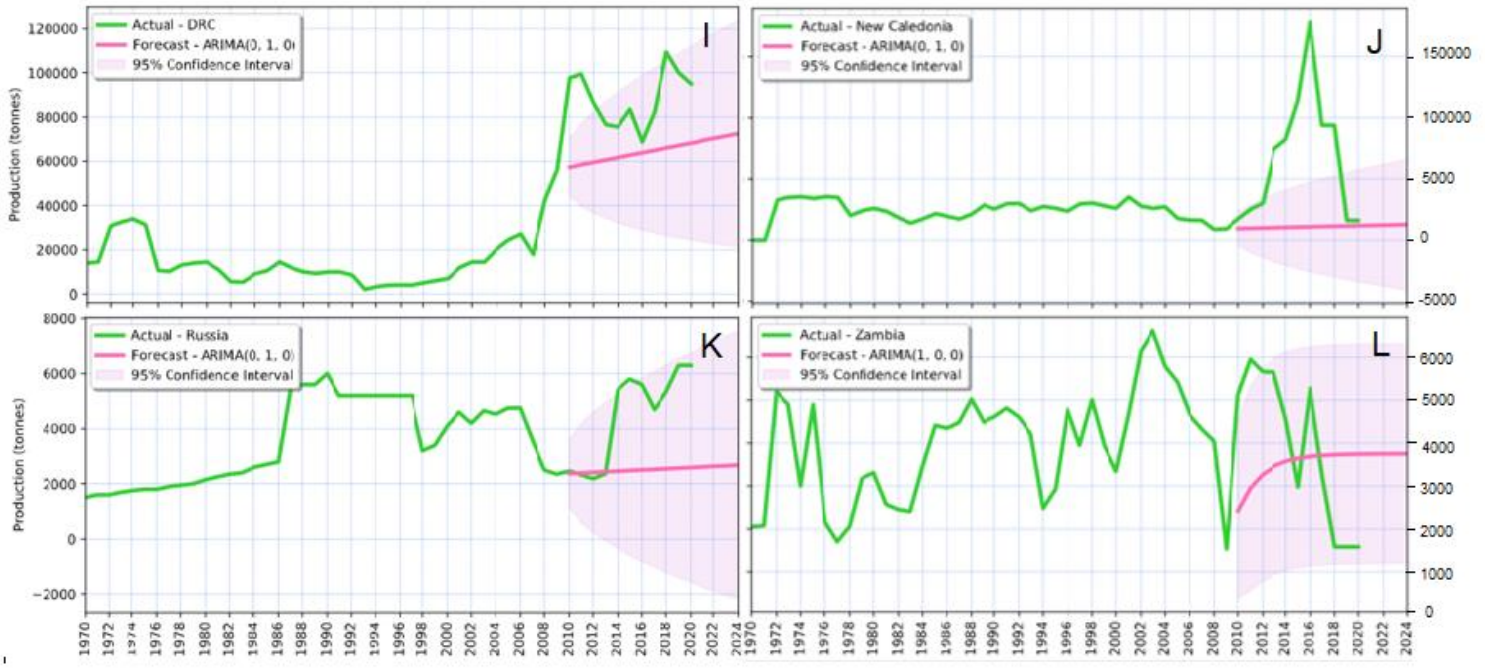
Year	South Africa	USA	Uganda	Vietnam	Zambia	Zimbabwe	World
1970					2052		23160
1971					2079		24357
1972					5200		47601
1973					4900		49330
1974					3000		49332
1975					4900		50300
1976					2175	0	27143
1977					1704	0	27091
1978					2063	17	29298
1979					3176	205	31807
1980					3310	115	33732
1981					2570	94	28612
1982					2446	98	21381
1983	400				2407	73	19597
1984	500				3472	77	25238
1985	500				4415	91	30391
1986	650				4344	76	33290
1987	263				4479	111	35776
1988	206				5025	122	35555
1989	199				4488	111	35035
1990	249				4614	121	34691
1991	209				4817	118	24679
1992	234				4610	100	27027
1993	243				4211	113	19608
1994	258				2480	126	18837
1995	190				2934	109	22808
1996	244				4799	106	24107
1997	316				3949	126	25024
1998	296				5011	100	31154
1999	306				3946	129	31173
2000	397				3342	79	32940

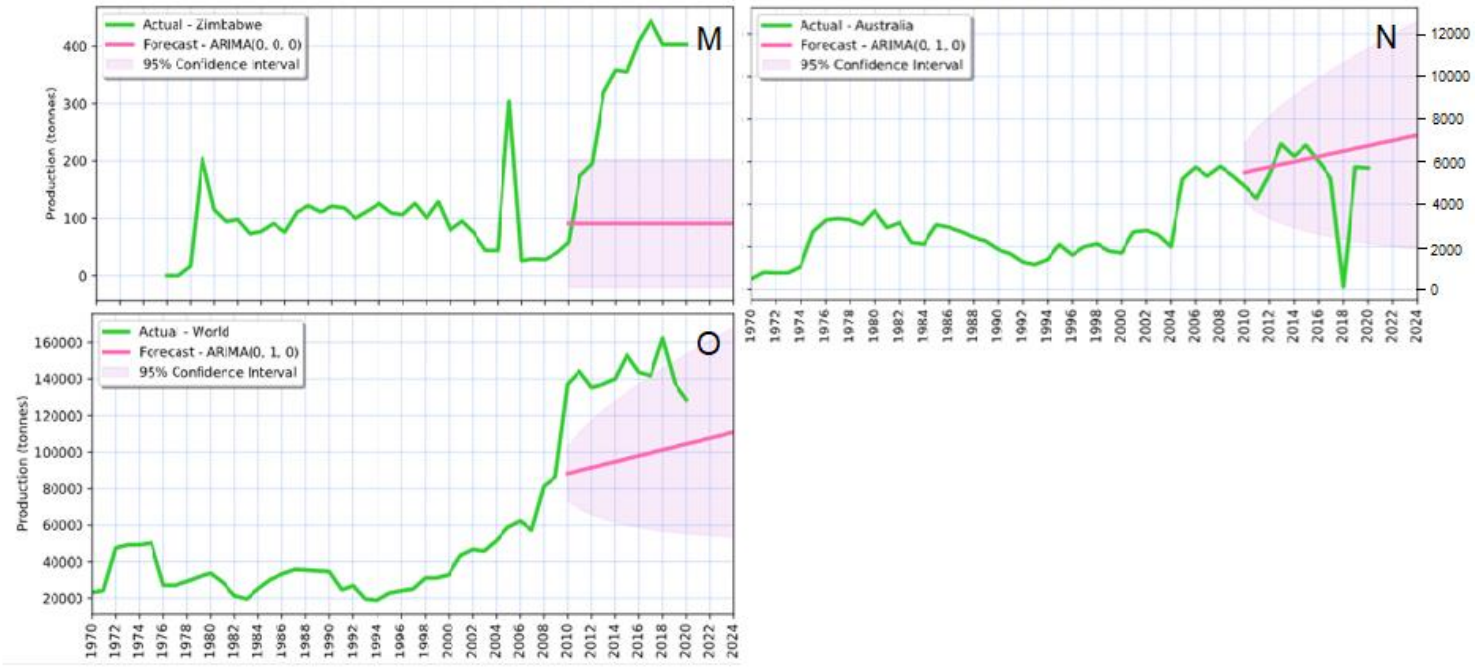
2001	373				4665	95	43415
2002	366				6144	74	46739
2003	271				6620	44	45815
2004	309				5791	44	51591
2005	268		638		5422	304	58942
2006	267		674		4665	26	62321
2007	307		698		4335	29	57318
2008	244		663		4041	28	81409
2009	238		673		1535	39	86560
2010	1680		568		5134	58	137123
2011	862	0	673	0	5956	174	144274
2012	1102	0	556	0	5665	195	135386
2013	1294	0	181	0	5658	319	137072
2014	1332	120		223	4562	358	140022
2015	1362	760		277	2979	355	153437
2016	1101	690		134	5276	409	143603
2017	1062	640		0	3240	445	141681
2018	1007	630		0	1585	403	162317
2019	2100	500					137990
2020	1800	600					128600

Appendix D: Cross-validation graphs






Actual - DRC
Forecast - ARIMA(0, 1, 0)
95% Confidence Interval
I
Actual - New Caledonia
Forecast - ARIMA(0, 1, 0)
95% Confidence Interval
J
Actual - Russia
Forecast - ARIMA(0, 1, 0)
95% Confidence Interval
K
Actual - Zambia
Forecast - ARIMA(1, 0, 0)
95% Confidence Interval
L
Production (tonnes)


Actual - Zimbabwe
Forecast - ARIMA(0, 0, 0)
95% Confidence Interval
M
Actual - Australia
Forecast - ARIMA(0, 1, 0)
95% Confidence Interval
N
Actual - World
Forecast - ARIMA(0, 1, 0)
95% Confidence Interval
O
Production (tonnes)